# WATERSHED MODELING AND RISK ASSESMENT OF ERGENE RIVER BASIN

by

Musa Rahmanlar

B.S., Civil Engineering, Boğazici University, 2006

M.S., Civil Engineering, Boğazici University, 2009

Submitted to the Institute for Graduate Studies in
Science and Engineering in partial fulfillment of
The requirements for the degree of
Doctor of Philosophy

Graduate Program in Civil Engineering
Boğaziçi University
2019

WATERSHED MODELING AND RISK ASSESMENT
OF ERGENE RIVER BASIN

APPROVED BY:

Prof. Atilla Akkoyunlu .....
(Thesis Supervisor)

Prof. Ahmet Doğan .....

Prof. Cem Avcı .....

Prof. Mustafa S.Yazgan .....

Prof. Orhan Yenigün .....

DATE OF APPROVAL: 30.01.2019

# ACKNOWLEDGEMENTS

First, I would like to express my sincere gratitude to my thesis supervisor, Prof. Atilla Akkoyunlu for his guidance and support throughout the preparation of this thesis. Without his sympathy, patience and guidance, the accomplishment would be impossible.

I would also like to thank Prof. Mustafa S. Yazgan and Prof. Cem Avcı for their kind and supportive attitude to me. I wish to express my appreciation to Prof. Ahmet Doğan and Prof. Orhan Yenigün for their final comments and contributions to my thesis.

I extend my sincere thanks to Assoc. Prof. A. Ufuk Şahin for his kind and supportive attitude to me and showing high interests and valuable advices to my thesis.

I want to convey special thanks to Dr. İzzet ARI for sharing his experience on climate change and climate models.

I want to convey special thanks to Yusuf Eşidir and Orçun Erpiş who spent their invaluable time and energy with me also my friends, Mehmet Tarık Yılmaz, Halit Özdilek, Mustafa Bulut who encourage me during my thesis study.

I also want to convey special thanks to Bülent Çakın and Bülent Selek from DSI General Directorate and Dr. Yakup Karaarslan from Ministry of Agriculture and Forestry for their support for the data about the Ergene River.

My heartfelt gratitude goes to my wife: Simge Rahmanlar for her encouragement and lifelong supports. Last, I want to thank my wife again, greatest thanks for all.

# ABSTRACT


## WATERSHED MODELING AND RISK ASSESMENT OF ERGENE RIVER BASIN

Protection of water resources in terms of quality and quantity is one of the main challenges for the developed and developing countries. Especially, pollution caused by industrialization and agriculture makes difficult to manage water resources.

Ergene Basin, which has been exposed to population growth, migration, industrial development and agricultural pollution since the 1980s, was the focus of this study. Hydrological characteristics of the basin can be modeled thanks to advances in geographical information systems, hydrologic and water quality models.

In this study with using ArcSWAT, Ergene Basin was modeled with the combined effects of land use and climate. Additionally, the hydrology and water quality of the basin were evaluated by ArcSWAT according to future climate and land use change scenarios.

In this context, the flow data of the İnanlı and Hayrabolu streams were used for calibration and validation process of the model and high degree of accuracy was obtained. Total nitrogen and phosphorus values of the model were compared with İnanlı water quality monitoring point values. Results of model revealed that it can be used for future scenarios of Ergene Basin.

After this stage land use change predictions were calculated for Ergene Basin with using CORINE land use 1990, 2000 and 2012 which were obtained from European Environment Agency. In addition for the estimation of 2030 and 2050 land use maps, potential land use change map was created with CA_MARKOV analysis by using driving factors such as distance to city center, main roads and rivers.

In order to examine the effects of climate change, precipitation and temperature data were created for Ergene basin according to RCP4.5 and RCP8.5 climate scenarios of Meteorology General Directorate.

Generated future land use and climate data were used as input for the validated ArcSWAT model. The future flow and nutrient estimation of the basin were calculated and compared according to different scenarios.

Also, Mann-Kendal, Rho-Spearman statistical tests were used to make inferences for the future from historical data. Additionally with ARIMA model, the trend towards future has been revealed. Total nitrogen and phosphorus values were compared with the ArcSWAT model outputs.

To sum up, the current and future status of the region in terms of water flow quantity and quality is modeled with ArcSWAT by taking into account the land use and climate effects. This study was one of the rare studies in Turkey able to integrate climate variability and land use change on water resources.

# ÖZET


## ERGENE NEHRİ HAVZASININ RİSK ANALİZİ VE HAVZA MODELİ

Su kaynaklarının nitelik ve nicelik bakımından korunarak yönetilmesi, gelişmiş ve gelişmekte olan ülkelerin en büyük problemlerinden birisidir. Özellikle endüstri ve tarımın yarattığı kirlilik, su kaynaklarının yönetimini daha zor hale getirmektedir.

1980'lerden bu yana nüfus artışı, göç, endüstriyel gelişim ve tarımsal kirliliğe maruz kalan Ergene Havzası bu çalışmanın odak noktası olmuştur. Coğrafi Bilgi Sistemi teknolojisi, hidroloji ve su kalite modellerinde yaşanan gelişmeler sayesinde bölgenin hidrolojik yapısı modellenebilmektedir.

Bu çalışmada, ArcSWAT modeli kullanılarak Ergene Havzası günümüz arazi kullanımı ve iklimine göre modellenmiştir. Ayrıca gelecekteki arazi kullanımı ve iklim senaryolarına göre ArcSWAT modeli kullanılarak havzanın hidrolojisi ve su kalitesi üzerine değerlendirmeler yapılmıştır.

Bu kapsamda, İnanlı ve Hayrabolu gözlem istasyonlarının akış verileri modelin ölçümleme ve doğrulama sürecinde kullanılarak yüksek doğruluk dereceleri elde edilmiştir. İnanlı su kalitesi izleme noktasından elde edilen değerler ile modelin toplam azot ve fosfor değerleri kıyaslanmıştır. Günümüz koşullarına göre yeterli sonuçlar veren modelin gelecek senaryoları için kullanılabileceği anlaşılmıştır.

Bu aşamadan sonra, Avrupa Çevre Ajansı'ndan elde edilen 1990, 2000 ve 2012 CORINE arazi kullanım haritaları, Ergene havzasının geleceğe yönelik arazi kullanım tahmini için kullanılmıştır. Ayrıca şehir merkezine, ana yollara, nehirlere uzaklık gibi etki haritaları kullanılarak CA_MARKOV analizi ile potansiyel arazi kullanım değişim haritası oluşturulmuş; 2030 ve 2050 yılları için arazi kullanım haritaları tahmin edilmiştir.

İklim değişikliğinin etkilerinin incelenebilmesi için Meteoroloji Genel Müdürlüğü tarafından kullanılan RCP 4.5 ve RCP 8.5 iklim senaryoları ile gelecekteki yağış ve sıcaklık değerleri Ergene havzası için ortaya konulmuştur.

Elde edilen gelecek arazi kullanımı ve iklim verileri doğrulanmış ArcSWAT modeline girilerek havzanın gelecekteki akış ve besin tahmini farklı senaryolara göre hesaplanmış ve karşılaştırılmıştır.

Ayrıca, Mann-Kendal, Rho-Spearman istatistiki testleri kullanılarak geçmiş verilerden geleceğe yönelik çıkarımlar yapılmış, ARIMA modeli ile de geleceğe yönelik eğilim ortaya konmuştur. Toplam azot ve fosfor değerleri ArcSWAT modeli çıktıları ile kıyaslanmıştır.

Sonuç olarak bölgenin su akış miktarı ve kalitesi bakımından mevcut ve gelecekteki durumu hakkında arazi kullanımı ve iklim etkileri de göze alınarak tespitler yapılmıştır. Söz konusu çalışma Türkiye'de gelecekteki arazi kullanımı ve iklim verilerini dikkate alan ve buna bağlı olarak geleceğe yönelik akış ve kirlilik tahmini yapan ender araştırmalardan biridir.

# TABLE OF CONTENTS

ACKNOWLEDGEMENTS ..... iii
ABSTRACT ..... iv
ÖZET ..... vi
TABLE OF CONTENTS ..... viii
LIST OF FIGURES ..... x
LIST OF TABLES ..... xv
LIST OF ACRONYMS / ABBREVATIONS ..... xvii
1. INTRODUCTION ..... 1
1.1. Subject Matter of Hydrology ..... 3
1.2. History of Hydrology and Modeling ..... 6
1.3. Hydrological Models ..... 9
1.4. The Soil and Water Assessment Tool Model ..... 11
1.5. Other Supporting Tools ..... 14
1.5.1. Land Use and Cover Change ..... 15
1.5.2. Land Use and Cover Change Models ..... 18
1.5.3. Climate Modelling ..... 21
2. LITERATURE REVIEW ..... 26
3. MATERIAL AND METHODS ..... 29
3.1. Materials ..... 29
3.1.1. Study Area: Ergene Basin ..... 29
3.1.2. Climate ..... 30
3.1.3. Landuse ..... 33
3.1.4. Geological Structure ..... 36
3.1.5. Hydrogeology ..... 37
3.1.6. Population ..... 38
3.1.7. Agriculture and Livestock ..... 39
3.1.8. Industry ..... 41
3.2. Methods ..... 42
3.2.1. Ergene SWAT Model ..... 42
3.2.2. Data Input ..... 43

3.2.3. Calibration & Validation ..... 54
3.2.4. Water Quality ..... 55
4. MODEL RESULTS ..... 60
4.1. Calibration of Model ..... 60
4.2. Validation of Model ..... 67
4.3. Nutrient Loads ..... 69
4.4. Water Budget ..... 71
4.5. Land Use Estimation ..... 73
4.5.1. Driving Force Analysis of LUCC in Ergene Basin ..... 76
4.5.2. Future Land Estimation ..... 78
4.6. Weather Scenarios and Effect of Climate Change ..... 85
4.7. Future Hydrology and Nutrient Estimation with SWAT ..... 89
4.8. Nutrient Load Estimation with Statistical Tests ..... 93
4.8.1. Mann & Kendall Test ..... 93
4.8.2. Spearman's Rho Test ..... 94
4.8.3. Time Series Models and ARIMA Model ..... 95
4.8.4. Application of Statistical Tests and ARIMA Model on Ergene Basin ..... 97
5. RESULTS AND DISCUSSIONS ..... 111
REFERENCES ..... 117
APPENDIX A: CLIMATE SCENARIOS ..... 125
APPENDIX B: 2006 AND 2012 CORINE MAPS ..... 128
APPENDIX C: MATLAB CODE OF MOVING AVERAGE TEST ..... 129
APPENDIX D: MATLAB CODE OF ARIMA TEST ..... 130

# LIST OF FIGURES


Figure 1.1. Illustration Hydrological Cycle ..... 3

Figure 1.2. An Engineering View of the Hydrologic Cycle ..... 4

Figure 1.3. Hydrological System Concept. ..... 5

Figure 1.4. The Steps of Data Input of SWAT Model. ..... 13

Figure 1.5. CORINE Land Cover Classes. ..... 16

Figure 1.6. A Flow Chart of IDRISI Modeling Process. ..... 19

Figure 1.7. Steps for Climate Modelling. ..... 21

Figure 1.8. Climate Model Projections. ..... 22

Figure 1.9. Temperature and Precipitation Forecasting According to RCP Scenarios. ..... 24

Figure 3.1. Study Area – Ergene Basin Map. ..... 29

Figure 3.2. Average Temperature and Precipitation Data of Meteorological Stations in Ergene Basin between 2013-2018. ..... 30

Figure 3.3. Temperature Distribution for Winter Season and Summer Season for Ergene Basin. ..... 31

Figure 3.4. Monthly Average Precipitation , Average Temperature for all Meteorological Stations in Ergene Basin Between 2013-2018 years .. 32

Figure 3.5. The Land Use Classes. ..... 33

Figure 3.6. The Land use Classes of Ergene Basin According to CORINE Codes. ..... 34

Figure 3.7. The Land Use Data Change Analysis Steps. ..... 35

Figure 3.8. Geological Map of Ergene Basin. ..... 36

Figure 3.9. Hydrogeological Map of Ergene Basin. ..... 37

Figure 3.10. ArcSWAT Model Data Input Needs ..... 42

Figure 3.11. ArcSWAT DEM Model ..... 44

Figure 3.12. ArcSWAT Water Delination Model ..... 44

Figure 3.13. Ergene Model Subbasin ..... 45

Figure 3.14. CORINE Classification Versus ArcSWAT Landuse After Reclassification. ..... 47

Figure 3.15. Soil Map According to Scale National Soil Database. ..... 49

Figure 3.16. ArcSWAT Soil Map After Reclassification. ..... 50

Figure 3.17. ArcSWAT Slope Map After Reclassification. ..... 50

Figure 3.18. ArcSWAT Slope Map after Reclassification. ..... 51

Figure 3.19. Meteorological Stations used in Model ..... 53

Figure 3.20. 2003-2011 years Hydrological Observation Stations Flow Data. ..... 54

Figure 3.21. Hydrological Stations Used in Model ..... 55

Figure 3.22. ArcSWAT Point Load Map. ..... 56

Figure 4.1. Sensitivity Analysis of Parameters for Calibration. ..... 63

Figure 4.2. Model & Observation Flow Data Comparison for Hayrabolu Stream 65

Figure 4.3. Model & Observation Flow Data Comparison for İnanlı Stream. ..... 66

Figure 4.4. Model and Observed data Comparison According to Months and Determination Coefficient of Hayrabolu Stream. ..... 67

Figure 4.5. Model and Observed data Comparison According to Months and Determination Coefficient of Hayrabolu Stream. ..... 68

Figure 4.6. TN, $R^2$ of Model for İnanlı Stream. ..... 70

Figure 4.7. TP, $R^2$ of Model for İnanlı Stream. ..... 70

Figure 4.8. Hydrological Cycle of Model..... 71

Figure 4.9. CORINE Land Cover Legend for 1990 of Ergene Basin. ..... 73

Figure 4.10. CORINE Land Cover Legend for 2000 and 2012 of Ergene Basin..... 74

Figure 4.11. Driving Factors Map of Ergene Basin. ..... 77

Figure 4.12. Projected 2012 Map & Projected Potential for Transition..... 79

Figure 4.13. Projected 2012 Lands Use Map vs Observed 2012 Land Use Map..... 80

Figure 4.14. Projected Lands Use Map & Potential for Transition for 2030. ..... 81

Figure 4.15. Projected Lands Use Map & Potential for Transition for 2050. ..... 82

Figure 4.16. Comparison of Projected 2030 and 2050 Land Use Maps..... 83

Figure 4.17. CORINE 1990,2000, 2012 Land Use Maps and Constructed 2012, 2030, 2050 Land Use Maps. ..... 84

Figure 4.18. Precipitation vs Time Graph of Lüleburgaz Station. ..... 85

Figure 4.19. Tmin & Tmax vs Time Graph of Lüleburgaz station. ..... 86

Figure 4.20. Ergene Precipitation Trend vs RCP 4.5 and 8.5 Trend..... 87

Figure 4.21. Temperature Forecast 2013-2100 RCP 4.5..... 88

Figure 4.22. Comparison of Average Annual Flow According to Scenarios..... 89

Figure 4.23. Comparison of Average Monthly Flow According to Scenarios..... 90

Figure 4.24. Difference Map of Current Flow with Estimated Flow Scenarios..... 90

Figure 4.25. Comparison of Annual TN Concentration According to Scenarios..... 91

Figure 4.26. Comparison of Monthly TN Concentration According to Scenarios... 91

Figure 4.27. Comparison of Annual TP Concentration According to Scenarios. .... 92

Figure 4.28. Comparison of Monthly TP Concentration According to Scenarios . . 92

Figure 4.29. MK and SR Moving average concentration and ARIMA results for o-$PO_4$ İnanlı and İpsala stations ..... 98

Figure 4.30. MK and SR Moving average concentration and ARIMA Results for o-PO4 Lüleburgaz and Uzunköprü stations ..... 99
Figure 4.31. o-$PO_4$ concentration distribution of stations according to years ARIMA ..... 100
Figure 4.32. MK and SR Moving average concentration and ARIMA results for $NH_4$ İnanlı and İpsala stations ..... 101
Figure 4.33. MK and SR Moving average concentration and ARIMA results for NH4 Lüleburgaz and Uzunköprü stations ..... 102
Figure 4.34. $NH_4$ concentration distribution of stations according to years for ARIMA ..... 103
Figure 4.35. MK and SR Moving average concentration and ARIMA results for Al İnanlı and İpsala stations ..... 104
Figure 4.36. MK and SR Moving average concentration and ARIMA results for Al Lüleburgaz and Uzunköprü stations ..... 105
Figure 4.37. Al concentration distribution of stations according to ARIMA ..... 106
Figure 4.38. MK and SR Moving average concentration and ARIMA results for Cl İnanlı and İpsala stations ..... 107
Figure 4.39. MK and SR Moving average concentration and ARIMA results for Cl Lüleburgaz and Uzunköprü stations ..... 108
Figure 4.40. Cl concentration distribution of stations according to ARIMA ..... 109
Figure A.1 Precipitation Forecast 2018-2100 RCP 4.5. ..... 125
Figure A.2. Temperature Forecast 2013-2100 RCP 8.5. ..... 126
Figure A.3 Precipitation Forecast 2013-2100 RCP 8.5. ..... 127
Figure B.1. CORINE 2006 and 2012 Map Comparison. ..... 128

Figure C.1. MATLAB Code of Moving Average Test. ..... 129

Figure D.1. MATLAB Code of ARIMA Test ..... 130

# LIST OF TABLES


Table 1.1. Model Features Comparison. ..... 20

Table 3.1. 2006 vs 2012 CORINE Area Classification of Ergene Basin. ..... 36

Table 3.2. Population Distribution of Ergene Basin ..... 38

Table 3.3. Agricultural Areas of Ergene Basin. ..... 40

Table 3.4. Organized Industrial Zones of Ergene Basin. ..... 41

Table 3.5. Summary of Input Data. ..... 43

Table 3.6. ArcSWAT Generic Land Cover Codes ..... 46

Table 3.7. Ergene Watershed according to ArcSWAT Generic Land Cover Classification ..... 46

Table 3.8. 1/25 000 Scale National Soil Database. ..... 48

Table 3.9. SWAT HRU Options ..... 52

Table 3.10. Information about Meteorological Stations. ..... 52

Table 3.11. Ergene Meteorological Station Data Availability. ..... 53

Table 3.12. Ergene Basin Domestic Loads. ..... 56

Table 3.13. Ergene Basin Industrial Loads. ..... 58

Table 3.14. Ergene Total Loads for Sub-basins ..... 59

Table 4.1. Calibration Parameters Used in Studies. ..... 62

Table 4.2. Parameter Calibration Results of Study. ..... 64

Table 4.3. Statistical Performance Indicators for Calibration and Validation of Streams ..... 69

Table 4.4. Water Table of Ergene Basin Comparison Model, Before and After 2000 Year ..... 72

Table 4.5. Corine Land Cover Legend for Ergene Basin in Arcmap for 1990-2000-2012. ..... 75

Table 4.6. Land Use in the Ergene Basin for the 1990-2000-2012 Years. ..... 76

Table 4.7. Land Use Transition Matrix of 2000 to 2012..... 78

Table 4.8. CORINE 2012 & Generated 2012 Maps Area Comparison. ..... 80

Table 4.9. Land Use Transition Matrix of 2012 to 2030..... 81

Table 4.10. Land Use Transition Matrix of 2012 to 2050..... 82

Table 4.11. Comparison of Constructed Maps..... 83

Table 4.12. RCP 4.5 and 8.5 Temperature and Precipitation Change Scenarios for Ergene Basin for 100 years..... 86

Table 4.13. MK and SR test Results for o-$PO_4$..... 100

Table 4.14. MK and SR test results for $NH_4$..... 103

Table 4.15. MK and SR test results for Al..... 106

Table 4.16. MK and SR test results for Cl..... 108

# LIST OF ACRONYMS / ABBREVATIONS

| | |
|---|---|
| AGNPS | Agricultural Nonpoint Source |
| ANN | Artificial Neural Network |
| AOGCM | Atmosphere–Ocean General Circulation Model |
| AR | Autoregressive |
| ARIMA | Autoregressive Integrated Moving Average |
| BASINS | Better Assessment Science Integrating Point and Nonpoint Sources |
| CORINE | Coordination of Information on the Environment |
| CA | Cellular Automata |
| CLC | CORINE Land Cover Model |
| CLUE | Conservation of Land Use |
| DEM | Digital Elevation Model |
| EBM | Energy Balance Model |
| EEA | European Environmental Agency |
| EMIC | Earth System Model of Intermediate Complexity |
| EPA | U.S. Environment Agency |
| ESM | Earth System Model |
| ESP | Earth System Physics |
| FAO | Food and Agriculture Organization of the United Nations |
| GDM | General Directorate of Meteorology |
| GHG | Greenhouse Gases |
| GIS | Geographic Information Systems |
| GWLF | Generalized Watershed Loading Function Model |
| HEC | U.S. Army Corps of Engineers Hydrologic Engineering Centers |
| HRU | Hydrological Response Units |
| HSPF | Hydrologic Simulation Program-Fortran |
| IPCC | Intergovernmental Panel on Climate Change |

| | |
|---|---|
| LCM | Land Change Model |
| LUCC | Land Use/Cover Change |
| LULC | Land Use / Land Cover |
| MA | Moving Average |
| MoD | Ministry of Development |
| MoEF | Ministry of Environment and Forestry |
| MoEU | Ministry of Environment and Urbanization |
| MoFWA | Ministry of Forestry and Water Affairs |
| MoAF | Ministry of Agriculture and Forestry |
| MCA | Markov Chain Analysis |
| MK | Mann-Kendall |
| MUSLE | Modified Universal Soil Loss Equation |
| NCAR | Center for Atmospheric Research |
| NSE | Nash Sutcliffe Model Efficiency |
| RCM | Regional Climate Model (or RegCM) |
| RCP | Representative Concentration Pathway |
| RS | Remote Sensing |
| SHW | State Hydraulic Works |
| SR | Spearman’s Rho |
| SWAT | Soil and Water Assessment Tool |
| SWMM | Storm Water Management Model |
| TN | Total Nitrogen |
| TP | Total Phosphorus |
| TURKSTAT | Turkish Statistical Institution |
| US | United States |
| USDA | The United States Department of Agriculture |
| USGS | The United States Geological Survey |
| WMS | Watershed Modeling System |

# 1. INTRODUCTION

Water resources are irreplaceable for mankind's quality of life. Within this scope, studies are carried on all over the world on management of water resources. After the industrial revolution, human habitat has shifted from rural to urban life. If past trends are examined, urbanization has increased in worldwide, and the trend seems to continue in the same way. As a result of this situation, the pressure on the environment has increased. Changing environmental factors can lead to change in the land use and even the climate. Especially urbanization cause pollution of underground and surface water resources, increase of the flood risk and decrease of groundwater level. The number of unexpected changes in climate is increasing and there is non-stationarity in climate and water related events (Milly *et al*., 2008). Regions, that have adequate water sources currently, may not have it in the upcoming years. In addition to these changes, the impact of land use/land cover change on water sources will be inevitable. The influences of land use and climate change on water resources and the adaptation strategies are developed on a global scale in the Assessment Reports of the Intergovernmental Panel on Climate Change (IPCC 3rd, 4th and 5th Reports) (IPCC 2001, 2007, 2013).

The urbanization is not much different from the world in Turkey. The cities, which are defined as metropolitan cities, have expanded with unplanned growth due to excessive population growth. The concept of urbanization in Turkey also comes to mind considering the biggest city in Turkey, Istanbul province. However, the pressure created by Istanbul actually affects the neighboring provinces of Edirne, Kırklareli and mostly Tekirdağ. These three cities are located in Ergene Basin which has importance for the Marmara region and Turkey in terms of both industry and agriculture. Due to importance of region for Turkey, Ergene basin was the focus of this study. Also, after 2008 the pollution in the region attracted the attention of decision-makers and since 2011, investments have applied to protect the region such as domestic wastewater treatment plants, organized industrial zone water treatment facilities and deep sea discharge. The approximate cost of government investments is around 2 billion Turkish Liras (MoD, 2012).

The most important problem in the region is the increasing irregular urbanization and the pressure created by this urbanization in agricultural areas, forest areas and water resources (Kocaman *et al.*, 2011). 30 years ago, Ergene River's water quality was sufficient for use of drinking and agricultural irrigation but the rapid development of basin's provinces in the few past decades has resulted in growing pressure on the local environment (Hallı *et al*., 2014). It has been estimated that if water pollution in the region continues at this rate, problems that will be encountered 25-30 years later will be unrecoverable (Akın *et al*., 2007). Besides, it is estimated that climate change and land use change has potential effects on environment. Therefore, this study aims to examine the integrated effects of climate variability and land use change for water resource management of Ergene basin.

First part of this study is related about fundamental principles of hydrology and modeling.

The second section of this study is composed of literature review which are related with land use, climate change, hydrological modeling and researches about Ergene region.

Region characteristics such as climate, land use, geological structure etc. were defined in section three. And also hydrological, land use and climate change models which were used in this study introduced in this section.

In the fourth section of this study, ArcSWAT model was used for modelling Ergene basin in terms of hydrology and water quality for the years 2003-2010. Flow data of the İnanlı and Hayrabolu streams for 2003-2004 years are used for warm period of the model. And the data of 2005-2007 years are used for calibration period of the model. 2008-2010 years' data were used for validation of the model. In the end, high $R^2$ and NSE values were obtained from model. Also, total nitrogen and phosphorus outputs are obtained from the model and compared with İnanlı stream water quality observations. Then, land use change predictions are created by using 1990, 2000 and 2012 year Coordination of Information on the Environment (CORINE) project maps. IDRISI program constructed 2030 and 2050 year land use maps by using differences in CORINE maps of the region. After that, by using RCP 4.5 and RCP 8.5 climate scenarios, the basin was examined for the effects of climate

change. Precipitation and temperature values were generated by the help of down scaled climate scenario. Finally, the future land use and climate data were used as input for the validated ArcSWAT model and the basin's estimated reaction according to future land use and climate scenarios were calculated. In addition, in order to verify the ArcSWAT model outputs, the statistical analysis namely Man-Kendall, Spear man-Rho are applied for water quality station. Estimated future trends are also compared with ARIMA model.

To sum up, ArcSWAT gave satisfactory results in modeling of Ergene basin in terms of flow and water quality. Furthermore, in the creation of future-oriented scenarios IDRISI (land use change model) and climate change models made a significant contribution by providing realistic estimates. Also statistical tests played an effective role in predicting values unpredictable by ArcSWAT. These results showed that climate and land use change would have impact on Ergene basin. Besides, this study concluded that the basin will be under attack by a considerable amount of pollutants (TP, TN, $Cl^-$) which creates some risks for the environment as well as the human's life.

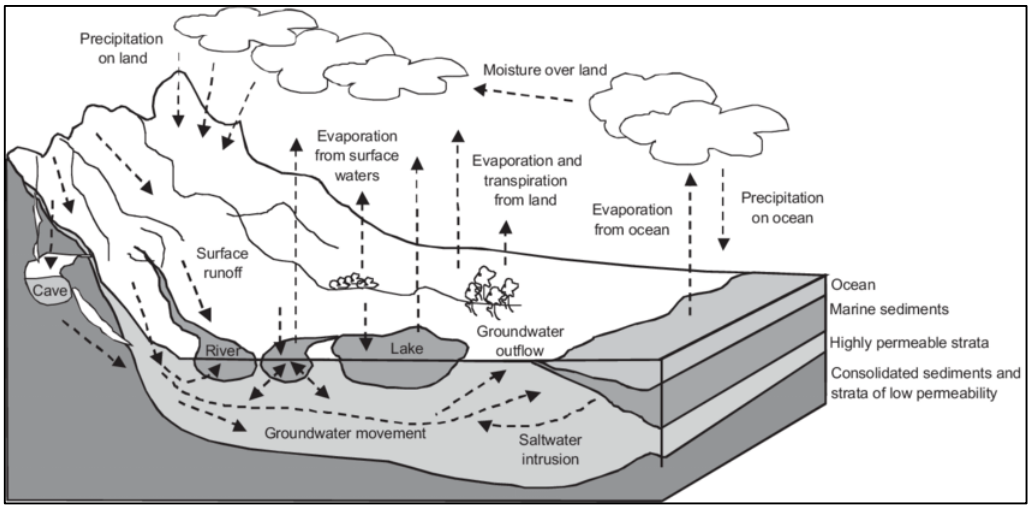


Figure 1.1. Illustration Hydrological Cycle (Danielopol *et al.*, 2003).

## 1.1. Subject Matter of Hydrology

Hydrological cycle is the most important phenomenon used in watershed management. It can be defined as the movement of water in a cyclic manner, proceeding from the sea to the atmosphere by evaporation, and then precipitation to earth, where water

runs back to the sea through either streams or groundwater flow. Figure 1.1 depicted the cyclic movement which is used in all hydrological calculations in an illustrative way.

Real events in the hydrological cycle are simplified for easy implementation from an engineering point of view. Eagleson (1970) demonstrated the cycle as shown in Figure 1.2. Actual events happening in nature is of course far more complex than this simple illustration.

Precipitation, stream flow, evaporation and infiltration are the most important elements of the hydrological cycle. Hydrologists and engineers are concerned with the part of the cycle that takes place on Earth. Normal conditions and values associated with hydrological cycle are not in the scope of engineers, but extreme values are important for them. To satisfy human needs, hydraulic structures must be designed considering the extreme values of droughts, floods, or to overcome the misdistribution of water over geographic locations and time, and so on.

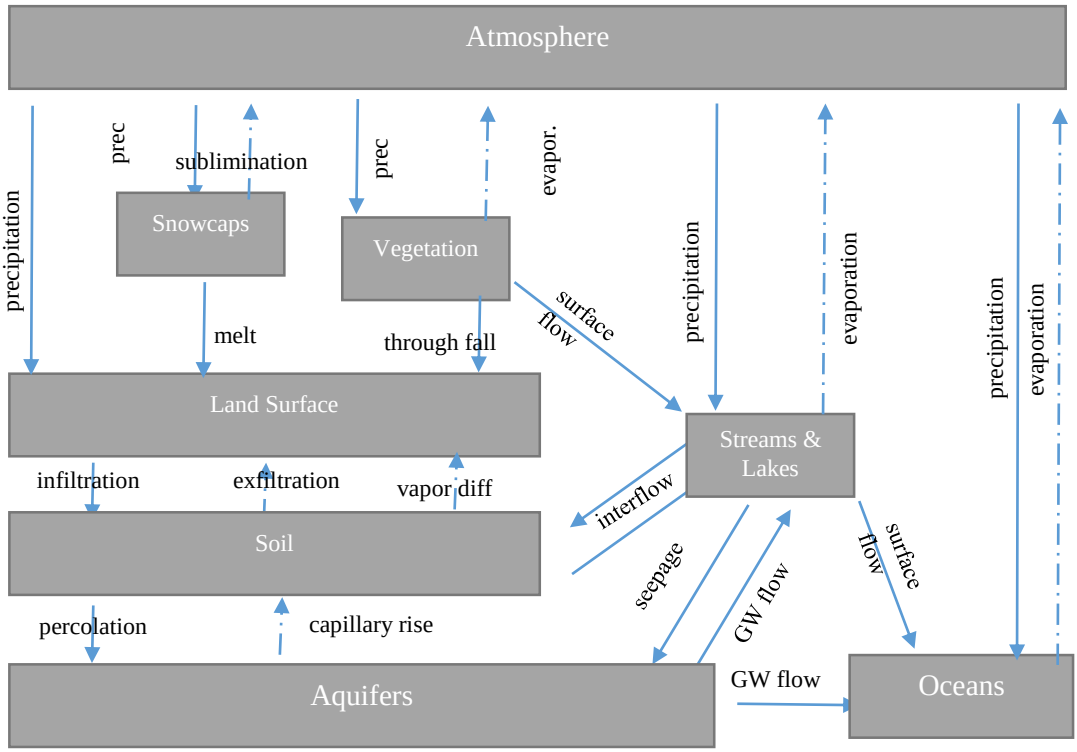


Figure 1.2. An Engineering View of the Hydrologic Cycle (Eagleson, 1970).

It is not easy to apply the well-known equations of mass, state and momentum in hydrology. Due to the fact that the systems are heterogeneous and anisotropic, many complications arise. These complications include: existence of unknown parameters, uncertain values of parameters, complexity of the determination of parameters varying according to time and space, the unknown physical behavior of the system, etc. Because of these complications of the system approach, approximate and statistical methods are used for solving problems in hydrology.

A system can be defined as a set of connected parts that form a whole. Components of hydrological cycle, such as precipitation, evaporation, runoff, etc. can be treated as the elements forming a system. These components should be studied together to analyze the united system, or they can be divided into clusters of small groups like subsystems. The interactions between subsystems and the system itself should be analyzed and the results should be combined. A hydrological system can be defined as a constraint structure or volume in space. The system includes water and other inputs like air, heat, energy, etc. The system operates on these elements internally, and as output different quantity and quality of input items arise. As an example, if a basin is considered as the system, rainfall and runoff will be the input and output respectively.

Figure 1.3. Hydrological System Concept.

The actual system is simplified by approximations to form a hydrologic system with inputs and outputs being the hydrologic variables. Transformation equations are used to link inputs and outputs in order to express the system. (Equation 1.1)

$$Q(t) = \phi . I(t) \tag{1.1}$$

Where $I(t)$ is the input, $Q(t)$ is the output, and $\phi$ is the system transfer function, as shown in Figure 1.3.

The wide range of time and space scales can be used to investigate the hydrologic systems. For example, transpiration from a certain crop may be considered as a micro scale problem, or studying rainfall-runoff relationship of a basin can be considered as a meso-scale, whereas continental water budget study is an example of a macro scale problem.

The inflow and outflow of a reservoir can be formulated with a transfer equation as follows (Equation 1.2).

$$\frac{dS}{dt} = I(t) - Q(t) \tag{1.2}$$

Where $I(t)$ is the inflow, $Q(t)$ is the outflow, and $dS/dt$ is the change in storage. The inputs of a reservoir may be precipitation (P), surface flow (SF), subsurface flow (I) and base flow (GWF), the outputs may be evaporation (E), seepage (S) and the water taken from reservoir (W). The equation will become:

$$\Delta S = P + SF + I + GWF - S - W - E \tag{1.3}$$

## 1.2. History of Hydrology and Modeling

Water has always been one of the most important matter for humankind, the calculation for hydrology started from ancient civilizations of the world. The irrigation systems built in Mesopotamia are considered as the oldest water works known in the world. Elevated gardens of Babylonians involved a solution to a difficult and complex problem encountered by people living in Mesopotamia in those days, the flood problem. Hammurabi, the king of Babylon, is known to institute the first legislative law about water. Similarly, in countries such as China, India, and Egypt hydraulic measurements were also made to overcome a flood problem (Biswas, 1970).

Hydrology was firstly defined as a science by Pierre Perrault, Edme Mariotte and Edmund Halley. Perrault measured rainfall and evaporation in the Seine basin, and Mariotte tried to measure the flow in the Seine River. Halley confirmed that the source of moisture, precipitation is the adequacy of oceanic evaporation. He demonstrated the equality between the amount of evaporation from Mediterranean and the amount of water in the rivers, which flow back to Mediterranean. These three scientists did their researches in a modern scientific manner, thus they may be accepted as the founders of the science of hydrology (Usul, 2005).

Bernoulli, Cassini, Chezy, Pitot, Ramazinni, and Ventury are known to be the important scientists of the 18$^{th}$ century. At the beginning of the 20$^{th}$ century, quantitative hydrology was not developed much, to solve practical hydrological problems, empirical approaches were being used. 1900-1930 period can be considered as Period of Empiricism, and 1930-1950 as Period of Rationalization. Horton, Mead and Sherman were the important representatives of rationalization period of science of hydrology.

The aim of all of these researchers was to create mathematical solutions namely mathematical models for hydrological problems. Mathematical modelling can be defined as an interpretation of real-life circumstances and relations by using mathematics in it (Haines *et al*., 2007). Another definition of mathematical models is translation of real-life problems into mathematical language, solving within a symbolic system, and the solutions tested back within the real-life system (Verschaffel *et al*., 2002). In both definitions mathematical modelling is stated as a method of simulating real-life situations with mathematical equations to forecast future behavior. The best model can be defined as the model that gives realistic results using least parameters.

Hydrological models are classified into different groups according to their operating procedure. Their concepts are not so much different from each other. Despite there are lots of classifications, one of the most known classifications is empirical, conceptual and physically based models (Jajarmizadeh *et al*., 2012).

Empirical Models are derived from the results of statistical analysis of a large number of trials. The properties and processes of hydrological system have no influence on model

data. Therefore these models are also called experimental or data driven models. Simultaneous input and output time series are main sources of mathematical equations and the physical processes of the catchment have no direct effect on these equations. These models are only valid within the defined boundaries. Unit hydrograph is an example of this method. Statistical methods namely regression and correlation models are used for the functional relationship between inputs and outputs. Artificial neural network (ANN) and fuzzy regression are two example techniques that are widely used in hydro informatics methods.

Conceptual models identifies all components of hydrological processes. Physical elements are represented by a number of interconnected reservoirs which are recharged by rainfall, infiltration and percolation and their potentials are reduced by evaporation, runoff, drainage etc. These model types use semi empirical equations. They use both field data and statistical data. The calibration procedure requires large data set of meteorological and hydrological records. In this model type the effect of land use change cannot be predicted with great accuracy. Interpreting land use is difficult due to the curve fitting operation used in calibration process.

In physically based models real phenomenon is represented in a mathematically idealized way. These models are also called mechanistic models which use principals of physical processes. Mechanistic models use state variables which are measurable and functions of both space and time. Finite difference equations are used to represent the hydrological processes of water movement. Huge number of parameters are required for describing physical characteristics of study area. But, calibration does not require extensive hydrological and meteorological data. Large amount of data such as soil properties (moisture content, hydraulic conductivity), land use types, topography, dimensions of basin, river network etc. are required in this method. By using large amount of parameters model can interpret lots of information and thus many shortcomings of the two previous models can be overcome by this model (Devi, 2015).

Technological development in recent years deeply changed the concept of hydrology, and made hydrologic analysis possible in larger scale. Iterations take a big part in estimating

most of the hydrological equations that are generally based on complex mathematical equations. Application of mathematical models become much wider in science of hydrology related with advances in computer capacity. Special purpose application software called as “hydrological models” developed to solve certain hydrologic problems. Nowadays, even personal computers have enough capacity and speed that is adequate for hydrological calculations.

### 1.3. Hydrological Models

By the help of digital computers in 1950s and 1960s, precipitation run-off simulations as a hydrologic model was created. The purpose of the model is to estimate stream flow using observed weather conditions. First known hydrologic model which is named as Stanford Watershed Model stimulates hydrological cycle elements including precipitation, evaporation, infiltration surface flow and groundwater flow (Donigian, 2006).

Later a series of hydrological models was coded by U.S. Army Corps of Engineers Hydrologic Engineering Centers (HEC). Among these, in 1973, “HEC-1” model was developed for simulating flood scenarios, and to compute water surface profile for a given river geometry HEC-2 was developed in 1976. Another most widely used model, Storm Water Management Model (SWMM) is developed by Crawford and Linsley which is known as the first major conceptual model in 1966. It has taken into consideration 16 to 20 parameters of hydrology. SWMM (now HSPF) was developed by U.S. Environment Protection Agency (EPA) to determine hydrographs and estimate sewage loads.

EPA has a special importance for modelers, due to their state-of-art models which are so crucial for hydrological processes. EPA developed Better Assessment Science Integrating Point and Nonpoint Sources (BASINS) model in 1994. BASINS has enough tools to perform watershed and water quality analysis. Before BASINS, environmental databases, models, tools were running individually. It integrated all of them with preprocessing and post processing utilities. In other words, it combined tools and data into a solo modeling set. The core watershed model used in BASINS is the HSPF. The most important properties of HSPF and the USGS softwares was integrated and enhanced in

BASINS since 1994. HSPF has also been incorporated into the U.S. Army Corps of Engineer's Watershed Modeling System (WMS), for the purpose of making availability for the use of joint tools and approaches by federal organizations, besides other modeling authorities.

HSPF is a bulk watershed model which simulates runoff and point source contributions by integrating with hydrologic and water quality processes in reaches (Bicknell *et al*, 1996). Like other physical based models, HSPF needs large amount of site data to accurately modeling hydrology and water quality of a watershed. It should be noted that it is also extremely data intensive and over-parameterized model.

EPA has nearly 20 popular surface water models that are distributed free of charge. These models are: AQUATOX, BASINS, DFLOW, HSPF, QUAL2K, RUSLE2, SERAFM, SWMM, WASP, WHATIF, and WMOST.

Watershed Modeling System is developed in 1998 in Brigham Young University to perform all functions of HEC-1. This software gives hydrologic analysis of basins. Danish Hydraulic Institute developed MIKE series, which is an example of physical based model, to make the modeling of the basin or river network and give hydrologic solutions.

Geographic Information Systems (GIS), and Remote Sensing (RS) technologies become applicable for hydrologic models in late 1990's. To make it compatible with GIS and RS technologies, most of the models listed above were updated. To exemplify MIKE-GIS is an interface software that uses MIKE's mathematical model.

Hydrological models have a great influence on the development of other models. Especially number of water quality models have increased due to developments in hydrological models. Water quality, erosion and flow models are based on hydrological models. The integrated management of the basin idea arose from the requirement of combining these separate models. The need for integrated watershed management also ensured the emergence of basin/watershed models.

SWAT as a widely used, physically based hydrological model developed in cooperation with the USDA-ARS and the Texas A & M University. Model is used in the calculation of the possible effects of climate change, land use and evaluation of best management practices for water budget and water quality modeling. (Arnold *et al*., 1995). This model is re-altered for ArcGIS software to be applicable ArcMap software. The model's new name become ArcSWAT. It is also compatible with GIS based other software which make the model stronger. In this study ArcSWAT program was used to model watershed.

Watershed model is a good tool to figure out relationship between land use activities, water hydrology and quality process happening within a watershed. Point source loads like nutrients (total phosphorus, total nitrogen, etc.), flow and sediment loads from watersheds can be simulated continuously by several models. AGNPS, GWLF, MIKESHE, WATFLOOD, HECHMS, HEC 2000, SWRRB and SWAT are most important and widely used models. Strengths and limitations vary from model to model. Flow, sediment transport, erosion and nutrient transport can be modelled in most of the physically-based distributed basin models. They can also calculate temporal and spatial hydrological processes, change land use / land cover and determine how climate change affects this mechanism. HSPF and SWAT models are the most popular ones among others.

### 1.4. The Soil and Water Assessment Tool Model

The Soil and Water Assessment Tool (SWAT) is one of the most widely used for water quality and hydrology modeling of watersheds. It was developed for exploring the effects of land management practices on water and pollution loadings on a daily basis. Simulation of different physical processes like percolation, evapotranspiration, lateral subsurface flow, return flow, groundwater flow, surface runoff, ponds and channel routing in basin can be provided by SWAT model. "Channel Hydrology" and "Land Hydrology" are two important subdivisions of SWAT simulations, where first one is used for stream and reservoir water quantity and quality and second one for chemical substances and pollutant loadings to water sources (Ertürk *et al*., 2014). For this study, the first component of SWAT is the most important part of the model.

As mentioned in last chapter, hydrological model is based on the water-balance equation (Equation 1.4) in the soil profile, with terms representing processes of surface runoff, infiltration, precipitation, evapotranspiration, percolation, lateral flow and groundwater flow (Neitsch *et al*., 2011). In this study, only the basic equilibrium formula has been given. Equations used by SWAT model are not given in detail, they can be found in the SWAT manual.

$$SW_t = SW + \sum_{i=1}^{t}(R_i - Q_i + ET_i - P_i - QR_i) \tag{1.4}$$

$SW$ : Soil water content
$i$ : Time in days for the simulation period t
$R_i$ : Daily precipitation
$Q_i$ : Runoff
$ET_i$ : Evapotranspiration
$P_i$ : Percolation
$QR_i$ : Return flow

For calculation of surface runoff, SWAT use two distinct approaches: the SCS curve number procedure, which considers only the rainfall volume and does not cover rainfall intensity and duration, and the Green & Ampt infiltration method which simulates not only impacts of precipitation intensity and period but also the infiltration processes. Green & Ampt method requires sub-daily precipitation data. The kinematic storage model for the sub-surface flow is used by the model. Simulation of groundwater flow with empirical equations can be provided by SWAT (Neitsch *et al*., 2011).

To estimate evapotranspiration Priestly-Taylor, Hargreaves, and Penman-Monteith methods are used by SWAT. The amount of required input data varies among the methods. These models take into account plant growth component of plant. Temperature, water, nitrogen or phosphorus stress are input data for plant growth (Abdelwahab *et al*., 2018).

Basin concentration time is calculated using Manning's formula by summing overland flow time and channel flow time (Xu *et al*., 2009).

Modified Universal Soil Loss Equation (MUSLE) calculates total eroded sediment by utilizing the surface runoff volume, the peak runoff rate, the Universal Soil Loss Equation related other values.

While the model was established; basin's characteristic features such as meteorology, topography, soil classes, land use and cover types are used as input. As a result of the combinations of these inputs, drainage areas are divided into hydrological processing units, called HRU, according to their hydrological properties. Each sub basins are evaluated in terms of their own HRU values. Balance of water in HRU's at four type of storage volumes are considered. These are snow, soil profile, shallow aquifer, and deep aquifer. Flow, sediment yield, and nutrient loading are calculated by the model for each sub basin, and then they are moved through channel network by utilizing hydrologic routing method.

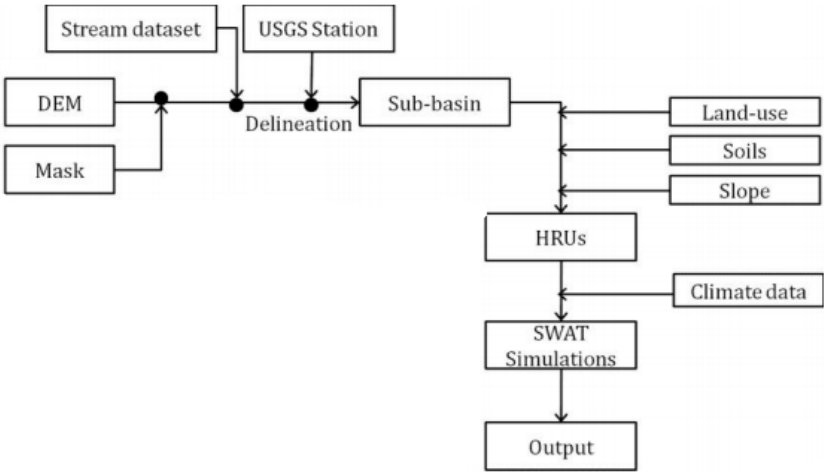


Figure 1.4. The Steps of Data Input of SWAT Model.

Despite SWAT uses FORTRAN database for calculations which is MS-DOS formatted, it has a well-designed user interface with ArcSWAT. In the SWAT model watershed data is defined by four modules. The first module is the Digital Elevation Model (DEM) module which delineate watershed and creates sub basins by using the data derived from the DEM. The second is the hydraulic response unit (HRU) tool, which integrates and overlay land use, soil and slope map data in order to characterize the HRUs. The third is the weather generator, which associates meteorological data like temperature, precipitation, radiation with watershed. And last module is input editor, which allows to create inputs such

as inlets, point sources, etc. and modify all the model parameters. Figure 1.4 summarized the steps of data input of SWAT model. All of these modules and data detailed under the "Ergene SWAT Model" heading.

SWAT has well prepared documentation which is essential for modeling basins. A helpful documentation and manual increase popularity of program among researchers. But main reason of popularity is the powerful aspects of SWAT which makes it much stronger against other hydrological models. SWAT is physically based model which makes it much stronger than empirical and conceptual models. Model can be integrated with GIS programs like ArcMAP, MapINFO. Model can use GIS inputs through its interface. Model allow users to limit basin area and also user defined basin can be integrated as input for model. Especially watershed delineation module is the most powerful tool of SWAT. Model can calculate stream direction and shape through the shape of DEM. SWAT's land use database classifications are compatible with European standards. For instance CORINE land use classification can easily be applicable to SWAT model. And also model has extensive crop growth model and databases which is an advantage for agricultural area cases. Also despite SWAT is a FORTRAN based model, huge watershed sizes can be studied via the HRU capability. To sum up, powerful aspects of SWAT are ability to predict climate and management impacts; water quality loadings and fate capabilities; provided flexibility in basin discretization and continuous time feature. Success of the model in a particular watershed is directly related with the quality of input data. Most of hydrological models need input parameters that cannot be obtained from field measurements. And therefore calibration is so crucial for these types of models to adjust such parameters for optimizing the simulated values with observed data. The original design objective of the SWAT model was to operate in large scale, ungagged basins with little or no calibration efforts.

## 1.5. Other Supporting Tools

For the good management of the water resources of the basin, basin has to be modeled with considering different aspects. In order to evaluate the hydrology of the basin in an accurate way, land use and climate should be examined in a realistic manner. A watershed model (like SWAT) gives results by combining climate and land use effects. Therefore land

use classification, models of Land Use / Cover Change (LUCC) and climate change are necessary tools for modeling basins current and future conditions.

### 1.5.1. Land Use and Cover Change

An area where living and non-living things, interact with environmental occasions is defined as the land. In terms of land's use and the covering layer characteristics the use of it can vary. Most of the people confuse land cover and land use terms. Land cover refers to physical elements, together with natural vegetation, covering the surface of the land (soil, water, vegetation etc.). On the other hand, land use implies that humanity benefits from land and this term covers land management practices like forestry, cities, industry areas, nature conservation areas etc. (Verburg *et al*., 2009).

In year 1985 European Commission took action for implication of the environmental information system. In first years of this project terminology and methodology of the system was defined. The system was named as Coordination of Information on the Environment (CORINE). At the Dobris Conference held in 1991, European Environment Ministers requested the implementation of this project within the framework of the European Union Aid Program in Central and Eastern European countries. CORINE databases were completed in 13 countries with this support. The basic idea was to create a standard database of all European land segments in the context of common evaluation criteria.

CORINE project serves four main purposes:

- Collecting information on the state of the environment according to the priority issues determined for all Member States of the European Union,
- Collecting data and harmonizing information within Member States or at international level,
- Ensuring the consistency of the information and the compatibility of the data,
- Generating "Land Use" maps according to the criteria of European Environment Agency.

In addition, with the CORINE project, it is ensured that the environmental information collected by various studies at different levels (International, Union, National and Regional) is monitored over the years.

Figure 1.5. CORINE Land Cover Classes (EEA, 2006).

CORINE project land use/cover classification is composed of three hierarchical levels determined by the European Environment Agency. First level of land use classification compose of five main groups as artificial surfaces, agricultural areas, forest and semi natural areas, wetlands and water bodies. Second level consist of 15 classes and 44 subclasses are

located under these classes (Figure 1.5). It is stated in the CORINE Technical Manual that additional national classes can be used at the third hierarchical level, but this should be added to the third level in terms of the integrity of the European data standard. Within the scope of CORINE Project, the scale is determined to be 1/100.000, a minimum cartographic unit that means the smallest area to be mapped, is 25 ha, geometric accuracy better than 100 m and working precision is 1/25.000.

CORINE land use maps are used for determining current environmental factors. Most of the hydrological models use CORINE data as a base map. Also land use maps allow users to forecast future land use trends. This study utilized 1990, 2000 and 2012 year CORINE maps for evaluation of current and future conditions of the basin.

It is known fact that land use maps enables to compare certain time land applications. As a result of environmental factors, Earth's movement in a certain equilibrium may be subject to partial changes. Nonetheless, the extent of human-driven changes is much more than that. Activities of people transform the natural land cover of the earth and the use of the land gradually. Land use causes land cover change. A place that transformed into settlements, trade and industry zones was a place covered with forest, agricultural land, and pastures 30-40 years ago. Change in natural environment is unavoidable due to the increase in consumption which caused by the increase in population and human needs. Changes in the LUCC not only affect biodiversity, climate change and global warming but also the vulnerability of people and places indirectly (Altürk, 2017; Verburg *et al*., 2009).

Rapid changes in land covers should be determined faster in order to develop a bunch of economic and ecological decisions, rational use of water resources and to take environmentally sensitive land-use decisions. In the past, it was hard to monitor the destruction of forestland, drying of wetlands, misuse of agricultural areas, coastline changes. In the last 20-30 years detection of LUCC is more cost-effective and more accurate thanks to satellite systems and also decision support mechanisms such as land use/cover change models are supportive tools for identifying and estimating environmental conditions (Altürk, 2017).

### 1.5.2. Land Use and Cover Change Models

Various aspects of global environmental change is crucial for LUCC that attracted scientists' and decision makers' attention. Lots of models were investigated to understand LUCC. Most of the land use models supports exploration of future scenarios to assist in land management over the last two decades (Veldkamp *et al*., 2001). LUCC models can be categorized in various ways, such as non-spatial, spatial, dynamic and static, etc.

There are many LUCC models accepted by researchers. Some of these models are IDRISI, DINAMICA, LCM, CLUE (or CLUE-s). Each model is a software with inputs and outputs at different resolutions, spatially different at international, national, regional and local scale. In each model, spatial changes for the future are shaped in line with scenario analyzes involving different economic, social and political decisions.

Models generally differ from each other by,

(i) the used algorithms for calibration of the model
(ii) the way simulating land cover changes
(iii) the methods for assessing land cover's model performance
(iv) adaptation of the user's demands

CLUE-s (Conversion of Land Use and its Effects) model has broad application to wide range of topics, including deforestation, tropical deforestation, urbanization, biofuel crops, agricultural intensification, farmland abandonment (Verburg *et al*., 2009).

Markov Chain Analysis (MCA) is a sum of the visible, stochastic modeling processes used for the forecast change model. The MCA calculates the probability of a cell being changed from one land use category to another within a given period of time. The possibility of change from one state to another is called the transition. MCA calculates transition matrices with the possibility of changing from one land category to another land category and the changes that may occur in cell numbers for each land use category from this matrix. An MCA transition matrix "P" is expressed as follows;

$$P = \begin{bmatrix} P_{11} & P_{12} & \dots\dots\dots\dots P_{1n} \\ P_{21} & P_{22} & \dots\dots\dots\dots P_{2n} \\ P_{n1} & P_{n2} & \dots\dots\dots\dots P_{nn} \end{bmatrix} \tag{1.5}$$

$$\sum_{j=1}^{n} P_{i,j} = 1$$

P : MCA transition matrix

Pi,j : Land cover type in the first and second period

Pij : Possibility of transition from land use type “i” to land use type “j”

DINAMICA Environment for Geoprocessing Objects as a land use dynamic models uses transition probability maps to study the processes of land-use modification. The maps that simulate landscape dynamics are based upon the genetic algorithm and weight of evidence methods with using Markov chain matrices.

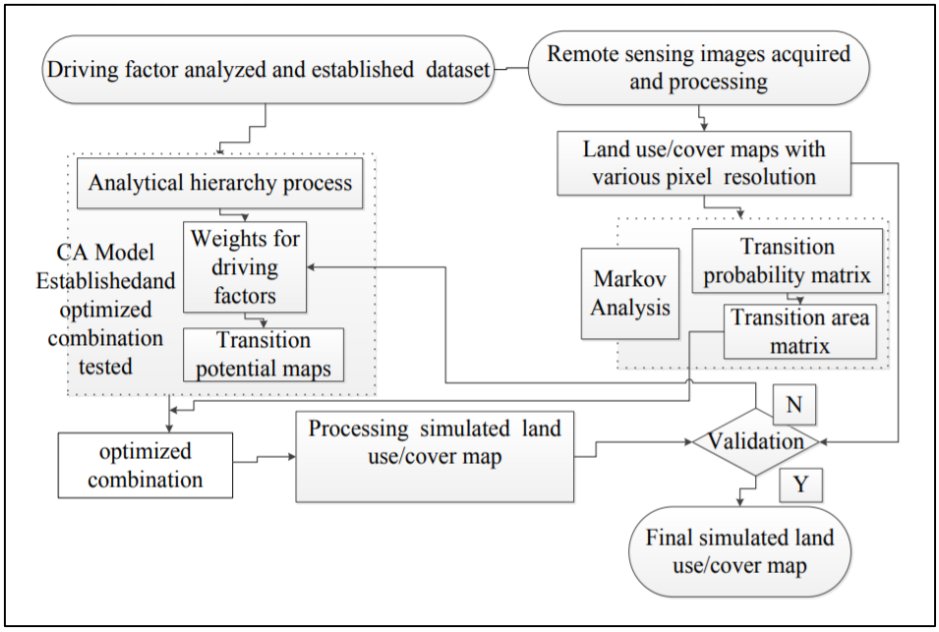


Figure 1.6. A Flow Chart of IDRISI Modeling Process (Lin *et al*., 2015).

A CA (Cellular Automata) model is a discrete dynamical system where space and time are defined as discrete units. Both in space and time, cellular automata are

homogeneous and discrete but local in the interactions. In nature most of the processes governed by local and homogeneous underlying rules. In CA-based models there is a strong ability to represent nonlinear, spatial and stochastic processes.

Markov Model summarizes the land use change over a specified period of time with using a series of transition probabilities. The probabilities used for prediction of land cover properties. The dynamic changes of landscape pattern can be quantitatively predicted with the Markov model, however this model is not good at dealing with the spatial pattern of landscape change. Otherwise, prediction of any transition among any number of categories can be provided by Cellular Automata (CA) (Lin *et al*., 2015). Most of the researchers have applied Cellular Automata with Markov (CA_Markov) model to following LUCC and future predictions because of the advantages for instance high efficiency with data, its dynamic simulation capability, simple calibration for simulating multiple land covers and complex patterns. In this study IDRISI, CA_Markov model is used for land use estimation. Basic principles of this model is summarized in Figure 1.6.

Table 1.1. Model Features Comparison.

| Program | Analysis of Drivers | Expert knowledge integration | Data Driven | Expected goodness of fit (GF)/ over fitting risk (OFR) |
|---|---|---|---|---|
| CA_MARKOV | Multicriteria Evaluation | Yes | Yes | Acquire Expert Knowledge, satisfactory GF without OFR |
| CLUE | Logistic Regression | No | Yes | Poor GF, OFR unlikely |
| DYNAMICA | Wight if Evidence | Yes | Yes | High GF with OFR |
| LCM | Genetic Algorithm | No | Yes | High GF with OFR |
| | Logistic Regression | No | Yes | Poor GF OFR unlikely |

Markov matrix used to calculate the amount of land cover change for each transition by CA_MARKOV, DINAMICA and LCM. However in CLUE model the amount of each land cover category forecasted outside the model. In IDRISI different methods are used for calculation of an annualized Markov matrix. During the simulation period, the assumption of Markov projections will stay the same; that situation may create an incorrect assumption in some cases. In DINAMICA different matrices could be used by models in the calibration

period or the amount of change was obtained from other approaches. Comparison of four models were summarized in Table 1.1.

### 1.5.3. Climate Modelling

Observations and following change in the climate system are possible with direct measurements including remote sensing and investigation of paleoclimate objects (Stocker *et al.*, 2013). Instrumental measurements with paleoclimate reconstructions provide information based on historical trend and projections of changes in earth system elements such as the atmosphere, the land surface, the cryosphere and the ocean (Stocker *et al.*, 2013). The change in the climate systems and their projections are required to be modeled for better understanding of drivers of climate change and impacts and responses of it (Flato *et al.*, 2013). The climate models provide a suitable tool to study the various influences on the Earth's climate. Climate models which are well developed in terms of scientific principles, assist to explain reasons and impacts of climatic changes at global and regional level (IPCC, 2007a). Climate change projections requires some elements such as emission scenarios, carbon cycle models which give increasing number of radiative forcing, climate models with number of future scenarios and downscaling for region by increasing resolution. Figure 1.7 presents a basic process of climate modelling.

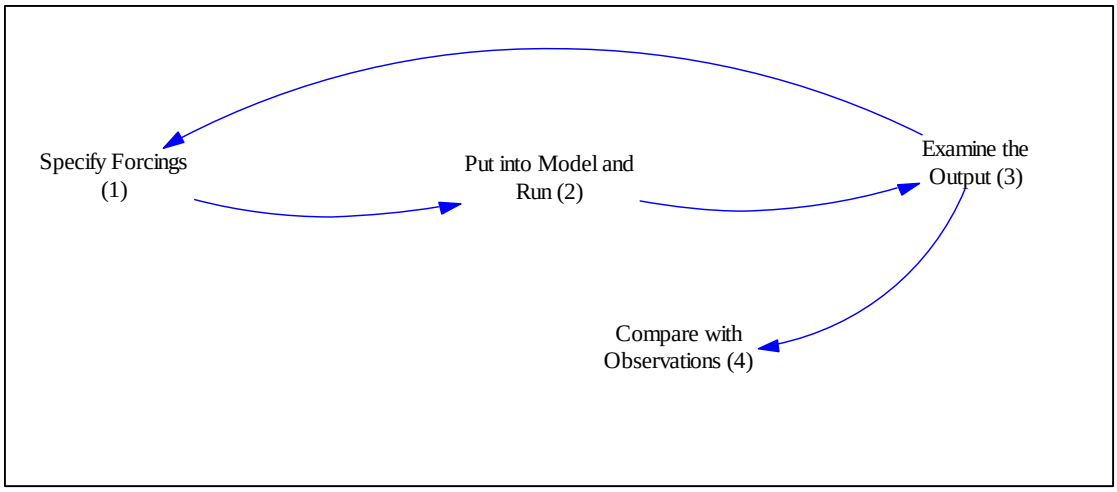


Figure 1.7. Steps for Climate Modelling.

In order to understand drivers and main reasons of climate change attribution exercise is essential. Internal variability, external factors and feedbacks which are activated by the external factors, cause climate change. External factors which can be either natural or anthropogenic origins can be distinguished by the climate models. The model set some hypothesis such as:

(i) $H_o$ (null hypothesis) : The observed record is consistent with effect of natural climate variability

(ii) $H_1$ (experimental hypothesis): The observed record is consistent with natural and anthropogenic drivers.

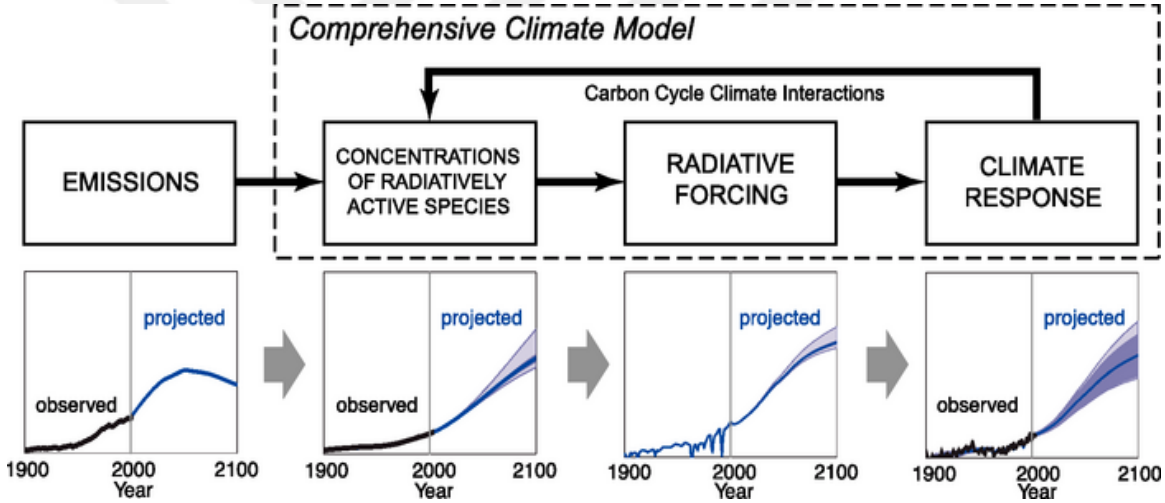


Figure 1.8. Climate Model Projections (IPCC, 2007a).

Models are run many times to compare the results with observed climate systems. The effects of natural internal processes are estimated by using observed variations in the climate change without external factors ($H_o$). Then the effects of greenhouse gases (GHG) are inserted in the models with naturel drivers, the model is run with simulations to explain global warming that has occurred over the past centuries ($H_1$). Therefore the attribution of climate change, either natural or external can be estimated by climate models. According to results of hypothesis, the model is established with its required parameters for projections of changes for future. Figure 1.8 shows the steps for comprehensive climate model starting from emissions as external drivers to climate response and carbon cycle. It is said that 20$^{th}$ century global warming cannot be explained without anthropogenic factors (IPCC, 2001).

It is very likely that the observed increase in global average temperature is caused by observed increase in anthropogenic GHG concentration (IPCC, 2018).

Climate models have a hierarchy ranging from simple climate models such as Energy Balance Model (EBM) to comprehensive models such as Earth System Models (ESMs). (Flato *et al.*, 2013; Stocker *et al.*, 2013). The models include historical climate data analysis, detection and attribution of climate change, projections of near and long terms change in earth climate and downscaling regional and local projections (Flato *et al.*, 2013). Main models types are listed below (Flato *et al.*, 2013; Stocker *et al.*, 2013):

- Atmosphere–Ocean General Circulation Models (AOGCMs) are used for understanding of dynamics of climate system (atmosphere, ocean, land and sea ice). They provide high resolution.
- Earth System Models (ESMs) expand on AOGCMs to involve biogeochemical cycles and feedbacks such as carbon cycle, the Sulphur cycle.
- Earth System Models of Intermediate Complexity (EMICs) are set for research on specific questions and longer time scale to understand climate feedbacks.
- Regional Climate Models (RCMs or RegCMs) are developed with limited area and higher resolution to understand impacts of climate change in an area.

Besides these models types, there are different impacts models such as hydrological, ecological, economy, health and cryosphere. Similar to other models, climate models are subject to uncertainty in assessments reports of Intergovernmental Panel on Climate Change (IPCC) (IPCC, 2007, 2007a; Flato *et al.*, 2013; Stocker *et al.*, 2013). Uncertainty in projection of climate change arises at all stages of modelling processes. There are different sources of uncertainty: Emission scenarios, carbon cycle models, climate models, downscaling and impacts. In emissions scenarios, IPCC SRES developed 40 emissions scenarios (IPCC, 2000). There are basically 4 storylines about the economic and population growth, technology development and diffusion, coherence of global economy. In carbon cycle models, it is necessary to convert emissions into concentration of radiative active species. Concentration of GHG emissions in the atmosphere depends on sinks and sources.

IPCC did not use dynamic carbon cycle models, it transforms emissions into concentration in the atmosphere (Cox. P. M. *et al.*, 2000; Friedlingstein *et al.*, 2006). However, IPCC used 25 General Circulation Models (GCM) during the projection of climate. Each model has different specifications. There is considerable confidence that GCMs provide credible quantitative estimates of future climate change (IPCC, 2007a). Confidence in models has increased due to improved simulation and model resolution, computational methods and parameterization. Assumption of models, computational methods and parameterization leads to different results. This variation is driven by uneven distribution of solar heating, individual responses of the atmosphere, ocean and land, the interaction between these and physical characteristics of region. Scientists need to deal with downscaling to obtain credible information at spatial scales with using different techniques.

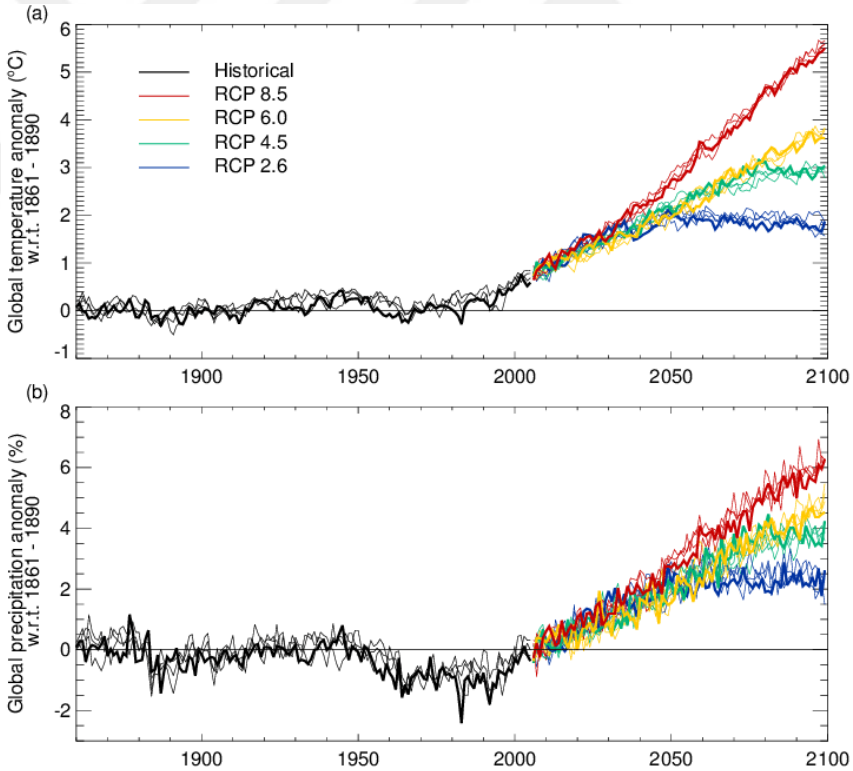


Figure 1.9. Temperature and Precipitation Forecasting According to RCP Scenarios.

Climate Change and the efforts of solution seeking on it are developing. Climate models are the best tools in these efforts to foresee how the climate system will react to the climatic forces. Climate models are to be downscaled using Dynamic Downscaling methods, these are efforts of getting both higher resolution and real-like output results.

Climate projections are obtained via Global Climate Model Outputs which are in the scope of IPCC-AR5 and downscaled to regional and local with province scale.

Three different climate forecasting simulations are used by General Directorate of Meteorology report (GDM, 2015). These models are HadGEM2-ES, MPI-ESM-MR, CNRM-CM5.1. In this study Had-GEM2-ES simulation is chosen due to data availability.

Despite HadGEM2-ES model uses 4 different climate scenarios which are also widespread global scale (RCP 2.6, 4.5, 6.0, 8.5), in this study RCP 4.5 and RCP 8.5 scenarios were applied as climate scenarios. Temperature and Precipitation forecasting values of HadGEM2-ES model were shown in Figure 1.9.

# 2. LITERATURE REVIEW

Conceptualizing a problem, and developing a problem-solving approach is sometimes a confusing process that needs problems and reasons to be investigated separately, considering every aspect behind them. The reasons and problems should be summarized by models to get an efficient solution. For Ergene basin, an effective model can be constructed by analyzing the current conditions and also effects of future risks like climate change and land use/land cover changes on the water resources.

The first objective of this research was to set up a hydrological model and water quality model which should be capable of analyzing current situation and future estimation. Second aim was to figure out the impact of climate changes by using forecasted land use/land cover on water resources in quantity. Last goal was to evaluate water quality and determine pollution of water bodies for future scenarios.

Usage of LUCC models become widespread after technological improvements of geographic information systems and remote sensing. These technologies provide high accuracy for land use planning. Land use simulation models use different calculation methods, the most popular ones are cellular automata, artificial neural network and Markov chains. Han *et al*. (2015) modeled Beijing and resulted by the help of Land Cover Simulation that cultivated land converts to urban built-up land, in the future. Price *et al.* (2015) tried to determine with the CLUE-S model which regions in Switzerland face urbanization and landfill risk. In the context of globalization, decentralization, market-oriented developments and political interventions, five different scenarios for 2035 were discussed. In another study in Turkey it is concluded that urban areas were expanded and the agricultural lands were adversely affected by this enlargement (Erdoğan *et al*. 2015). Sullivan *et al.* (2004), Investigated camel catchment to prove hydrological response and land use change relation. Lin et al. (2015) analyzed catchment runoff according to different land uses. Anand et al. (2018) studied on water balance for different land uses.

Water plays a vital role in reducing and adapting to the impacts of climate change. It is expected that nearly 5 billion people will experience water stress in 2025 (Arnell, 1999). Therefore the climate change effects have to be taken into account for modeling a watershed. Many researches were studied about climate change and effects on water sources. Piao *et al*. (2010) investigated the impacts of climate change on water resources and agriculture in China. Ficklin (2009) used model to measure climate change sensitivity for agricultural watershed. Looking at the studies from Turkey, Ertürk *et al*. (2014) searched for climate change impacts on Köyceğiz-Dalyan watershed Western Mediterranean Region by using SWAT. Scenarios related with climate change and land use were used to forecast the present and future climate change impacts on water resources. Özdemir *et al*. (2014) modeled the Sarısu-Eylikler River Basin with SWAT to investigate the impact of climate changes on flows and to manage a sustainable watershed. According to the model results, due to climate changes, there is a danger of flood and change of the region's product pattern.

For watershed modeling most of researchers uses SWAT model because of its advantages. Abdelwahab *et al*. (2018) used the Annualized Agricultural Nonpoint Source (AnnAGNPS) and Soil and Water Assessment Tool (SWAT) to generate simulations in Mediterranean Watershed to model soil erosion. And results showed that how strong correlation between observed and simulated stream flow which may result in soil erosion and sediment load. Andrade *et al*. (2018) modelled soil moisture and discharge in northeastern Brazil by using SWAT to evaluate the effects on them. Čerkasova *et al*. (2018) evaluated SWAT model with the method which uses MATLAB scripts in order to improve Hydrologic Response Unit (HRU) definition procedure. Thavhana *et al*. (2018) calibrated SWAT to simulate runoff for the Luvuvhu River catchment area.

Also, there are examples that SWAT program is used in Turkey boundaries. Ertürk *et al*. (2010) worked on Melen Watershed which seen as an alternative water source for İstanbul province. One dimensional stream water quality model was used to water quality assessment. Köyceğiz (2019) estimated flow with SWAT and artificial intelligence methods. Güngör (2018) modeled the hydrology of the Filyos river basin by (SWAT) model for the determination of hydrological components. Güzel (2010) worked on SWAT model to calculate surface runoff, groundwater flow and precipitation for Köyceğiz Dalyan

watershed. Özcan (2016) used SWAT to evaluate practices of agricultural management in terms of sediment, total phosphorus and total nitrogen for Lake Mogan. Gölpınar (2017) studied daily flow data obtained from current observation stations to integrate in SWAT model. In addition to test the applicability of the model to agricultural basins. Akıner *et al.* (2012) studied in Melen Basin; missing and future rainfall data was obtained by artificial neural networks technique. The model was established with estimated precipitation data for the basins future surface flow. The study also showed that the water transfer from Melen to Istanbul can be done by water forecasting.

There are also studies that have been done for Ergene watershed. Some of researches are related with water hydrology and quality some of them directly related with sustainability index and land use estimation. Altürk (2017) explored land use changes in Ergene Basin by CLUE model. Gök (2015) explored watershed sustainability index for Ergene watershed. Paçal (2017) developed hydrological and water quality model of Ergene Basin using SWAT.

To sum up, in recent years integrated basin management concepts become popular in investigating environmental problems. Because in a system a reaction triggers other reaction which affects another, this interaction is called as chain reaction. Therefore in order to develop solutions for environmental problems, researchers need to consider many interconnected reactions together. Climate change has direct influence on water quantity and quality as expected, but also variations in regional hydrological cycles are closely related to LUCC (Lee *et al*. 2007). As it is a known fact that the water management and land management are undistinguishably linked. Land use change is the most important factor for environmental management through its influence on ecosystems, water budgets, water hydrology and quality, carbon cycling, and livelihoods (Lambin *et al*. 2000). However, it is unclear whether the LUCC or climate change that affect the hydrological process of the basins contribute more to this process (Altürk, 2017). Studying both effects together is a new concept for science, therefore in this study both climate and land use changes were used as future input data to estimate Ergene basin's hydrology and water quality.

# 3. MATERIAL AND METHODS

## 3.1. Materials

### 3.1.1. Study Area: Ergene Basin

Ergene Basin with an area of 14 560 km$^2$, is 63% of the surface area of Thrace, constitutes 1.37% of the Turkey surface area. Ergene Basin is located in the middle of the Thrace region, which is in the northwestern part of the Turkey. According to the geographical coordinate system the basin is located at 42°05'42”- 40°48'06” North Latitude between 26°20'04”'- 28°13'00” East Longitude and surrounded by the borders of the Northern Bulgaria, Marmara Basin and Meriç Basin. The east-west length of the Ergene Basin is 160 km, the north-south length is 140 km.

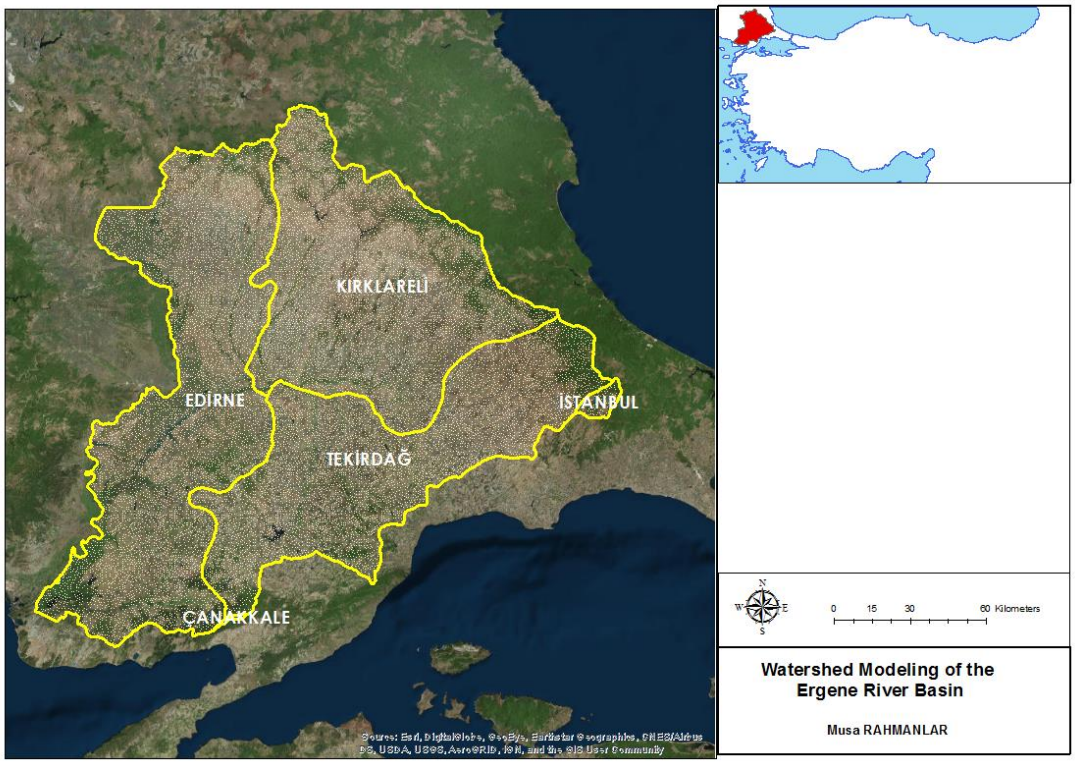


Figure 3.1. Study Area – Ergene Basin Map.

The Ergene Basin, where there is an obvious asymmetry difference between the north and south, has a highly faulted and fragmented topographic view of the plain from the north and the monotonous south (Altın, 2000). The highest point of the basin area where the average elevation is 162 m is Mahya Hill (1031 m). Istranca (Yildiz) Mountains stretches from the North of Edirne to Lalapasa, Kirklareli, Kofçaz, Demirköy, Vize, Saray towns and remaining between Black Sea coasts. Ganos Mountains that located in the south of the region stretches from the region covering Enez, Kesan, Malkara ve Sarköy towns to Tekirdag. In Turkey one of the existing 13 sedimentation basins is Ergene Basin (Hazar, 1997). The provinces in the basin are Tekirdağ, Edirne and Kırklareli. As shown in figure 3.1, also the basin has İstanbul and Çanakkale parts, but in this study these regions are neglected due to areas proportion which is so small (<%0,001) (MoFWA, 2013).

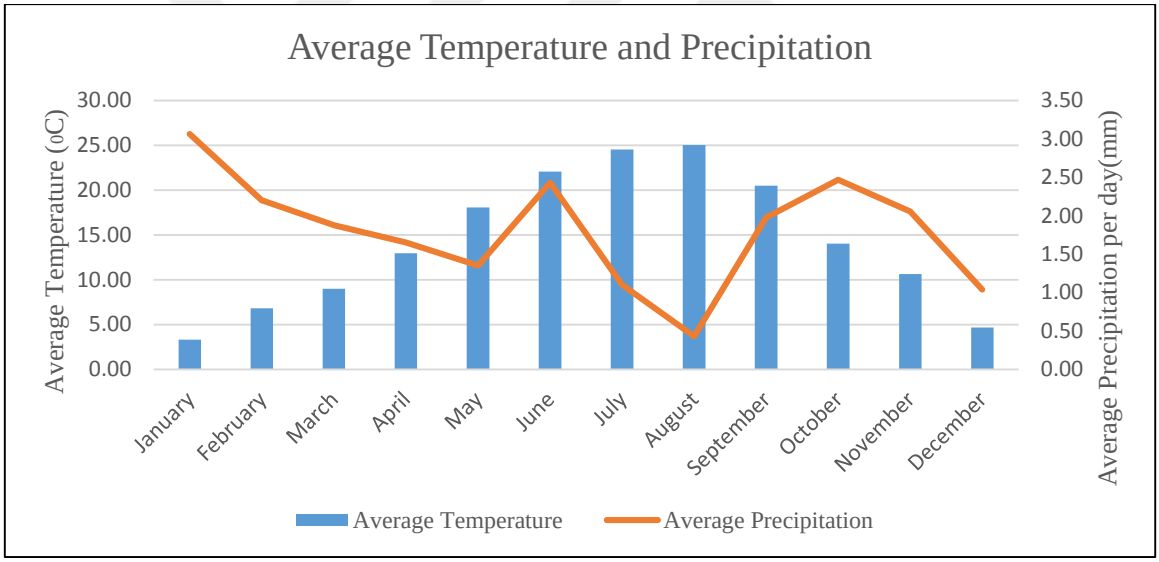


Figure 3.2. Average Temperature and Precipitation Data of Meteorological Stations in Ergene Basin between 2013-2018.

### 3.1.2. Climate

Various climate types are seen in Ergene basin. Generally dry and hot summers, rainy and cold continental climate prevails in winters. Due to the cold air waves coming from the Balkans, the type of snowfall and the freezing temperatures in winter are seen continuously. Also, Mediterranean Sea and Blacks Sea climate types have influence on the region.

As can be seen from figure 3.2, which was obtained from last 5 years average temperature of Ergene Region (2013-2018), warmest month of year is August and coldest one is January. June and October months have the highest precipitation rate according to region data.

(a) (b)

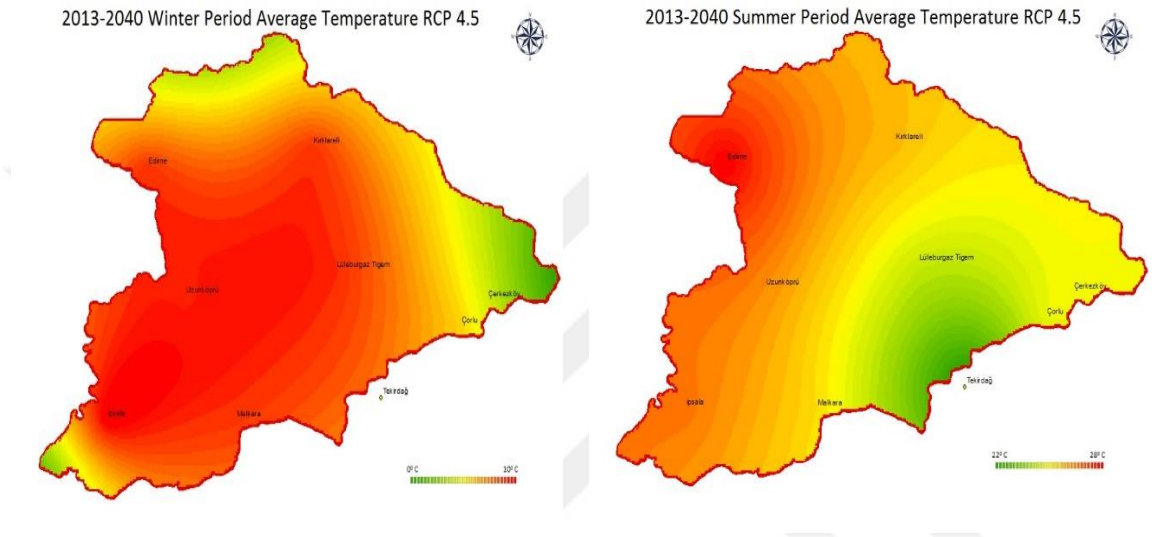


Figure 3.3. Temperature Distribution for Winter Season (a), Temperature Distribution for Summer Season (b) for Ergene Basin.

Different meteorological stations were used for this study due to differences among temperature and precipitation values (Figure 3.3). These differences are so important for creating a right model. Therefore all meteorological stations data were investigated and recorded. Besides temperature regions behave differently for winter and summer seasons. Therefore Edirne, Kırklareli, Çorlu, Tekirdağ, Uzunköprü, Lüleburgaz Tigem, İpsala, Malkara and Çerkezköy meteorological service stations are chosen for ArcSWAT model (Figure 3.4).

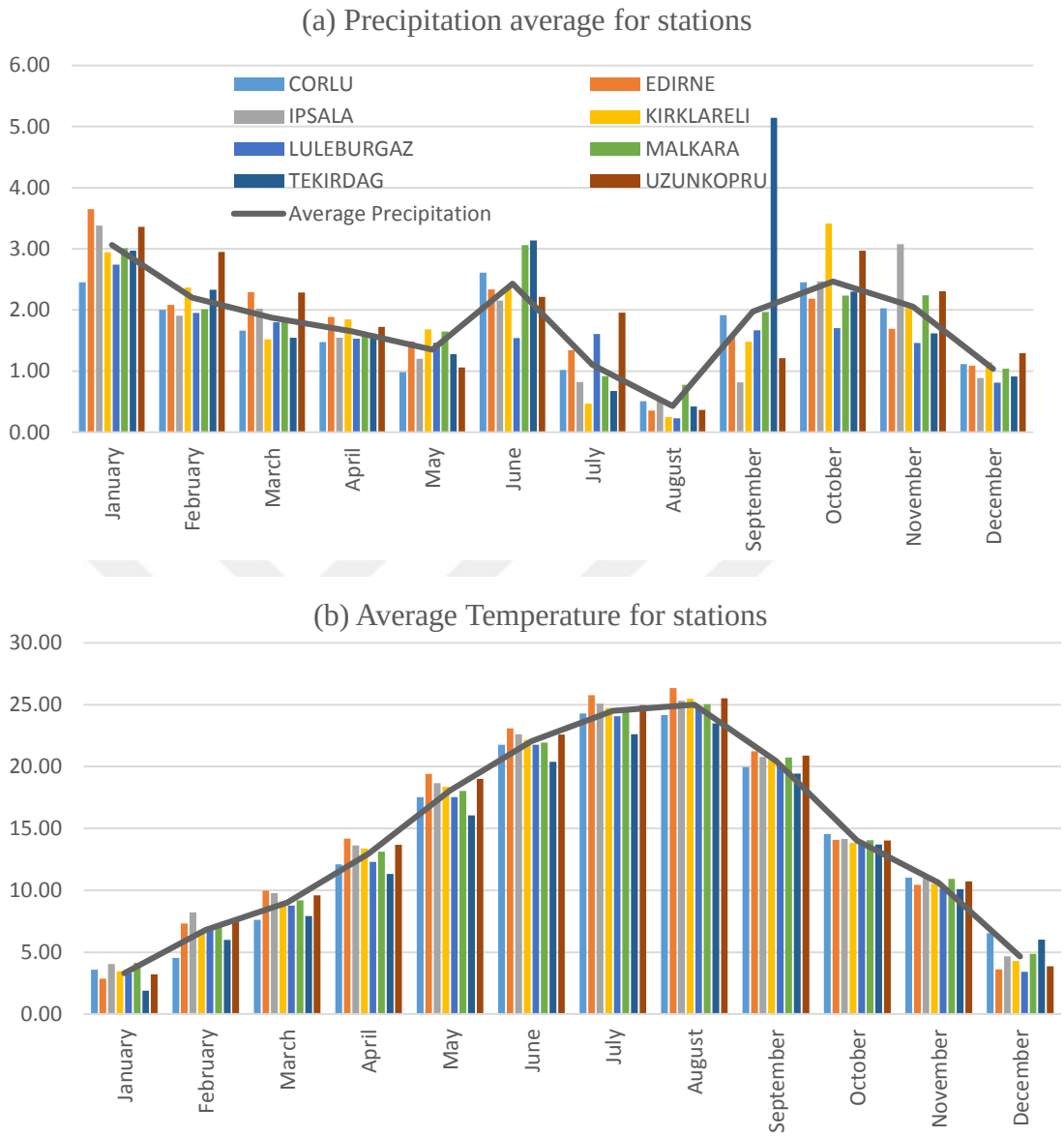


Figure 3.4. Monthly Average Precipitation (a), Average Temperature (b) for all Meteorological Stations in Ergene Basin Between 2013-2018 years.

### 3.1.3. Landuse

CORINE maps were used for Ergene basin to classify land use types. There are two sets of land use maps were constructed for Turkey as 2006 and 2012. 2012 year map was used as base map for hydrological modeling in SWAT program. For comprehending land uses CORINE classification was simplified and reclassified according to six classes. Land use/land cover areas were classified from CORINE data as agricultural areas, industrial areas, residential areas, forest areas, wetland areas and water bodies (Figure 3.5). This simplification assisted to compare 2012 and 2006 land use maps.

Figure 3.5. The Land Use Classes.

According to the results of CORINE 2012 data; the largest area of Ergene Basin covers agricultural areas with 77.19%. With 18,65%, forest and semi-natural areas are the second largest area occupying the basin. Artificial areas in the basin constitute an area of 3.24%. Water surfaces cover approximately 1% of the basin. Detailed and simplified maps of the basin is illustrated in Figure 3.6. According to the CORINE classification; arable areas, mixed agricultural areas, pasture areas are all the agricultural areas of regions.

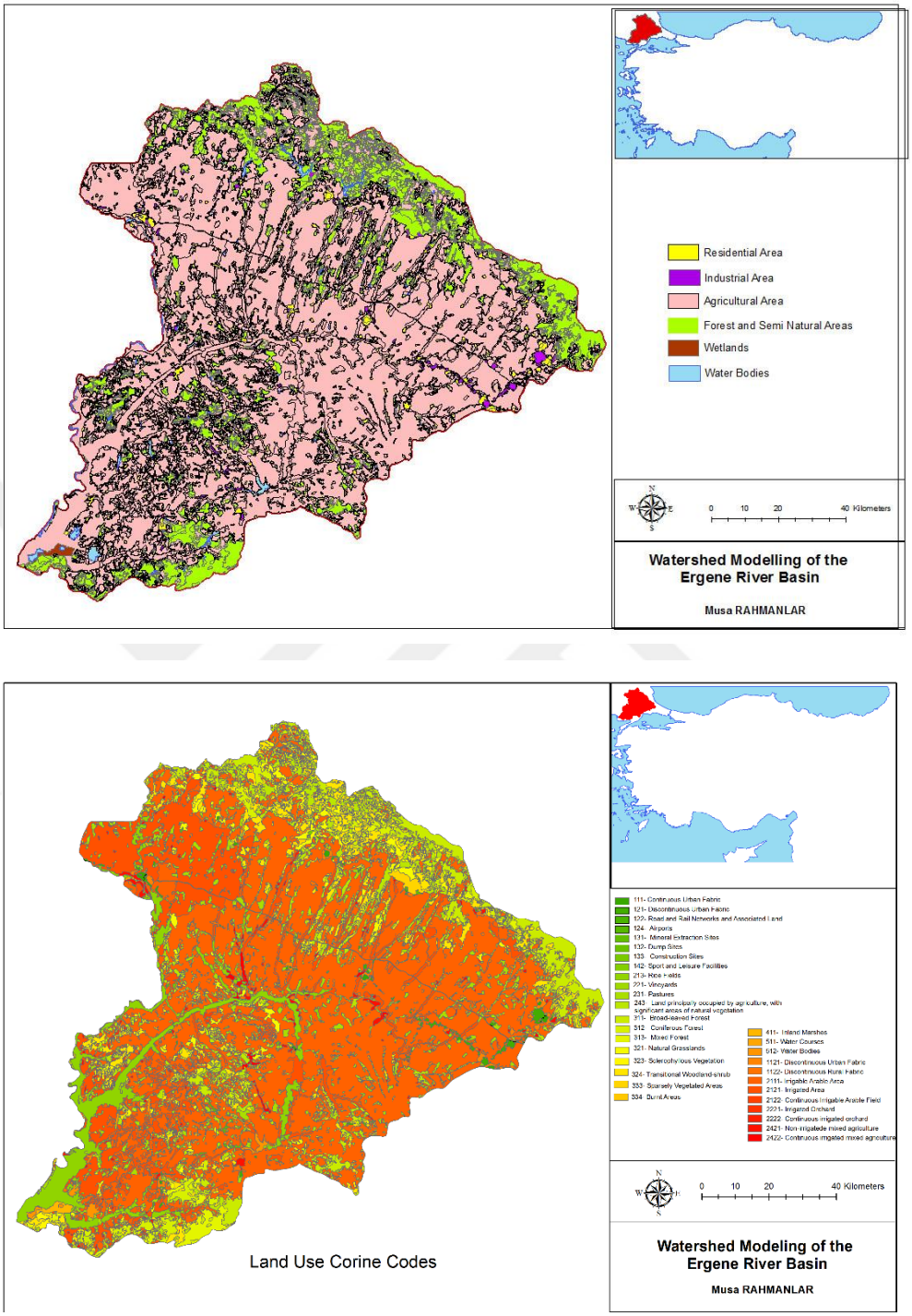


Figure 3.6. The Land use Classes of Ergene Basin According to CORINE Codes (Upper one is simplified to six classes).

In the watershed area dry agricultural methods are chosen (43.6%) rather than irrigated agriculture, irrigated agriculture is carried out only on streams and water bodies (lake, pond, dam, etc.) (4.7%) (MoEF, 2010). The main agricultural products grown in the

field are wheat, sunflower, canola and rice. In the watershed area where the settlement areas are distributed according to the water sources, the areas towards the water section line are used as pasture and forest areas.

Investigation of land use change has an importance to understand the trend of region. Therefore a short term comparison applied for the Ergene Basin. The land use cover change order is as follows: Preparing the data set for change analysis; acquisition of data; placing the data in a common projection system for comparison of the model; classification and mapping of images (Figure 3.7).

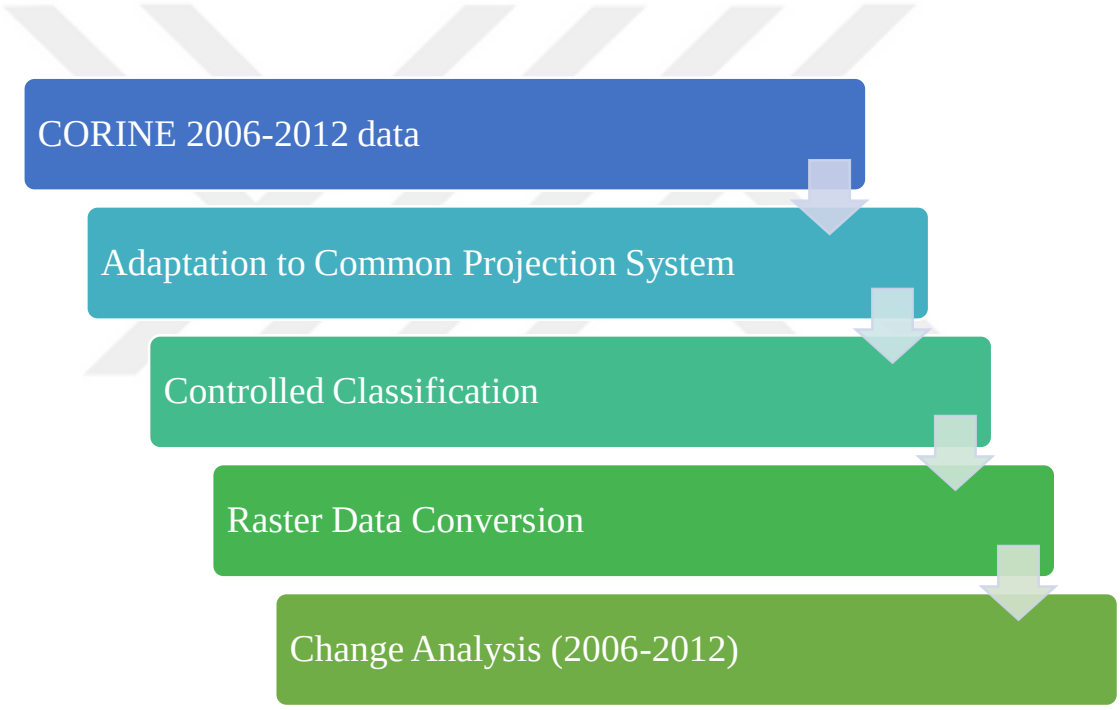


Figure 3.7. The Land Use Data Change Analysis Steps.

Again simplified map was created for CORINE 2006 land use map. And 2006 and 2012 images were compared by using ArcGIS program (Figure B.1). According to the results table 3.1 obtained. The percentage of land uses proved that there was a decrease in agricultural and residential areas. On the contrary, the percentage of industrial areas increased. These numbers proved that industrial potential of region increased between years 2006 and 2012. Also there was a risk of misclassification of land uses. For example a residential area might be miscoded as an agricultural area in year 2006 and when this place's land use compared with year 2012 data, it would show an increase in residential areas

despite this situation was not real. Therefore additional maps were used for estimation of future land use in high accuracy.

Table 3.1. 2006 vs 2012 CORINE Area Classification of Ergene Basin.

| | 2006 Corine | Percentage | 2012 Corine | Percentage | Difference | Percentage |
|---|---|---|---|---|---|---|
| Residential Areas ($km^2$) | 328,43 | 2.28% | 316 | 2.19% | -13 | -4.00% |
| Industrial Areas ($km^2$) | 136 | 0.95% | 150 | 1.04% | 14 | 9.17% |
| Agricultural Areas ($km^2$) | 11,274 | 78.30% | 11,115 | 77.19% | -159 | -1.43% |
| Forest Areas ($km^2$) | 2,538 | 17.63% | 2,684 | 18.64% | 146 | 5.43% |
| Wetland Areas ($km^2$) | 35 | 0.24% | 30 | 0.21% | -5 | -17.65% |
| Water Bodies ($km^2$) | 87 | 0.60% | 103 | 0.72% | 17 | 16.08% |
| Others | 1 | 0.01% | 2 | 0.01% | 1 | 49.04% |

### 3.1.4. Geological Structure

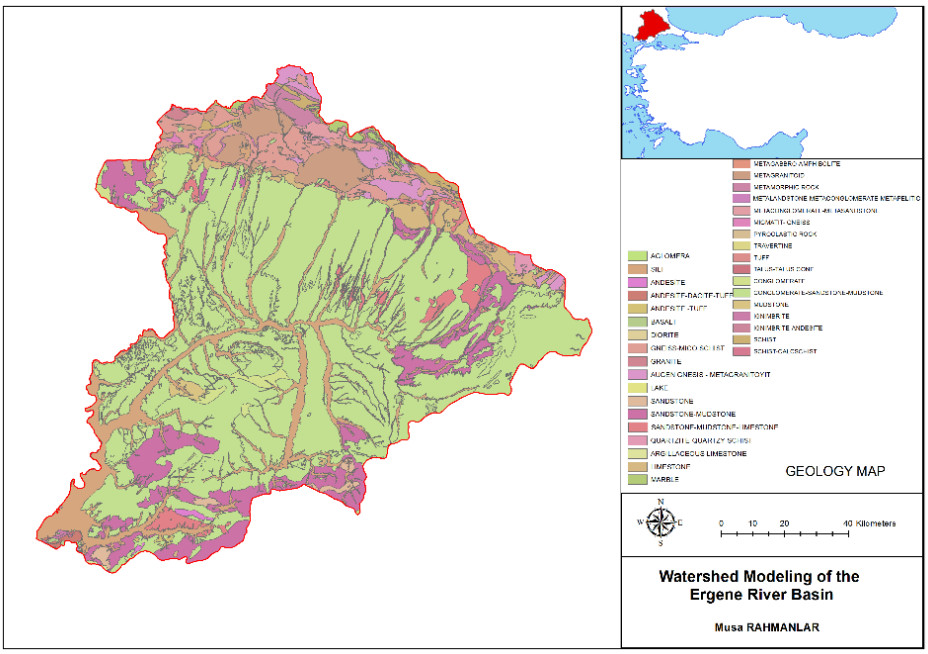


Figure 3.8. Geological Map of Ergene Basin.

Vertisol, Inceptisol, Alfisol, Entisol and Mollisol constitute soil types of the basin according to the new soil classification. Alfisol and Inceptisol are cultivable; Mollisol is

considerably fertile and significant and Vertisol that is accounts for about 30% of the basin is not suitable for agricultural purposes (Figure 3.8). 126.324 ha of the soil is exposed to severe erosion while 21.881 ha of the soil is exposed to the risk of very severe erosion (Haktanır *et al*., 2005). Despite geological maps shows some common characteristics of region, these characteristic can not always be adequate for analyzing behavior of soil. Therefore creating a soil map, it is important to check soil properties from literature survey or field experiments.

### 3.1.5. Hydrogeology

The source of Ergene River is Saray town of Tekirdağ and its ramifications (Sulucak Stream, Burgaz Stream, Teke Stream, Şeytandere stream and Hayrabolu Stream) are the most crucial surface water resource of the basin (Figure 3.9). The river joins with Çorlu Stream and afterwards flows to the west and flows into Meriç River in Uzunköprü town of Edirne. Ergene River extends 285 km in length with average annual flow rate is 27,270 $m^3$/ h (Hazar, 1997).

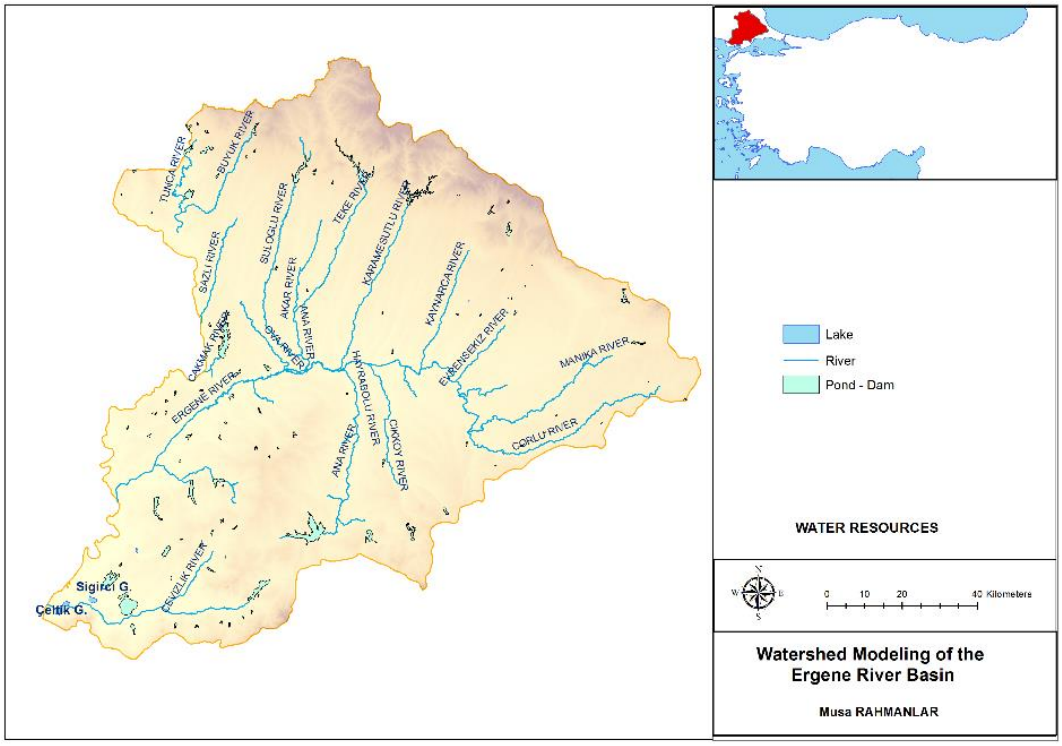


Figure 3.9. Hydrogeological Map of Ergene Basin.

The Ergene River is the most important stream of farmers in the Thrace Region with approximately 300,000 decares of 1st, 2nd and 3rd class agricultural areas. Ergene River is the most important branch of the river Meriç which is an international water. While the river and its tributaries keep water constantly, the basins are narrow and the amount of water they carry is small (MoEF, 2009). In the summer months when the water use increases, pollution in the river increases to very high levels due to the industrial loads (Güneş, 2009).

### 3.1.6. Population

Ergene Basin is located within the boundaries of Kırklareli, Tekirdağ and Edirne Provinces. The eastern and southern parts of the basin are located in Tekirdağ, in the northern part of Kırklareli, and in the western part of Edirne Province. While the population share of Edirne and Kırklareli provinces in the study area is decreasing, the population share in Tekirdağ Province increases due to the development of the industry. Especially in Çorlu and Çerkezköy districts, there is an increase in population with the effect of organized industrial zones. The population distribution of provinces of Ergene Basin is presented in Table 3.2 (TurkSTAT, 2017).

Table 3.2. Population Distribution of Ergene Basin

| Province | District | Population | Province | District | Population | Province | District | Population |
|---|---|---|---|---|---|---|---|---|
| EDİRNE | Enez | 10,434 | KIRKLARELİ | Babaeski | 48,229 | TEKİRDAĞ | Çerkezköy | 157,931 |
| | Havsa | 18,881 | | Demirköy | 8,482 | | Çorlu | 260,437 |
| | İpsala | 27,402 | | Kofçaz | 2,434 | | Ergene | 60,881 |
| | Keşan | 81,747 | | Lüleburgaz | 147,325 | | Hayrabolu | 32,035 |
| | Lalapaşa | 6,601 | | Merkez | 100,116 | | Kapaklı | 112,269 |
| | Meriç | 13,801 | | Pehlivanköy | 3,593 | | Malkara | 52,456 |
| | Merkez | 178,910 | | Pınarhisar | 18,513 | | Marmaraereğlisi | 24,598 |
| | Süloğlu | 7,159 | | Vize | 27,358 | | Muratlı | 28,127 |
| | Uzunköprü | 61,920 | | | | | Saray | 49,180 |
| | | | | | | | Şarköy | 31,518 |
| | | | | | | | Süleymanpaşa | 196,031 |
| Edirne | Total | 406,855 | Kırklareli | Total | 356,050 | Tekirdağ | Total | 777,914 |

### 3.1.7. Agriculture and Livestock

An important part of the basin is composed of agricultural land. While irrigated areas constitute 4.7% of the basin, dry farmland covers 43.6% of the basin area. Agricultural areas where irrigation systems are located are generally concentrated around river beds where slope is low. Irrigation in these regions is provided by dams which built by State Hydraulic Works. In addition, water can be irrigated with water drawn from the Ergene River and its side-arms by individual efforts. In the low slope areas of west of Keşan, where the Ergene River meets Meriç River, rice fields are intense.

In Edirne province wheat and sunflower are the prominent crops. These two crops are planted in 93% of field areas. And also, rice has a very important place for region by means of economy and ecology. Other important herbal products include barley, watermelon, and onion and so on. In addition, fodder crops such as oats, corn, vetch, alfalfa, and other vegetables, especially tomatoes, are produced to meet the region needs. In the province of Kirklareli, wheat takes the first place and its share in the cultivation varies between 55 and 60% over the years. Sunflower takes second place and its share in the cultivation is 20-25%. And for Tekirdağ region the most important field crop in province is wheat. Again sunflower takes second place (37%). The agricultural areas in the Ergene basin are presented in Table 3.3.

The fertilizer use of urea with nitrogen fertilizer (chemical fertilizers) is 113.695 tons per year in the provinces located within the catchment area of the Ergene Basin. The total amount of fertilizer used in Tekirdağ Province was 152.150 tons. In agricultural and forestry areas contaminant of phosphorus and nitrogen are amongst important pollutant sources because of using fertilizer. Also, heavily applied chemical fertilizers include more nitrogen in the basin. The fertilizers and pesticides used in agricultural activities around Ergene River contribute to the sediment load and pollution amount of the river. On the other hand, groundwater is used for water supply for irrigation purposes. This situation threatens to decrease at the water level.

Livestock is an important economic activity in this region. Especially in the districts of Muratlı and Hayrabolu cattle breeding; In Çorlu, poultry farming is dominant over the basin. There are 5 commercial poultry farms in the Çorlu district in the Upper Ergene Basin and 4 in the Muratlı district. Furthermore, there are 1 Angus farm in Çorlu-Şahpaz Village. In the livestock activities, Kırklareli Center is seen as the leading cattle, sheep and poultry husbandry. In addition, in Malkara, Uzunköprü and Babaeski, cattle breeding is carried out intensively in Keşan. There are also poultry farms in Hayrabolu Malkara and Kırklareli. According to animal husbandry data, small cattle husbandry is an important area with 825,162 units. Total number of cattle is 408,383. Waste from animal husbandry activities creates pressure in the region when they reach the receiving environment. Animal husbandry can reach groundwater depending on the operation and permeability of the area where animals are located.

Table 3.3. Agricultural Areas of Ergene Basin (decares).

| Province | District | Planted Area | Fallow Field | Vegetable Garden | Fruit Area | Total Area |
|---|---|---|---|---|---|---|
| Edirne | Enez | 124,314 | 1,039 | 1,108 | 3,817 | 130,278 |
| Edirne | Havsa | 384,768 | 208 | 3,700 | 2,660 | 391,336 |
| Edirne | İpsala | 468,243 | 0 | 5,547 | 4,209 | 477,999 |
| Edirne | Keşan | 514,408 | 0 | 20,676 | 8,004 | 543,088 |
| Edirne | Lalapaşa | 204,743 | 520 | 82 | 1,893 | 207,238 |
| Edirne | Meriç | 176,158 | 1,260 | 10,650 | 7,907 | 195,975 |
| Edirne | Merkez | 489,171 | 309 | 1,791 | 3,576 | 494,847 |
| Edirne | Süloğlu | 118,720 | 0 | 960 | 735 | 120,415 |
| Edirne | Uzunköprü | 595,277 | 3,118 | 13,024 | 26,108 | 637,527 |
| Kırklareli | Babaeski | 488,809 | 1,039 | 6,084 | 2,675 | 498,607 |
| Kırklareli | Demirköy | 1,549 | 598 | 645 | 720 | 3,512 |
| Kırklareli | Kofçaz | 76,533 | 246 | 209 | 1,738 | 78,726 |
| Kırklareli | Lüleburgaz | 773,538 | 5,629 | 2,716 | 4,362 | 786,245 |
| Kırklareli | Merkez | 509,564 | 5,592 | 5,123 | 9,403 | 529,682 |
| Kırklareli | Pehlivanköy | 81,625 | 1,570 | 240 | 1,200 | 84,635 |
| Kırklareli | Pınarhisar | 183,736 | 208 | 2,236 | 1,550 | 187,730 |
| Kırklareli | Vize | 187,401 | 2,599 | 5,260 | 1,905 | 197,165 |
| Tekirdağ | Çerkezköy | 48,794 | 0 | 5 | 137 | 48,936 |
| Tekirdağ | Çorlu | 301,154 | 0 | 521 | 3,377 | 305,052 |
| Tekirdağ | Hayrabolu | 765,165 | 0 | 940 | 3,467 | 769,572 |
| Tekirdağ | Malkara | 751,180 | 364 | 13,507 | 5,233 | 770,284 |
| Tekirdağ | Muratlı | 328,394 | 0 | 689 | 1,631 | 330,714 |
| Tekirdağ | Saray | 322,512 | 0 | 1,974 | 534 | 325,020 |
| | Total | 7,895,756 | 24,299 | 97,687 | 96,841 | 8,114,583 |

### 3.1.8. Industry

Biggest industrial centers of our country are located in Istanbul and Kocaeli region, but a result of lack place this Industrial zone shifted to eastern part of Thrace Region. With the establishment of Tekirdağ Çerkezköy Organized Industrial Zone in 1973, it has shown a rapid expansion starting from Çerkezköy and through the Çorlu Stream and Ergene River Basin. An important part of the industry in the Ergene Basin (80-85%) is the concentration around Çorlu-Çerkezköy. Çorlu-Çerkezköy has approximately 2000 facilities and the amount of industrial wastewater discharged to the receiving environment is over 300.000 $m^3$ / day. All three cities have industrial zones as shown in table 3.4. The region's distance to other industrial zones, ease of access, flat land and, more importantly, the richness of underground water resources, has made the region a center of attraction for the industrial facilities of the textile, leather, paper and chemical sectors based on groundwater consumption. The existence of approximately 2500 industrial facilities in the basin has a large population burden on the region. The water of the Ergene River, which gives life to the basin and the Thrace region, has polluted with the industrial and domestic wastewater that causes the water cannot be used in agriculture. With the industry moving out of Istanbul in a planned manner, many factories and facilities, most of which were unlicensed, moved towards the east of Istanbul that is to the west of Thrace, and especially in the vicinity of E-5, in the vicinity of Çerkezköy, Çorlu, Muratlı and Lüleburgaz. (Özkan *et al*., 2008). It is seen that there is 15-20% of the industry in Ergene Basin in Lower Ergene Sub-Basin. Kırklareli Center and Babaeski are the regions where industry is concentrated. Leading sectors are food and textiles. The Ergene River, which is contaminated by Çorlu, Çerkezköy and Lüleburgaz, is exposed to relatively less pollutant discharges when it enters the lower basin.

Table 3.4. Organized Industrial Zones of Ergene Basin.

| Province | Organized Industrial Zones |
|---|---|
| Edirne | Edirne |
| Tekridağ | Çerkezköy, Çorlu, Hayrabolu, Malkara, Muratlı |
| Kırklareli | Büyükkarıştıran, Pagder Aslan Özel |

To sum up region is threatened by many load sources as mentioned above. These load sources are summarized and revised for modeling region. New load tables are created for region as domestic and industrial loads which includes all load types which are shown in table 3.12 and 3.13.

## 3.2. Methods

### 3.2.1. Ergene SWAT Model

This chapter presents the SWAT model that applied to the Ergene Basin and input data requirements of the model. The model is running on ArcMAP platform of ESRI. The integrated ArcMAP user interface of the model is called ArcSWAT. ArcSWAT is a GIS based model which integrates three main components that are database management, processing, imaging of the computer technology (Ordu *et al*., 2007). Arc MAP is a popular program which is widely used in scientific studies. Thanks to the high number of users, the program continues development, so that new tool boxes have been emerging every day. In addition, other interfaces based on geographic information system can be applied to the program.

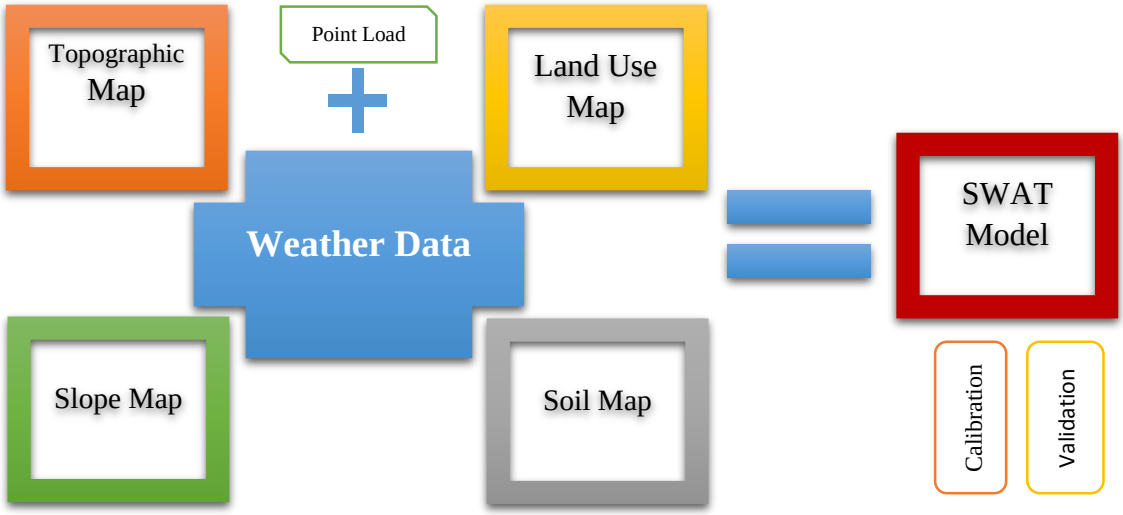


Figure 3.10. ArcSWAT Model Data Input Needs

### 3.2.2. Data Input

As mentioned in previous chapters SWAT program needs specific data sets. The basic input data of SWAT are topographic map, stream gage flow, point load coordinates, land use/land cover (LULC), soil map and weather data. These data needs are summarized in figure 3.10.

Table 3.5. Summary of Input Data.

| **Input Name** | **Data Source** |
|---|---|
| Digital Elevation Map | Turkish Ministry of Agriculture and Forestry |
| Slope Map | Created with ArcSWAT according to DEM |
| Soil Map | Turkish Ministry of Energy and Natural Resources-General Directorate of Mining Technical Research and Turkish Ministry of Agriculture and Forestry |
| Landuse Map | Turkish Ministry of Agriculture and Forestry |
| Climate, Temperature | Turkish State Meteorological Service |
| Climate, Precipitation | Turkish State Meteorological Service |
| Climate, Wind Speed | Turkish State Meteorological Service |
| Climate, Humidity | Turkish State Meteorological Service |
| Climate, Radiation | Turkish State Meteorological Service |
| River Hydrology (Flow) | General Directorate of State Hydraulic Works (obtained by protocol between DSİ and Boğazici University) |
| Water Quality | General Directorate of State Hydraulic Works (obtained by protocol between DSİ and Boğazici University) |

Digital Elevation Map (DEM), soil map, land use map, climate and weather, river hydrology and water quality data were obtained from public sources. These data sets were reconstructed for SWAT model as an input. The summary of input data was shown in table 3.5.

3.2.2.1. Digital Elevation Model. DEM is a specialized database that represents the relief of a surface between points of known elevation. The DEM is the most necessary data on which the entire system of SWAT is built. Therefore high resolution DEM map was obtained from Ministry of Agriculture and Forestry. A DEM with grid size of 20m × 20m (1:25.000), and WGS 1984 UTM Zone 35N coordinated was used in this study (Figure 3.11).

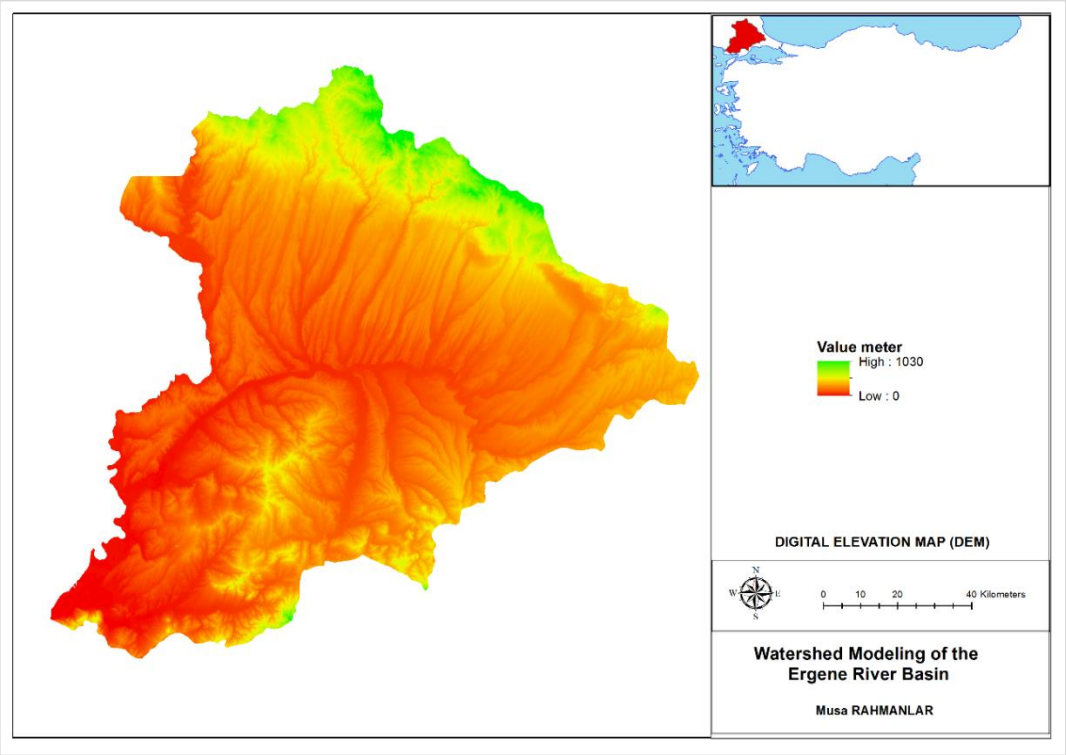


Figure 3.11. ArcSWAT DEM Model

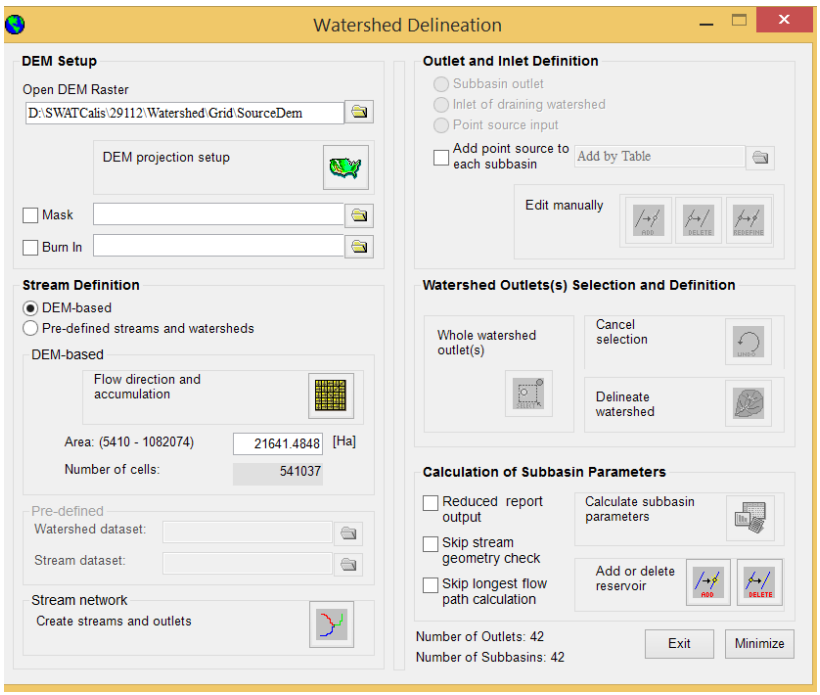


Figure 3.12. ArcSWAT Water Delination Model

Stream network creation was done in the environment of ArcSWAT using this DEM data. Watershed delineation module used DEM for creating stream network and sub basins. In addition threshold value for separation of sub basin was defined 21.641 ha by watershed delineator for optimum calculations.(Figure 3.12) The outlet points that were closed to stream gage and water quality monitoring points were selected specified in the generated river network for calibration of water quantity and quality.

Pollution sources of Ergene basin were constructed as point sources which were defined by generated table and integrated into the model (Table 3.12 & 3.13). Then the basin delineated into 42 sub basins (Figure 3.13). After sub basins defined Hydrological Response Units (HRU) module become active.

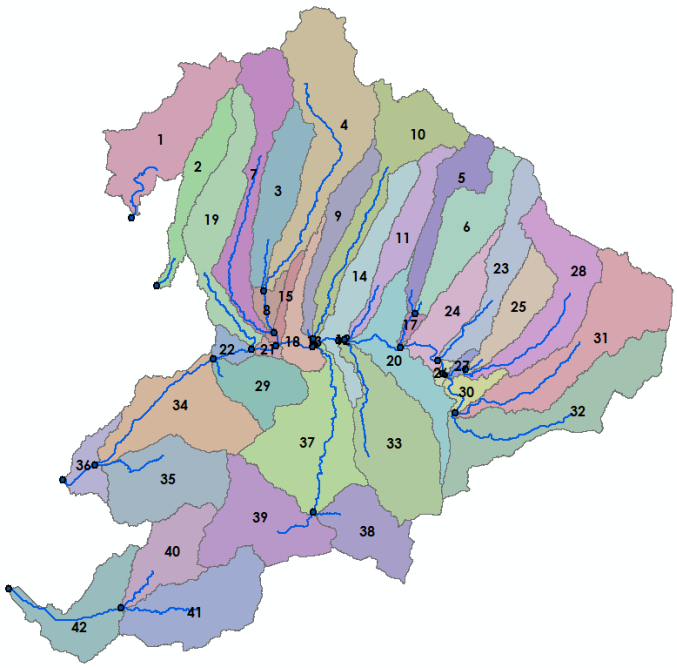


Figure 3.13. Ergene Model Subbasin

<u>3.2.2.2. Hydrological Response Units.</u> This module enables to calculate hydrological components of basin for different LULC, soils and slope by separating each sub basin to these characterizations. Therefore module requires three main components: Landuse, Soil, Slope maps.

Land use data (CORINE 2012) was obtained from the Ministry of Agriculture and Forestry. ArcSWAT classified land use of the basin under 22 classes which are shown in table 3.6 and also SWAT uses nearly 80 classes for determining plants. But CORINE codes system does not use same land classification of SWAT Program. Therefore all CORINE classification reclassified for input data and table 3.7 obtained. Both CORINE and ArcSWAT land use classification summarized in Figure 3.14.

Table 3.6. ArcSWAT Generic Land Cover Codes

| Landuse | Detail | Landuse | Detail |
|---|---|---|---|
| WATR | Water | FRSE | Evergreen Forest |
| URML | Urban Medium Density | FRST | Mixed Forest |
| URHD | Urban High Density | RNGB | Range Shrubland |
| UCOM | Urban Commercial | ORCD | Orchards/Vineyard |
| UINS | Urban Institutional | RNGE | Grasslands/Herbaceous |
| UIDU | Urban Industrial | PAST | Pasture/Hay |
| UTRN | Urban Transportation | AGRR | Row Crops |
| SWRN | South Western Range + Bare Rock | AGRC | Small Grains |
| SWRN | South Western Range + Quarries/Mines | AGRL | Generic |
| SWRN | South Western Range | WETF | Woody Wetlands |
| FRSD | Deciduous Forest | WETN | Emergent/Herbaceous Wetlands |

Table 3.7. Ergene Watershed according to ArcSWAT Generic Land Cover Classification

| SWAT Code | AGRC | AGRL | AGRR | FESC | FRSD | FRSE | FRST | ORCD | PAST | RNGB | RNGE | SWRN | SWRN | SWRN | UCOM | UIDU | UINS | URHD | URML | UTRN | WATR | WETF | WETN |
|---|---|---|---|---|---|---|---|---|---|---|---|---|---|---|---|---|---|---|---|---|---|---|---|
| CORINE Code & Color | 222<br>2222<br>2221 | 211<br>212<br>213<br>2112<br>2121<br>2122 | 244<br>243<br>242<br>241 | 141<br>142 | 311 | 312 | 313 | 221<br>223 | 231 | 324<br>322<br>323 | 321 | 332<br>3322 | 131<br>3321 | 333 | 121 | 121<br>132<br>133 | 121 | 111 | 112<br>1121<br>1122 | 122<br>123<br>124 | 511<br>512 | 411<br>412 | 421<br>422<br>423 |
| % | 0,01 | 62,8 | 10 | 0,1 | 4,8 | 1,3 | 1,5 | 1,3 | 5,5 | 7,5 | 1,5 | 0,01 | 0,01 | 0,4 | 0,1 | 0,6 | 0,1 | 0,1 | 2,28 | 0,2 | 0,5 | 0,1 | 0,1 |

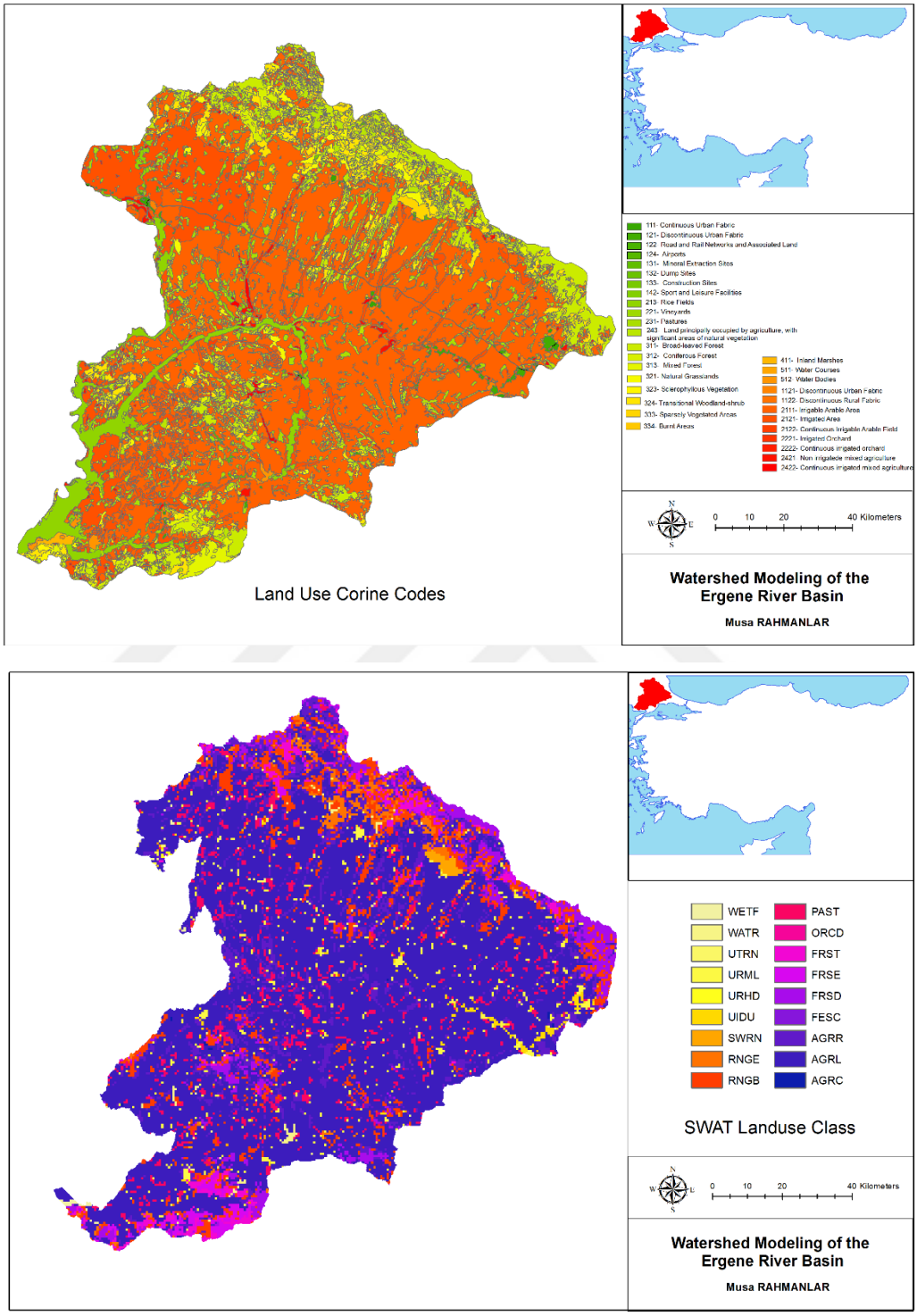


Figure 3.14. CORINE Classification Versus ArcSWAT Landuse After Reclassification.

Soil Data is crucial for calculation of hydrological response units. Therefore soil map quality directly effects the quality of the model. In other SWAT studies, most of researchers

used Soil Survey Geographic Database (SSURGO) or Food and Agricultural (FAO) soil library which is created for MWSWAT2012. But these sources are used generally for basic models. In this study, soil types were obtained from the Turkish Ministry of Energy and Natural Resources-General Directorate of Mining Technical Research and Turkish Ministry of Agriculture and Forestry. However, despite the fact that the Ministries are using FAO's 1/25.000 scale National Soil Database, this database is different from the classification used by SWAT. This database use sample large soil class group classification that is summarized in table 3.8. In this classification soils were scored according to Slope, Depth, Drainage, Impression, Salt, Alkali, Erosion Levels, Land Use Capability Classification, Land Use Capability Subclasses.

Table 3.8. 1/25 000 Scale National Soil Database.

| Large Soil Group Slope Depth Combination | | | | | | | | |
|---|---|---|---|---|---|---|---|---|
| Large Soil Group | | Slope Depth Combination | | | | | | |
| Symbol | Description | | Slope % | Depth (cm) | | | | |
| | | | | A Deep | B Med. Deep | C Shallow | D Very Shal. | E Litosolic |
| P<br>G<br>M | Red Yellow Podzolic Soils<br>Gray Brown Podzolic Soils<br>Brown Forest Lands | 1 | A<br>0 – 2 | 1 | 2 | 3 | 4 | 25 |
| N<br>CE<br>D | Lime-free Brown Forest Soils<br>Chestnut Soils<br>Reddish Chestnut color Soils | 2 | B<br>2 – 6 | 5 | 6 | 7 | 8 | 26 |
| T<br>E<br>B<br>U<br>F | Red Mediterranean Lands<br>Red Brown Mediterranean Lands<br>Brown Soils<br>Lime Brown Soils<br>Reddish Brown Soils | 3 | C<br>6 – 12 | 9 | 10 | 11 | 12 | 27 |
| R<br>V<br>Z<br>L | Rendzina Soils<br>Vertisol Soils<br>Sierozem Soils<br>Regosols Soils | 4 | D<br>12 – 20 | 13 | 14 | 15 | 16 | 28 |
| X<br>Y<br>A<br>H | Basaltic Soils<br>High Mountain Meadow Lands<br>Alluvial Soils<br>Hidromorphic Soils | 5 | E<br>20 – 30 | 17 | 18 | 19 | 20 | 29 |
| S<br>K<br>C<br>O | Alluvial Coastal Soils<br>Colluvial Soils<br>Salt Alkali Soils<br>Organic Soils | 6 | F<br>30 + | 21 | 22 | 23 | 24 | 30 |

Like landuse data, soil types input table have to be constructed according to region needs for SWAT input. In this step a literature survey is done and sample data were compared with Paçal (2017) and Altürk (2017) studies. These studies' soil data were compared with MSWAT2012-FAO database and according to results, new soil map were designed (Figure 3.15).

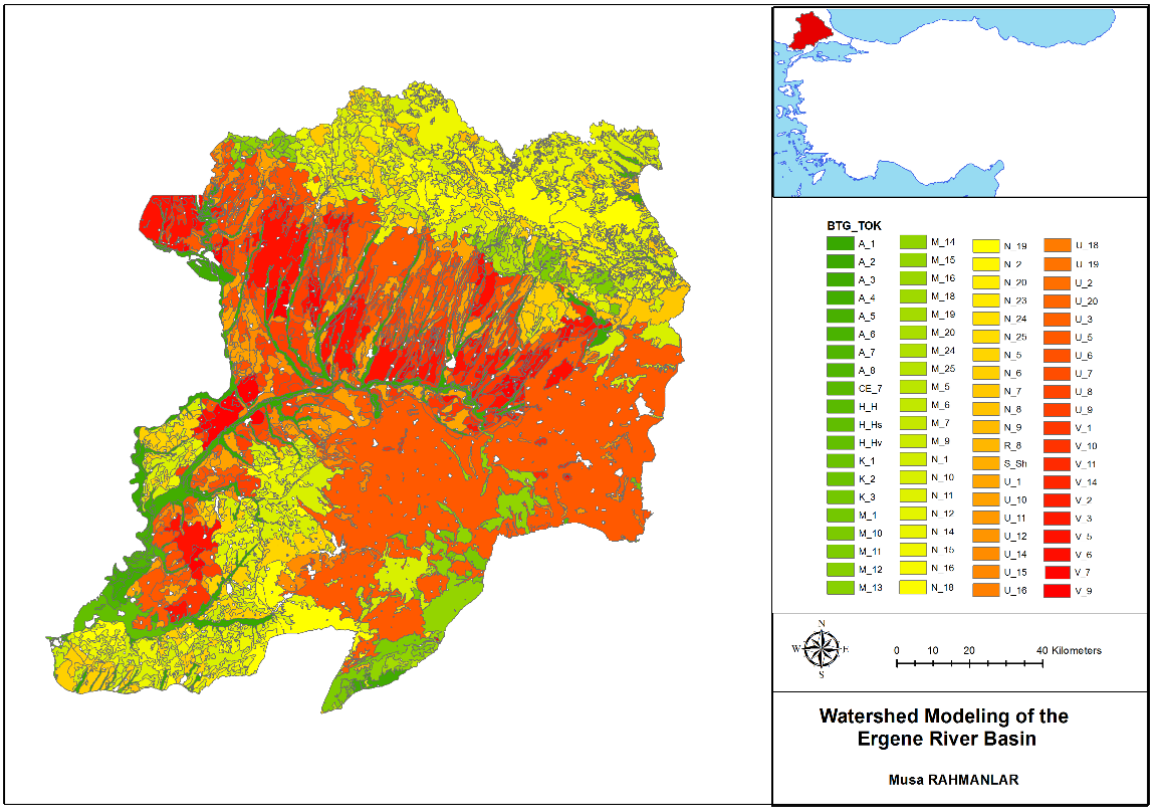


Figure 3.15. Soil Map According to Scale National Soil Database.

According to Scaled National Soil Database, the studied area in Ergene Basin consisted of hydromorphic soils (H) (0.44%), rendzinas (R) (0.02%), alluvial soils (A) (6.76%), brown forest soil (M) (3.66%). In the studied area, the main soil types were vertisols (V) (14.54%), brown soils without lime (U) (47.55 %) and brown forest soils without lime (N) (27.03%) (Figure 3.16).

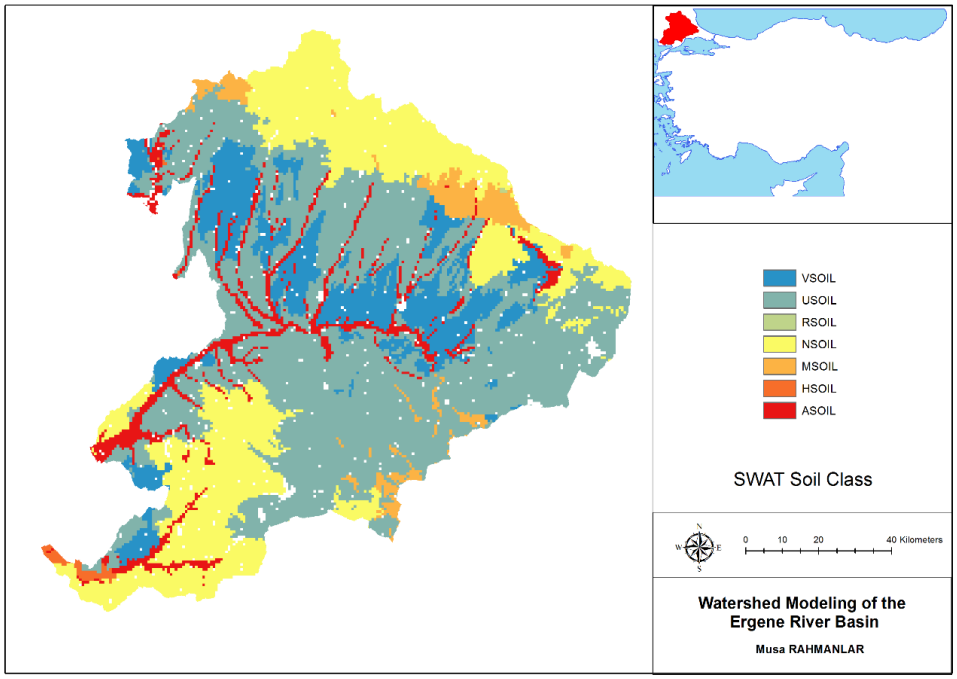


Figure 3.16. ArcSWAT Soil Map After Reclassification.

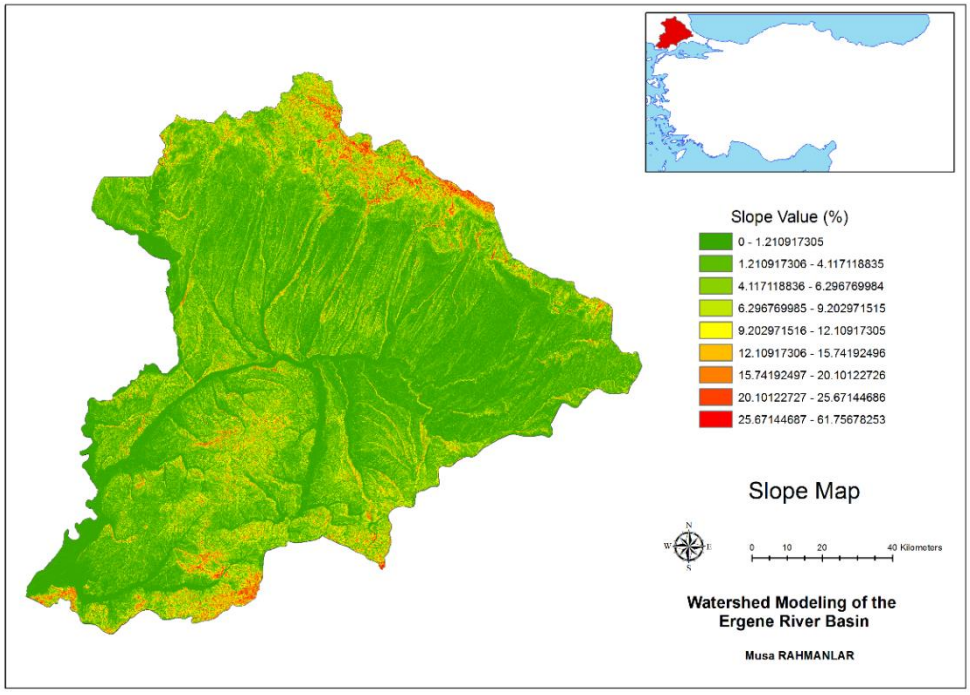


Figure 3.17. ArcSWAT Slope Map After Reclassification.

SWAT model can create its own slope map according to topographical data (DEM). User has to define slope boundaries for characteristics of the basin. According to user

knowledge, SWAT separates sub basins to multiple slope divisions. Therefore before modeling slope, slope percentage distribution of the basin have to be investigated. Slope map of Ergene Basin was constructed by using DEM data with ArcGIS program and boundaries of slope is defined according to general view of slope map (Figure 3.17). From results multiple slope modeling was selected as option. Region categorized by four main slope classes (0-1.5 %), (1.5-5 %), (5-15 %), (15-9999 %) (Figure 3.17).

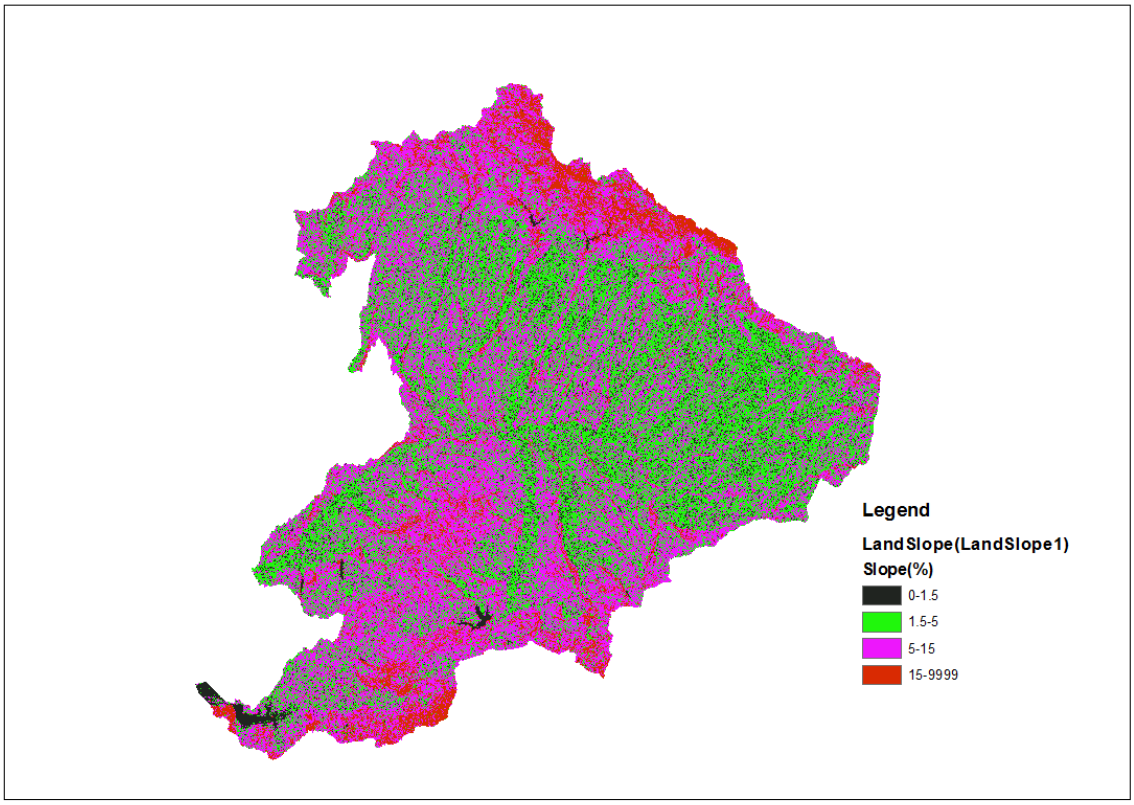


Figure 3.18. ArcSWAT Slope Map after Reclassification.

After defining three main input data, HRU definition menu becomes active. There are four methods for HRU definition: Dominant Landuse, Dominant HRU, Certain Number of HRU, Multiple HRU. First three methods are preferred from researchers to shorten the process time of SWAT. But for detail studies multiple HRU option is preferred to obtain realistic results. These methods are defined in Table 3.9. In this study, Multiple HRU option preferred to increase detail of watershed data.

Table 3.9. SWAT HRU Options

| | |
|---|---|
| Dominant Landuse | Landuse with biggest area applied whole basin |
| Dominant HRU | Largest potential HRU applied to whole basin |
| Certain Number of HRU | HRU's are limited according to maximum number |
| Multiple HRU | Unimportant percentage of landuse and soil are excluded |

3.2.2.2. Weather Data. SWAT requires daily meteorological data that could be obtained from measured data set or be generated by a weather simulation model. Essential climatic variables are temperature (min and max), precipitation, solar radiation, wind speed and humidity. Meteorological data obtained from Edirne, Kırklareli, Çorlu, Tekirdağ, Uzunköprü, Lüleburgaz Tigem, İpsala meteorological service stations. Malkara and Çerkezköy station were used for substitute station to obtain lack data of rest stations (Table 3.10).

Table 3.10. Information about Meteorological Stations.

| ICAO | State | District | Station Name | Height | Latitude | Longtitude |
|---|---|---|---|---|---|---|
| EDIR | EDİRNE | MERKEZ | Edirne | 51 | 41.6767 | 26.5508 |
| KIRL | KIRKLARELİ | MERKEZ | Kırklareli | 232 | 41.7382 | 27.2178 |
| CORL | TEKİRDAĞ | ÇORLU | Çorlu | 145 | 41.1798 | 27.816 |
| TEKR | TEKİRDAĞ | MERKEZ | Tekirdağ | 4 | 40.9585 | 27.4965 |
| UZKP | EDİRNE | UZUNKÖPRÜ | Uzunköprü | 45 | 41.2726 | 26.7056 |
| LULE | KIRKLARELİ | LÜLEBURGAZ | Lüleburgaz Tigem | 46 | 41.3513 | 27.3108 |
| IPSL | EDİRNE | İPSALA | İpsala | 81 | 40.89 | 26.39 |
| MALK | TEKİRDAĞ | MALKARA | Malkara | 207 | 40.8873 | 26.908 |
| CRKZ | TEKİRDAĞ | ÇERKEZKÖY | Çerkezköy | 160 | 41.2607 | 27.9196 |

ArcSWAT uses climate module which consist of six components. WGEN component is the main database for climate model. It defines meteorological stations characters as average weather data, standard deviation, maximum precipitation hours, dew points, etc. In year 2018 TAMU (owner and Creator Company of SWAT) prepared an access file to manage this complex database. The database constructed automatically according to statistical weather data (temperature, precipitation, wind speed, humidity, and radiation) inputs.

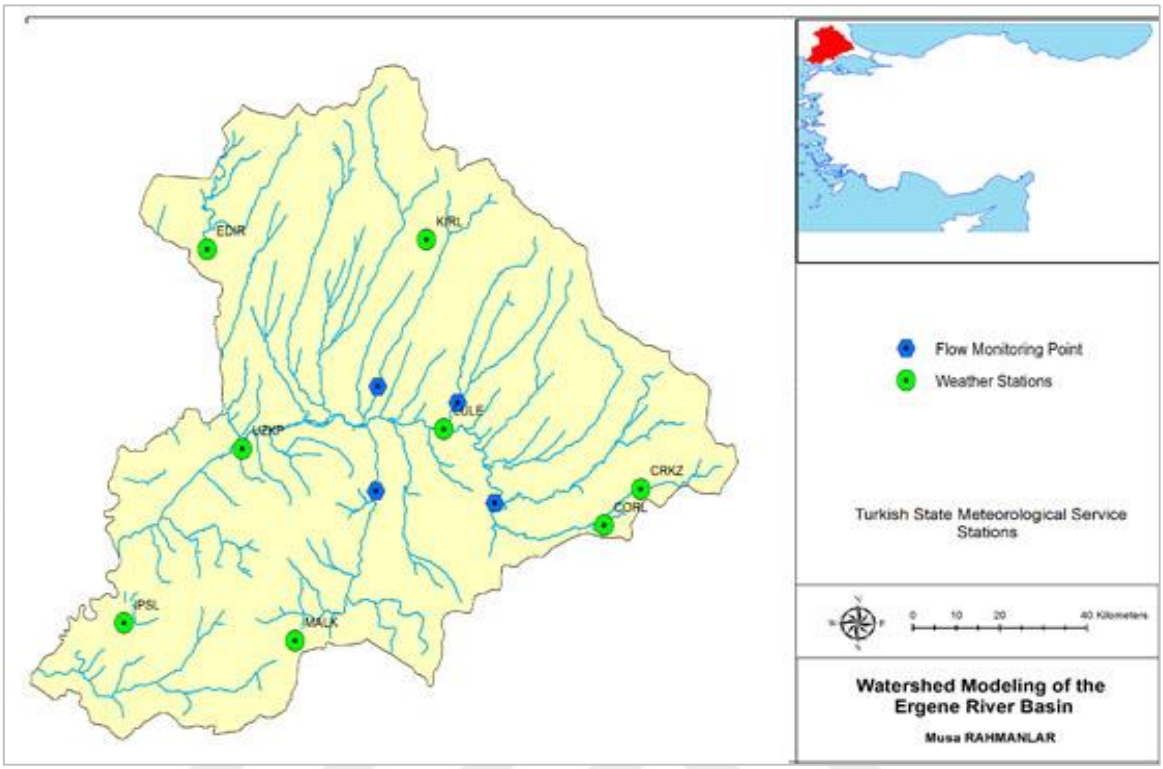


Figure 3.19. Meteorological Stations used in Model

Most of weather data sets have constructed between 1960-2017 years. Weather data availability of the region is summarized in below table. SWAT model needs daily data for modeling basin. It is usual that, in some season's climate data can not be recorded. SWAT model can not operate if the dates of climate data are incompatible, before model application input data are classified according to existence. To overcome this problem, neighbor stations were used as substitute data producers to complete daily records (Table 3.11).

Table 3.11. Ergene Meteorological Station Data Availability.

| Station Name | Max. Temprature | Min. Temprature | Avarege Humidity | Wind | Radiation | Daily Precipitation |
|---|---|---|---|---|---|---|
| **Edirne** | 1960-2017 | 1960-2017 | 1960-2017 | 1960-2017 | 1968-2009 | 1960-2017 |
| **Kırklareli** | 1960-2017 | 1960-2017 | 1963-2017 | 1960-2017 | 2007-2017 | 1960-2017 |
| **Çorlu** | 1960-2017 | 1960-2017 | 1960-2017 | 1960-2017 | N/A | 1960-2017 |
| **Tekirdağ** | 1960-2017 | 1960-2017 | 1960-2017 | 1960-2017 | 1983-2017 | 1960-2017 |
| **Uzunköprü** | 1965-2017 | 1962-2017 | 1965-2017 | 1962-2017 | 1985-2004 | 1965-2017 |
| **Lüleburgaz** | 1960-2017 | 1960-2017 | 1960-2017 | 1960-2017 | N/A | 1960-2017 |
| **Tigem İpsala** | 1963-2017 | 1963-2017 | 1963-2017 | 1963-2017 | 1976-2005 | 1963-2017 |
| **Malkara** | 1980-2017 | 1980-2017 | 1980-2017 | 1980-2017 | 1985-2006 | 1980-2017 |
| **Çerkezköy** | 2007-2017 | 2007-2017 | 2007-2017 | 2007-2017 | N/A | N/A |

### 3.2.3. Calibration & Validation

For calibration and validation steps, observed values are a need for testing the model. In Turkey, flow and water quality data are recorded by General Directorate of State Hydraulic Works (SHW). Flow data covers 2003-2010 years, water quality data covers 1985-2013 years.

Streams in the Ergene Basin's have different flow regimes. Lüleburgaz stream has highest flow capacity among others and also Şeytanderesi has the lowest. Also regimes can be varied according to ground water flows, snow melts and precipitation. For instance Lüleburgaz stream tripled its flow between years 2005 to 2010 (Figure 3.20).

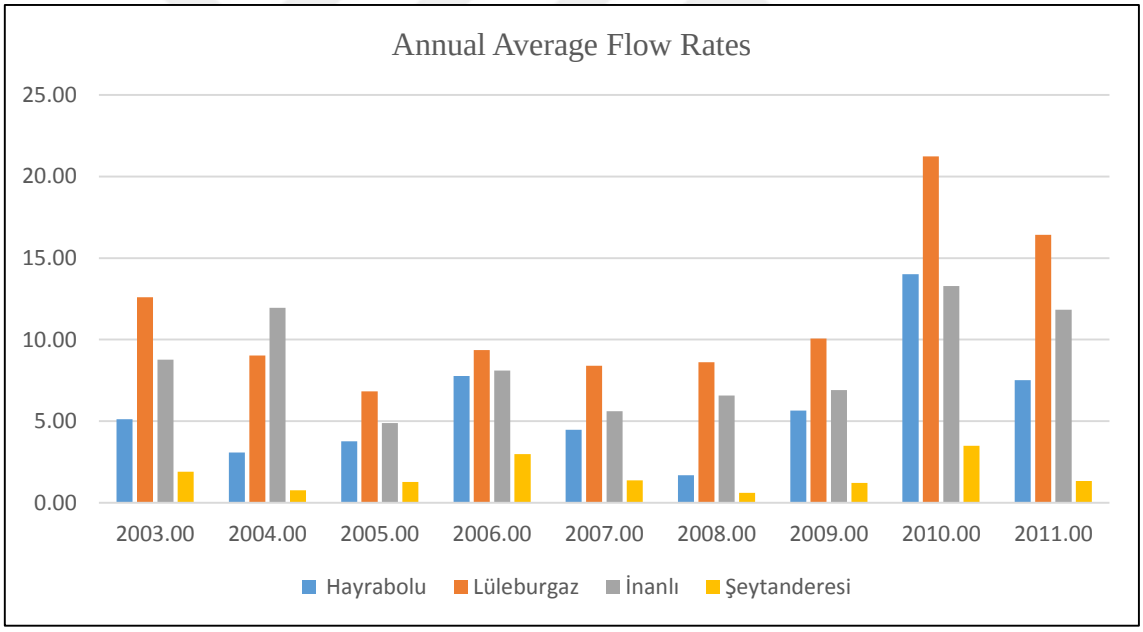


Figure 3.20. 2003-2011 years Hydrological Observation Stations Flow Data ($m^3$/sec).

SHW observation stations were chosen from different points in order to interpret the entire basin. 5 main observation points are shown in the figure 3.21. Due to flow regime, Şeytandere station neglected. In addition, Uzunköprü (Yenice-Görece) and Lüleburgaz stations are used as supplementary data stations for İnanlı stream which shows similar flow tendency with them. Quality of the observation data is a need for calibration. The lack of data may cause increase the potential of error therefore observation stations which have

continuous and accurate observation data were preferred. Thus İnanlı and Hayrabolu stations were used for calibration and validation step.

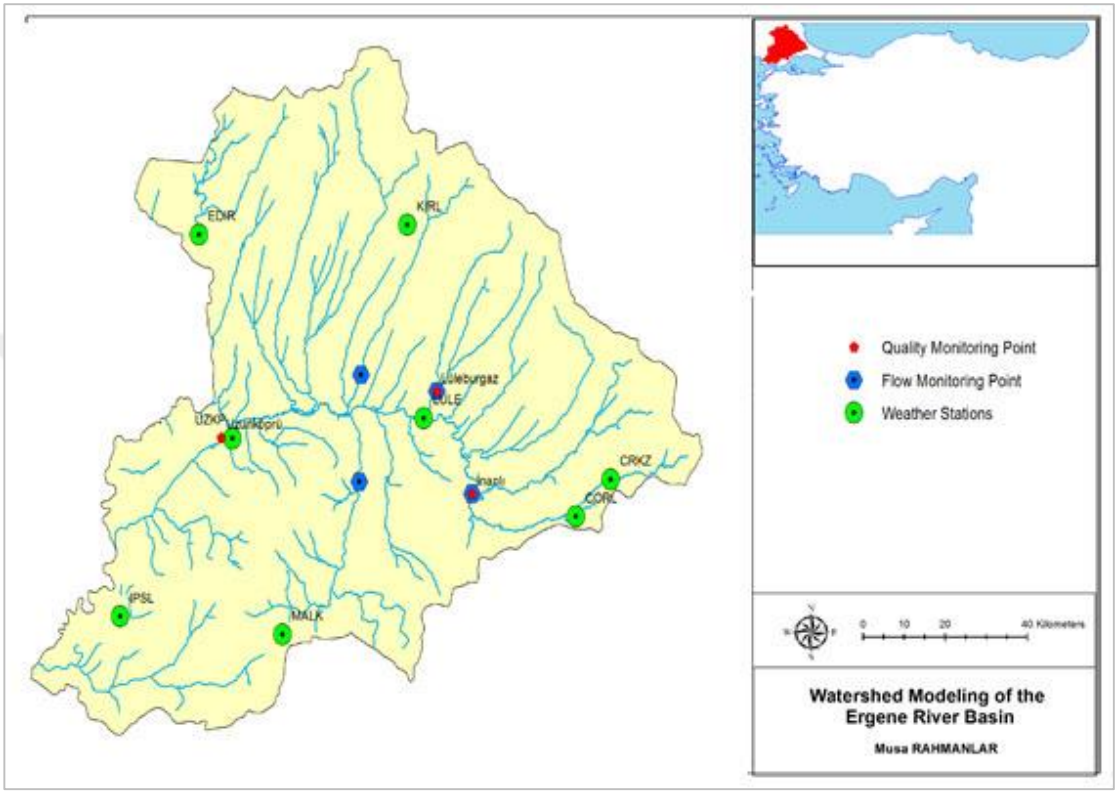


Figure 3.21. Hydrological Stations used in Model

### 3.2.4. Water Quality

SWAT builds a virtual basin which models flow according to LULC, weather, topography and slope data. After input process, SWAT becomes ready to summary real life hydrological events. Model can run for, daily, monthly and yearly time scale. Adding point loads is the last step of SWAT model. Industrial and domestic loads were obtained from the Ministry of Agriculture and Forestry. (Table 3.12 and 3.13) In order to integrate point load data to the SWAT program, the coordinates of them must be determined. SWAT suggests users to set up a hydrological model which gives satisfactory results before applying pollution loads into the model. Loads are defined as close to city centers (Figure 3.22).

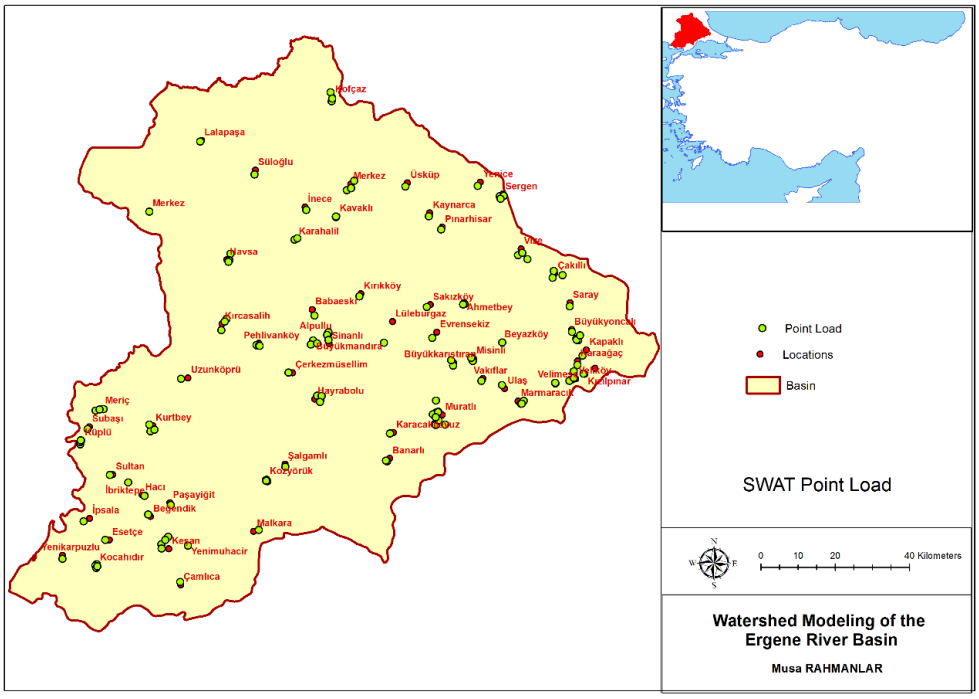


Figure 3.22. ArcSWAT Point Load Map.

34 points were described as domestic point sources, and 15 point were determined as industrial loads according to Ministry of Agriculture and Forestry's Reports. These data was classified according to sub basins of Ergene basin. Then these loads were used for SWAT input and shown in table 3.14.

Table 3.12. Ergene Basin Domestic Loads.

| Locations | m3/day Flow | kg/day NH4 | kg/day No3 | kg/day Org. P | kg/day Org. N | kg/day Orto P. | kg/day KOI |
|---|---|---|---|---|---|---|---|
| Edirne-İpsala-Yenikarpuzlu | 0.36 | 8.41 | 0 | 0.69 | 8.41 | 1.73 | 32.87 |
| Edirne-İpsala-Kocahıdır | 0.04 | 0.87 | 0 | 0.08 | 0.87 | 0.2 | 17.39 |
| Edirne-İpsala-Hacı<br>Edirne-İpsala- Hacı ,İbriktepe | 0.34 | 7.13 | 0 | 0.65 | 7.13 | 1.63 | 142.68 |
| Tekirdağ-Malkara-Kozyörük<br>Tekirdağ-Malkara-Malkara | 4.09 | 112.56 | 0 | 8.63 | 112.56 | 21.56 | 2251.25 |
| Tekirdağ-Çorlu-Marmaracık<br>Tekirdağ-Muratlı-Muratlı | 2.85 | 77.95 | 0 | 6.07 | 77.95 | 15.15 | 1511.16 |
| Tekirdağ-Saray-Büyükyoncalı | 1.27 | 35.37 | 0 | 2.7 | 35.37 | 6.74 | 707.47 |
| Tekirdağ-Saray-Saray | 2.98 | 82.69 | 0 | 6.31 | 82.69 | 15.74 | 1653.86 |
| Tekirdağ-Çorlu-Ulaş<br>Tekirdağ-Çorlu-Vakıflar | 0.83 | 21.68 | 0 | 1.79 | 21.68 | 4.46 | 381.58 |

Table 3.12. Ergene Basin Domestic Loads (cont.).

| Locations | m3/day Flow | kg/day NH4 | kg/day No3 | kg/day Org. P | kg/day Org. N | kg/day Orto P. | kg/day KOI |
|---|---|---|---|---|---|---|---|
| Kırklareli-Lüleburgaz-Büyükkarıştıran<br>Kırklareli-Vize-Çakıllı<br>Kırklareli-Vize-Vize | 3.1 | 35.5 | 18.83 | 3.9 | 35.5 | 9.74 | 747.04 |
| Tekirdağ-Çorlu-Misinli<br>Tekirdağ-Saray-Beyazköy<br>Kırklareli-Vize-Sergen | 0.18 | 3.8 | 0 | 0.35 | 3.8 | 0.87 | 76.05 |
| Kırklareli-Lüleburgaz-Ahmetbey<br>Kırklareli-Lüleburgaz-Evrensekiz | 0.52 | 13.47 | 0 | 1.11 | 13.47 | 2.77 | 237.08 |
| Kırklareli-Lüleburgaz-Lüleburgaz<br>Kırklareli-Pınarhisar-Kaynarca<br>Kırklareli-Pınarhisar-Pınarhisar | 16.89 | 33.07 | 186.1 | 11.17 | 33.07 | 27.87 | 2105.62 |
| Kırklareli-Pınarhisar-Yenice<br>Kırklareli-Babaeski-Babaeski<br>Kırklareli-Merkez-Kavaklı | 14.17 | 29.85 | 153.89 | 9.52 | 29.85 | 23.77 | 1795.76 |
| Kırklareli-Merkez-Merkez<br>Kırklareli-Babaeski-Karahalil<br>Kırklareli-Merkez-İnece | 0.43 | 11.15 | 0 | 0.92 | 11.15 | 2.29 | 196.17 |
| Edirne-Havsa-Havsa<br>Edirne-Süloğlu-Süloğlu | 1.61 | 40.51 | 0 | 3.34 | 40.51 | 8.33 | 537.47 |
| Kırklareli-Pehlivanköy-Pehlivanköy | 0.2 | 4.24 | 0 | 0.39 | 4.24 | 0.97 | 84.84 |
| Edirne-Uzunköprü-Kırcasalih | 0.24 | 6.36 | 0 | 0.52 | 6.36 | 1.31 | 112 |
| Edirne-Lalapaşa-Lalapaşa | 0.19 | 3.51 | 0 | 0.32 | 3.51 | 0.8 | 15.62 |
| Tekirdağ-Merkez-Banarlı<br>Tekirdağ-Merkez-Karacakılavuz | 0.51 | 12.63 | 0 | 1.06 | 12.63 | 2.65 | 228.18 |
| Tekirdağ-Hayrabolu-Şalgamlı | 0.17 | 3.47 | 0 | 0.32 | 3.47 | 0.79 | 69.35 |
| Tekirdağ-Hayrabolu-Çerkezmüsellim | 0.34 | 8.8 | 0 | 0.73 | 8.8 | 1.81 | 154.95 |
| Edirne-İpsala-Kocahıdır<br>Edirne-Keşan-Beğendik | 0.38 | 8.79 | 0 | 0.73 | 8.79 | 1.83 | 53.02 |
| Edirne-Keşan-Çamlıca | 0.12 | 2.51 | 0 | 0.23 | 2.51 | 0.57 | 50.27 |
| Edirne-Keşan-Keşan | 8.76 | 255.41 | 0 | 18.37 | 255.41 | 45.85 | 5254.09 |
| Edirne-İpsala-Esetçe | 0.11 | 2.78 | 0 | 0.23 | 2.78 | 0.57 | 48.93 |
| Kırklareli-Lüleburgaz-Sakızköy<br>Tekirdağ-Muratlı-Muratlı | 0.23 | 6.15 | 0 | 0.47 | 6.15 | 1.19 | 123.07 |
| Kırklareli-Babaeski-Alpullu, Büyükmandıra<br>Kırklareli-Babaeski-Sinanlı<br>Kırklareli-Lüleburgaz-Kırıkköy | 1.21 | 29.35 | 0 | 2.48 | 29.35 | 6.19 | 480.3 |
| Kırklareli-Merkez-Üsküp<br>Edirne-İpsala-Sultan<br>Edirne-Uzunköprü-Kurtbey | 6.28 | 14.57 | 57.58 | 4.05 | 14.57 | 10.11 | 736.57 |
| Edirne-Uzunköprü-Uzunköprü<br>Tekirdağ-Çerkezköy-Çerkezköy Kapaklı Velimeşe<br>Tekirdağ-Çerkezköy-Kapaklı, Karaağaç<br>Tekirdağ-Çerkezköy-Kızılpınar, Veliköy | 27.82 | 801.39 | 0 | 58.49 | 801.39 | 146.02 | 16303.26 |
| Tekirdağ-Çorlu-Velimeşe<br>Edirne-Uzunköprü-Kırcasalih | 0.12 | 3.18 | 0 | 0.26 | 3.18 | 0.65 | 56 |
| Edirne-Meriç-Küplü Subaşı Merkez<br>Edirne-Meriç-Meriç<br>Edirne-Meriç-Subaşı | 26.35 | 683.14 | 0 | 49.39 | 683.14 | 123.3 | 13977.62 |
| Edirne-Merkez-Merkez<br>Edirne-İpsala-İpsala | 0.62 | 16.26 | 0 | 1.34 | 16.26 | 3.34 | 286.12 |
| Kırklareli-Babaeski-Büyükmandıra Tekirdağ-Hayrabolu-<br>Tekirdağ-Hayrabolu-Hayrabolu | 2.54 | 70.19 | 0 | 5.37 | 70.19 | 13.42 | 1395.27 |

Table 3.13. Ergene Basin Industrial Loads.

| | m3/day Flow | kg/day NH4 | kg/day No3 | kg/day Org. P | kg/day Org. N | Orto P. | kg/day KOI |
|---|---|---|---|---|---|---|---|
| Tekirdağ-Çorlu-Marmaracık | | | | | | | |
| Tekirdağ-Muratlı-Muratlı | 44.50 | 289.85 | 136.40 | 30.53 | 596.75 | 55.83 | 17688.00 |
| Tekirdağ-Çorlu-Ulaş | | | | | | | |
| Tekirdağ-Çorlu-Vakıflar | 37.26 | 731.57 | 140.38 | 341.28 | 524.72 | 150.89 | 42170.10 |
| Kırklareli-Lüleburgaz-Büyükkarıştıran | | | | | | | |
| Kırklareli-Vize-Çakıllı | | | | | | | |
| Kırklareli-Vize-Vize | | | | | | | |
| Tekirdağ-Çorlu-Misinli | | | | | | | |
| Tekirdağ-Saray-Beyazköy | 7.53 | 143.88 | 3.33 | 70.25 | 139.18 | 36.49 | 7478.02 |
| Kırklareli-Vize-Sergen | 0.00 | 0.00 | 0.00 | 0.00 | 0.00 | 0.00 | 0.00 |
| Kırklareli-Lüleburgaz-Ahmetbey | | | | | | | |
| Kırklareli-Lüleburgaz-Evrensekiz | 10.22 | 186.65 | 10.46 | 73.38 | 111.99 | 32.51 | 9377.50 |
| Kırklareli-Lüleburgaz-Lüleburgaz | | | | | | | |
| Kırklareli-Pınarhisar-Kaynarca | | | | | | | |
| Kırklareli-Pınarhisar-Pınarhisar | | | | | | | |
| Kırklareli-Pınarhisar-Yenice | 6.53 | 48.10 | 5.24 | 39.61 | 61.06 | 17.29 | 2815.18 |
| Kırklareli-Babaeski-Babaeski | | | | | | | |
| Kırklareli-Merkez-Kavaklı | | | | | | | |
| Kırklareli-Merkez-Merkez | | | | | | | |
| Kırklareli-Merkez-İnece | 0.99 | 4.33 | 0.00 | 3.16 | 5.84 | 1.49 | 306.90 |
| Edirne-Havsa-Havsa | | | | | | | |
| Edirne-Süloğlu-Süloğlu | 0.25 | 2.45 | 0.29 | 0.91 | 1.55 | 0.41 | 97.35 |
| Kırklareli-Pehlivanköy-Pehlivanköy | 0.00 | 0.00 | 0.00 | 0.00 | 0.00 | 0.00 | 0.00 |
| Edirne-Uzunköprü-Kırcasalih | 0.50 | 9.08 | 2.91 | 1.42 | 4.51 | 0.78 | 93.50 |
| Kırklareli-Lüleburgaz-Sakızköy | | | | | | | |
| Tekirdağ-Muratlı-Muratlı | 38.18 | 734.36 | 0.00 | 289.05 | 530.81 | 132.59 | 33077.55 |
| Kırklareli-Babaeski-Alpullu | | | | | | | |
| Kırklareli-Babaeski-Büyükmandıra | | | | | | | |
| Kırklareli-Babaeski-Sinanlı | | | | | | | |
| Kırklareli-Lüleburgaz-Kırıkköy | | | | | | | |
| Kırklareli-Merkez-Üsküp | 0.70 | 13.94 | 3.69 | 2.15 | 5.47 | 1.32 | 158.95 |
| Edirne-İpsala-Sultan | | | | | | | |
| Edirne-Uzunköprü-Kurtbey | | | | | | | |
| Edirne-Uzunköprü-Uzunköprü | 0.20 | 15.40 | 1.46 | 3.29 | 9.21 | 1.30 | 206.80 |
| Tekirdağ-Çerkezköy-Çerkezköy | | | | | | | |
| Tekirdağ-Çerkezköy-Kapaklı | | | | | | | |
| Tekirdağ-Çerkezköy-Karaağaç | | | | | | | |
| Tekirdağ-Çerkezköy-Kızılpınar | | | | | | | |
| Tekirdağ-Çerkezköy-Veliköy | | | | | | | |
| Tekirdağ-Çorlu-Velimeşe | 101.00 | 874.14 | 5.42 | 437.35 | 1802.68 | 112.86 | 65468.98 |
| Edirne-Uzunköprü-Kırcasalih | 0.04 | 4.40 | 1.10 | 0.66 | 1.10 | 0.44 | 44.00 |
| Edirne-Meriç-Küplü | | | | | | | |
| Edirne-Meriç-Meriç | | | | | | | |
| Edirne-Meriç-Subaşı | | | | | | | |
| Edirne-Merkez-Merkez | 0.16 | 17.60 | 4.40 | 0.70 | 4.40 | 0.00 | 2.82 |
| Edirne-İpsala-İpsala | 0.00 | 0.00 | 0.00 | 0.00 | 0.00 | 0.00 | 0.00 |
| Kırklareli-Babaeski-Büyükmandıra | | | | | | | |
| Tekirdağ-Hayrabolu-Hayrabolu | 0.00 | 0.00 | 0.00 | 0.00 | 0.00 | 0.00 | 0.00 |

Table 3.14. Ergene Total Loads for Sub-basins.

| sub | Total, Flow | Total, KOI | Total, Orto P. | Total, Org. N | Total, NH4 | Total, No3 | Total, Org. P |
|---|---|---|---|---|---|---|---|
| Sub1 | 0.25 | 15.62 | 0.80 | 3.51 | 3.51 | 0.00 | 0.32 |
| Sub12 | 1.91 | 639.25 | 7.50 | 34.81 | 43.29 | 3.69 | 4.63 |
| Sub17 | 27.25 | 14185.94 | 125.39 | 698.42 | 716.18 | 7.31 | 52.04 |
| Sub18 | 23.42 | 4920.79 | 45.16 | 94.12 | 81.17 | 191.34 | 50.78 |
| Sub19 | 0.20 | 84.84 | 0.97 | 4.24 | 4.24 | 0.00 | 0.39 |
| Sub2 | 0.43 | 196.17 | 2.29 | 11.15 | 11.15 | 0.00 | 0.92 |
| Sub20 | 0.16 | 100.00 | 1.09 | 4.28 | 7.58 | 1.10 | 0.92 |
| Sub21 | 21.66 | 19305.22 | 71.42 | 254.73 | 404.05 | 20.91 | 149.32 |
| Sub26 | 10.63 | 8225.07 | 46.23 | 174.68 | 179.38 | 22.16 | 74.15 |
| Sub27 | 0.34 | 154.95 | 1.81 | 8.80 | 8.80 | 0.00 | 0.73 |
| Sub28 | 76.81 | 66401.24 | 267.55 | 1073.92 | 1481.03 | 0.00 | 579.05 |
| Sub29 | 42.34 | 44913.00 | 177.83 | 664.46 | 871.31 | 140.38 | 352.07 |
| Sub30 | 176.17 | 100971.40 | 329.85 | 3278.77 | 2043.33 | 141.82 | 532.43 |
| Sub31 | 1.02 | 456.35 | 5.31 | 25.26 | 25.26 | 0.00 | 2.13 |
| Sub32 | 6.48 | 943.37 | 11.41 | 23.78 | 29.97 | 59.03 | 7.34 |
| Sub33 | 0.34 | 142.68 | 1.63 | 7.13 | 7.13 | 0.00 | 0.65 |
| Sub35 | 2.70 | 1464.62 | 14.21 | 73.66 | 73.66 | 0.00 | 5.69 |
| Sub37 | 4.09 | 2251.25 | 21.56 | 112.56 | 112.56 | 0.00 | 8.63 |
| Sub38 | 8.86 | 5303.01 | 46.42 | 258.19 | 258.19 | 0.00 | 18.59 |
| Sub39 | 0.12 | 50.27 | 0.57 | 2.51 | 2.51 | 0.00 | 0.23 |
| Sub4 | 23.42 | 4920.79 | 45.16 | 94.12 | 81.17 | 191.34 | 50.78 |
| Sub40 | 0.42 | 70.41 | 2.03 | 9.66 | 9.66 | 0.00 | 0.81 |
| Sub5 | 3.72 | 1269.64 | 17.48 | 84.13 | 85.92 | 0.58 | 8.50 |
| Sub8 | 15.15 | 2102.66 | 25.26 | 35.69 | 34.18 | 153.89 | 12.68 |

# 4. MODEL RESULTS

2003-2010 years data was used for the model calibration and validation. Warm up period is applied for SWAT model to prepare model for groundwater flow estimation. In warm up period, model uses input data as a preparation step for calibration and validation. Model would not give results about this period. Therefore two year (2003-2004) period implied for Ergene basin. After that 2005-2007 years data was used for calibration period. During this period sensitive parameter analysis was done to determine which parameters are more significant. Obtained parameter values were used in validation step. Lastly, 2008-2010 years observation data was used for validation of the model.

## 4.1. Calibration of Model

A watershed model consists of huge parameters and factors which directly affect hydrological behavior of model. Number of parameters proportionally related with uncertainties of the model. Abbaspour (2008) summarized these uncertainties as: simplification of model, processes not included in model, processes included, but not applied from modeler. Sensitivity analysis is the process of specifying the rate of change in model input parameters related to changes in model output parameters.

The parameter sensitivity analysis was applied by using the SWAT-CUP program with SUFI-2 algorithm. SWAT-CUP model was preferred for its wide range applicability for all type of watersheds and its different techniques to assess the model uncertainty and calibration. There are two methods of uncertainty analysis in SUFI-2: One at a time analysis and the other one is global sensitivity analysis. One at a time analysis measure sensitivity of a parameter when rest parameters are constant. Global sensitivity analysis measure sensitivity of a parameter when all related parameters change simultaneously. In this study global sensitivity analysis was chosen for application.

Global sensitivity analysis determines each parameters sensitivity by “P-value” & “t-Stat”. P values determine the significance of sensitivity. Its value changes between “0” and

“1”; as closer to “0” value is most significant and “1” is less. A predictor that has a low p-value is likely to be a meaningful addition to the model because changes in the predictor's value are related to changes in the response variable. So that parameter is very sensitive. The t-stat is the coefficient of a parameter divided by its standard error. It is a measure of the precision with which the regression coefficient is measured. If a coefficient is “large” compared to its standard error, then it is probably different from 0 and the parameter is sensitive. To summarize: for high sensitivity, t values have to be far from zero and p values have to close to the zero value. Number of iteration is defined from SUFI-2 program, but generally model can easily reach good fit at the start of iteration procedure. For example, iterating 500 times causes waste of time, due to best fit obtained in $10^{th}$ iteration.

ArcSWAT has approximately 100 parameters for calibration but it is not possible to run all parameters in the sensitivity analysis. Besides, increasing number of parameters may cause the model not to fit observations. Therefore a literature survey was completed before calibration. Six studies were investigated from researches and shown in table 4.1. All of these studies were related with watershed modeling. The number of parameters which were taken into account were related with the study’s topic. Some of them just modeled the hydrology of model some of them also calculated water quality.

Parameters were determined according to response of model. But generally, as shown in table 4.1, four parameters are common for calibration step. These are Baseflow Recession Constant (ALPHA_BF.gw), Groundwater Delay Time (GW_DELAY.gw), Initial Curve Number for Moisture Condition II (CN2.mgt), Available Water Capacity of the Soil Layer (SOL_AWC.sol). And SWAT_CUP advice to calibrate Threshold Water Level in Shallow Aquifer for Baseflow (GWQMN) parameter for good results.

Table 4.1. Calibration Parameters Used in Studies.

| Parameters | Definition | Abdelwahaba *et al.* | Cerkasova *et al.* | Thavhana *et al.* | Andrade *et al.* | Paçal | Altürk |
|---|---|---|---|---|---|---|---|
| ALPHA_BF.gw | Baseflow alpha factor (days). | + | + | + | + | + | + |
| ALPHA_BNK.rte | Baseflow alpha factor for bank storage | | | + | | | |
| CANMX.hru | Maximum canopy storage | | + | | | + | |
| CH_K2.rte | Effective hydraulic conductivity in main channel alluvium | + | | + | | | |
| CH_N2.rte | Manning's "n" value for the main channel. | | | | + | + | + |
| CMN.bsn | Rate factor for humus mineralization of active organic nitrogen. | | + | | | | |
| CN2.mgt | SCS runoff curve number f | + | | + | + | + | + |
| ERORGN.hru | Organic N enrichment ratio. | | + | | | | |
| ERORGP.hru | Organic P enrichment ratio | | + | | | | |
| EPCO.hru | Plant uptake compensation factor. | | | | | + | |
| ESCO.hru | Soil evaporation compensation factor. | | | + | | + | |
| GW_DELAY.gw | Groundwater delay (days). | + | + | + | + | + | + |
| GW_REVAP.gw | Groundwater "revap" coefficient. | + | | + | | + | + |
| GWQMN.gw | Treshold depth of water in the shallow aquifer required for return flow to occur (mm). | + | + | + | + | | |
| HLIFE_NGW.pst | Half-life of nitrate in the shallow aquifer (days) | | + | | | | |
| N_UPDIS.bsn | Nitrogen uptake distribution parameter | | + | | | | |
| OV_N.hru | Manning's "n" value for overland flow. | + | | | | | |
| PPERCO.bsn | Phosphorus percolation coefficient. | | + | | | | |
| RCHRG_DP.gw | Deep aquifer percolation fraction. | | | + | | | |
| REVAPMN.gw | Threshold depth of water in the shallow aquifer for "revap" to occur (mm). | | | + | | | |
| SMFMX.bsn | Maximum melt rate for snow during year (occurs on summer solstice) | | + | | | | + |
| SOL_AWC.soL | Available water capacity of the soil layer. | + | + | + | + | | + |
| SOL_K.sol | Saturated hydraulic conductivity. | | + | + | + | | + |
| SOL_Z.sol | Depth from soil surface to bottom of layer. | | | + | | | |
| SURLAG.bsn | Surface runoff lag time. | | | + | | + | |

In our study, model was run for years 2003-2010 (8 years). 2 years (2003-2004) are used for warm up period, (2005-2007) 3 years for calibration period and 3 years (2008-2010) for validation period of SWAT model. 11 model input parameters (CN2, ALPHA_BF, GW_DELAY, GWQMN, CANMX, EPCO, ESCO, SOL_AWC, GW_REVAP, OV_N and RAINHHMX) were selected by using monthly flow data of Hayrabolu and Seytandere streams for sensitivity analysis and calibration period of the SWAT model.

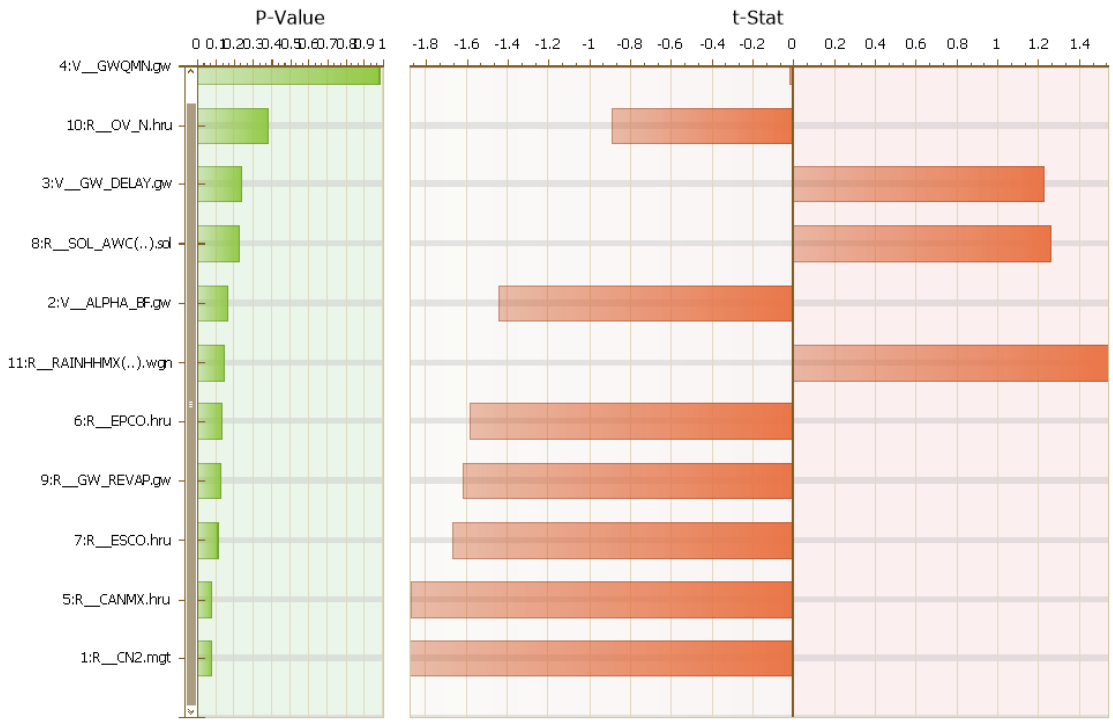


Figure 4.1. Sensitivity Analysis of Parameters for Calibration.

CN2 is a function of soil properties for moisture condition, ALPHA_BF is an indicator of recharge change of groundwater flow, GW_DELAY is the lag time between water enters shallow aquifer and exits the soil profile. GWQMN is limit depth value for return flow to occur. GW_REVAP is a factor related with water moves from shallow aquifer to unsaturated zone. CANMX is a function of density of plant cover, and known as maximum canopy storage. EPCO is another factor related with plants, its plant uptake these factors manage the depth distribution of water in soil layers for the fulfillment of plant evaporative and soil evaporative demand. SOL_AWC is the water capacity of the soil layer. OV_N is

manning's n value which is characterized according to land surface. Different from studies that investigated, RAINHMX parameter also observed. Many researchers advice to analyze weather and soil input data for sensitivity. Therefore due to different raining regime RAINHMX parameter added as sensitive parameter. This parameter has 0.1 probability value which shows its significance. Figure 4.1 also showed the global sensitivity analyses result for parameters. According to the analyses, CN2, was found to be the most sensitive in stream flow simulation, followed by CANMX, ESCO parameters. In this procedure, GWNQMN, OV_N were found to be less sensitive parameters. In this sensitivity analysis, the changes in both CN2 and CANMX had crucial effect on simulated stream flow. The majority of the parameters which were used for model were directly related with base flow and groundwater factors and surface water which signifies the groundwater component of the water balance in the watershed; this also highlighted the fact that the interaction between surface and groundwater played an important role in the overall dynamics of the basin. Table 4.2 showed the fitted values of the hydrological parameters for monthly calibration.

Table 4.2. Parameter Calibration Results of Study.

| Parameter_Name | Fitted_Value | Min_value | Max_value |
|---|---|---|---|
| 1:R__CN2.mgt | 0.073 | -0.2 | 0.2 |
| 2:V__ALPHA_BF.gw | 0.15 | 0 | 1 |
| 3:V__GW_DELAY.gw | 387 | 30 | 450 |
| 4:V__GWQMN.gw | 1.9 | 0 | 2 |
| 5:R__CANMX.hru | 18.33 | 0 | 100 |
| 6:R__EPCO.hru | 0.983 | 0 | 1 |
| 7:R__ESCO.hru | 0.75 | 0 | 1 |
| 8:R__SOL_AWC(..).sol | 0.916 | 0 | 1 |
| 9:R__GW_REVAP.gw | 0.179 | 0.02 | 0.2 |
| 10:R__OV_N.hru | 0.587 | 0.01 | 1 |
| 11:R__RAINHHMX(..).wgn | 89.583 | 0 | 125 |

Hayrabolu and İnanlı stream were used for calibration of the model, results were tested with SUFI-Cup model, and calibration results were shown in figure 4.2 and figure 4.3. For Hayrabolu stream, monthly $R^2$ value was obtained as 0.72 and Nash_Sutcliff value was calculated as 0.68, where p factor was 0.75 and r factor was 1.62. İnanlı stream had low

$R^2$ 0.55 due to anthropogenic effects of industry, its results were investigated for following years.

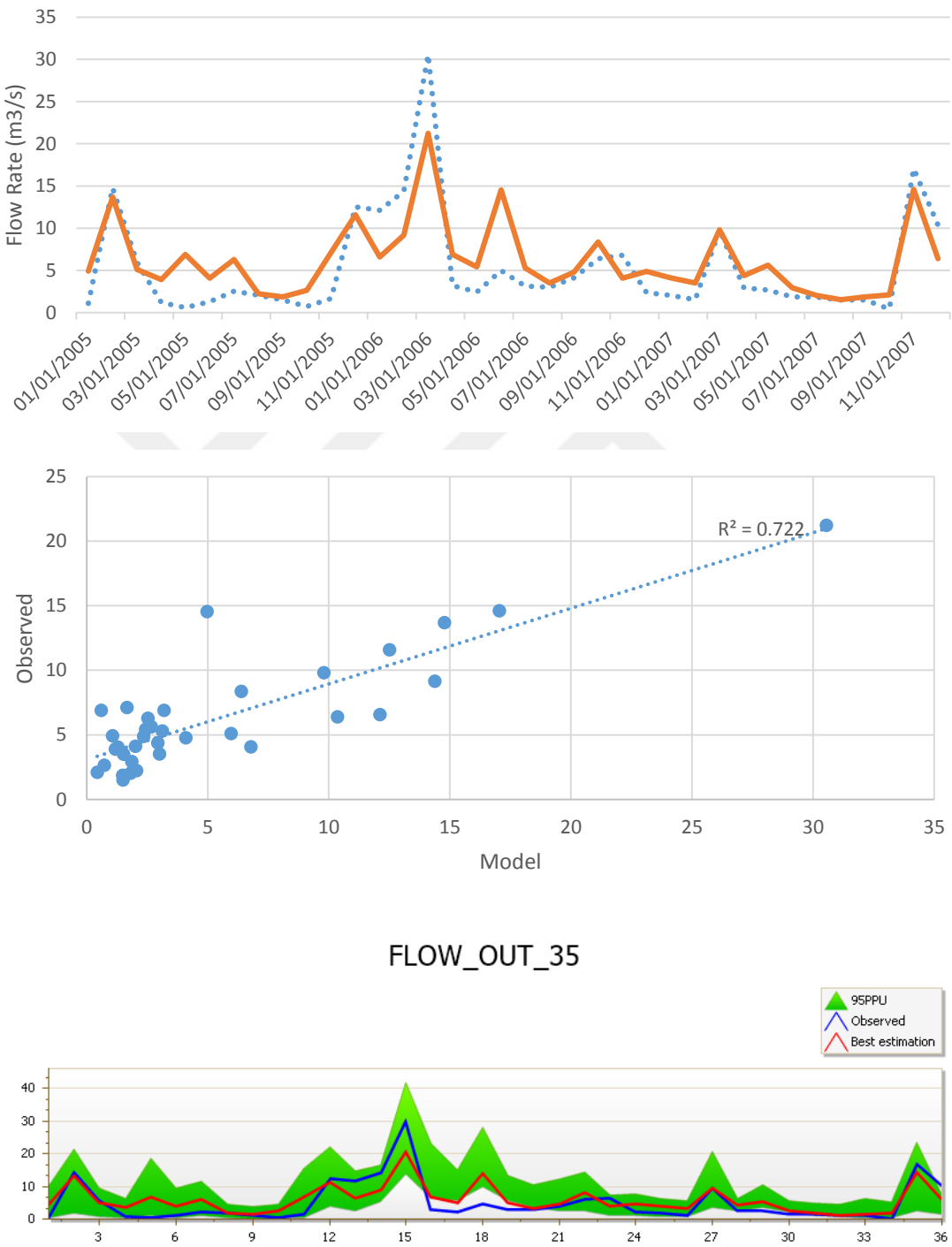


Figure 4.2. Model & Observation flow data comparison for Hayrabolu Stream. (First: Monthly comparison, Second: $R^2$ test, Third: Calibration with Swat CUP)

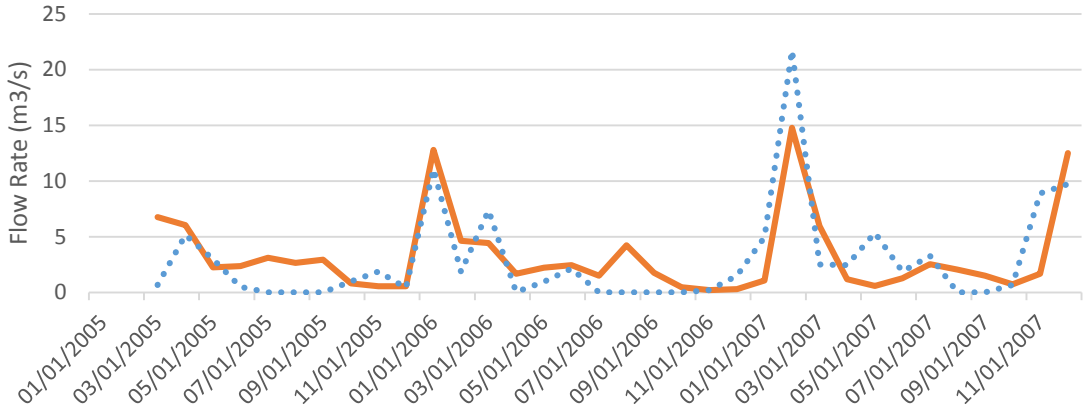


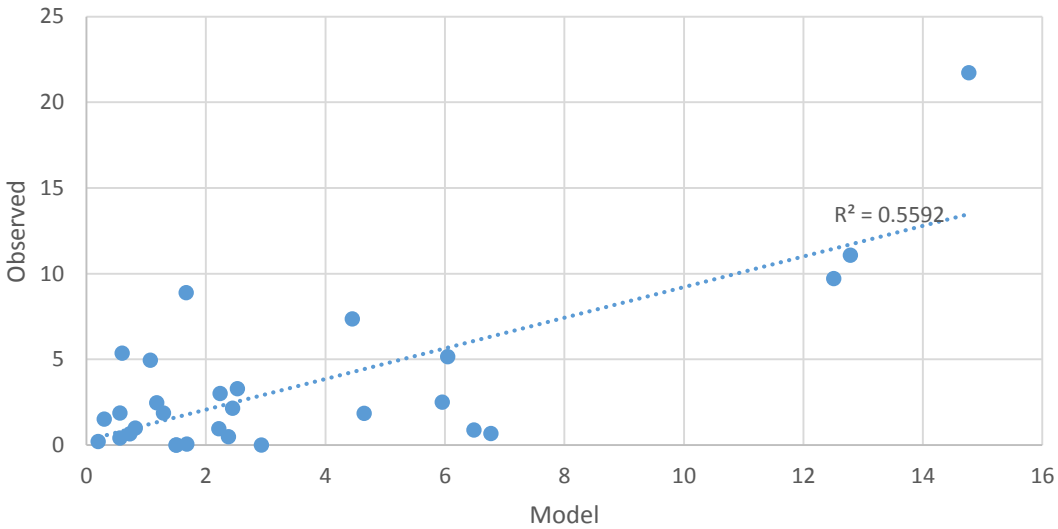


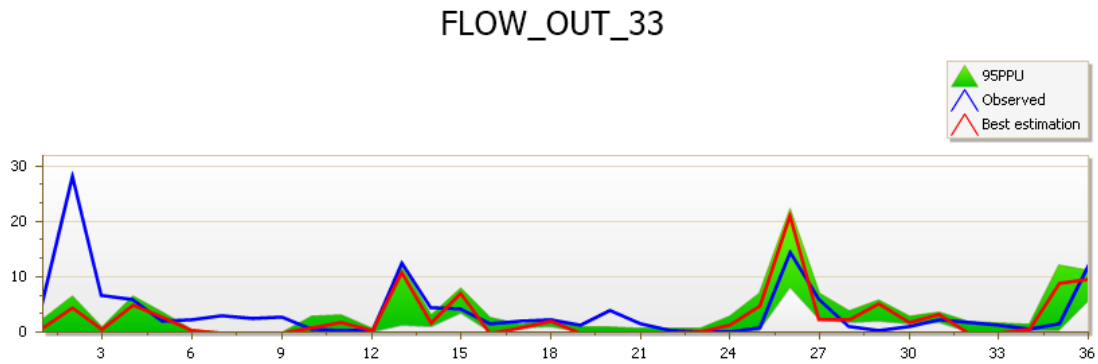


Figure 4.3. Model & Observation flow data comparison for İnanlı Stream. (First: Monthly comparison, Second: $R^2$ test, Third: Calibration with Swat CUP)

## 4.2. Validation of Model

It can be said that the model and observation results calibrated with SWAT-CUP software give statistically significant results both in the calibration phase and in the verification phase. The most important reason for the selection period of 2008-2010 for the validation period was the relationship between the model and observed data was very high for İnanlı and Hayrabolu streams. In some seasons, model could not give satisfactory results according to observed flows. One of the most important reasons for this was that the rainfall data observed in this period could not represent the exact precipitation-flow relationship in the basin. Another important factor affecting the statistical test results was that the measurement period of current data was short. Long-term observation data were needed for monthly calibration.

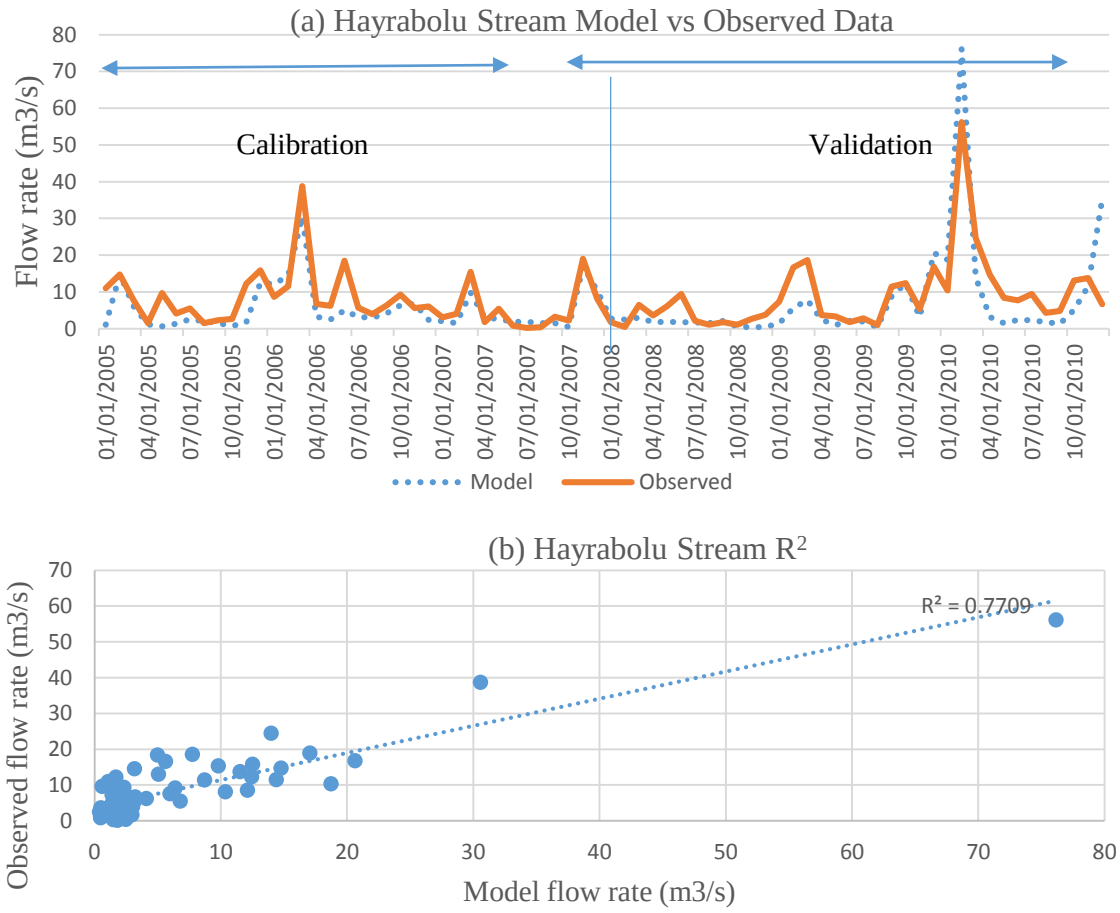


Figure 4.4. Model and Observed data Comparison According to Months (a) and Determination Coefficient of Hayrabolu Stream (b).

The results of the calibration and validation process of the model for the flow of the Hayrabolu and İnanlı streams were illustrated in Figure 4.4 and 4.5. The calibration and validation process was conducted using monthly time series. Generally, estimated flow of model was consistent with observed values of Hayrabolu and İnanlı streams. Especially, model reached peak values in the same period with the observed flow data.

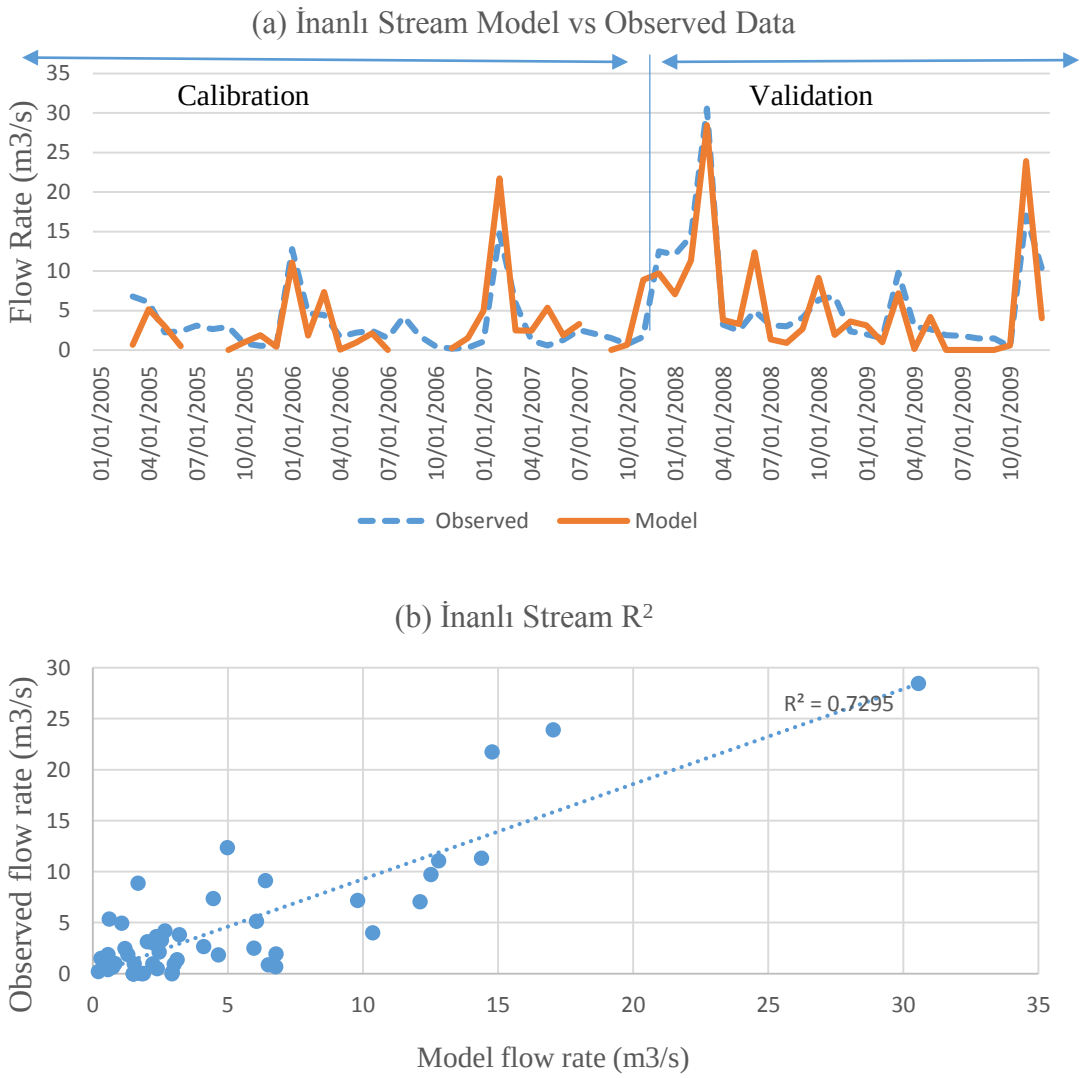


Figure 4.5. Model and Observed data Comparison According to Months (a) and Determination Coefficient of İnanlı Stream (b).

There are several statistical performance indicators for hydrological simulation. The most commonly reported for SWAT calibration and validation were the determination coefficient ($R^2$), the Nash–Sutcliffe model efficiency (NSE). The NSE varies between negative infinite and 1.0 (the optimal value). Values between 0 and 1 are generally regarded as acceptable performance levels and values “0” indicate that it is better to use the mean observed data than the predicted value of the model (Nash *et al.*, 1970). For Hayrabolu stream $R^2$ of model was obtained 0.72 for calibration and 0.77 for validation and NSE value was 0.68 and 0.64 respectively. Similar results calculated for İnanlı stream $R^2$ of model was obtained 0.55 for calibration and 0.72 for validation and NSE value was 0.49 and 0.48 respectively. The Nash–Sutcliffe Efficiency values for the calibration and validation of Hayrabolu was better than İnanlı stream. In an extensive literature review conducted by Moriasi *et al*. (2007) values over 0.5 for NSE for stream flow calibration were suggested acceptable, which was also found as satisfactory for our study. Model performances for streams flow related to both gaged streams were given in Table 4.3.

Table 4.3. Statistical Performance Indicators for Calibration and Validation of Streams.

| Hayrabolu stream | | | |
|---|---|---|---|
| Calibration | 2005-2007 | R2 = 0,72 | NS =0,68 |
| Validation | 2008-2010 | R2 = 0,77 | NS =0, 64 |
| İnanlı stream | | | |
| Calibration | 2005-2007 | R2 = 0,55 | NS =0,49 |
| Validation | 2008-2010 | R2 = 0,72 | NS =0, 48 |

## 4.3. Nutrient Loads

İnanlı, İpsala, Lüleburgaz and Uzunköprü are four stations on Ergene River which can monitor water quality data. İnanlı water quality monitoring point was selected for water quality calibration due to the existence of data. The model was calibrated manually with help of SWAT for nutrient loads of the year 2017. Point sources obtained from ministry of agriculture and forestry was given into the model as input. The validated stream flow data was used as stream flow for daily loading. The model was run. By changing in water quality

parameter default values in database, observed and simulated values of TN and TP were fitted. Nitrogen coming from rain (RCN), was increased. Our land is not wholly arid, so initial residue cover (RSDIN) was increased. CDN, denitrification exponential rate coefficient, SDNC, denitrification threshold water content, Nitrogen uptake distribution parameter (N_UPDIS) was manually calibrated. Figure 4.6, showed the monthly calibration results of nitrogen and phosphorus. The coefficient of determination ($R^2$) was 0.5639 for TN and 0.55 for TP, respectively (Figure 4.6 and 4.7).

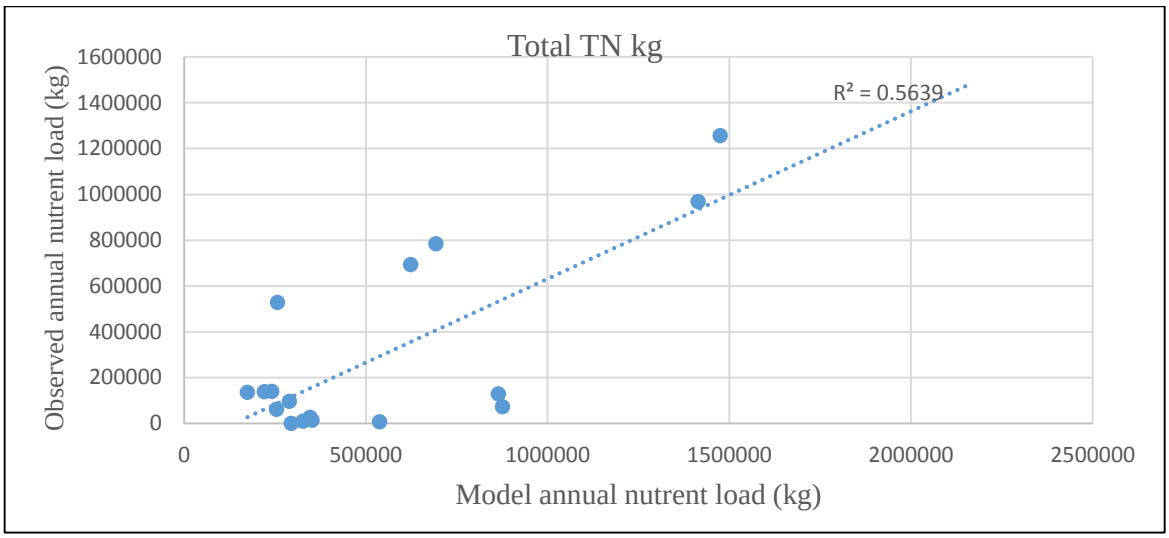


Figure 4.6. TN, $R^2$ of Model for İnanlı Stream.

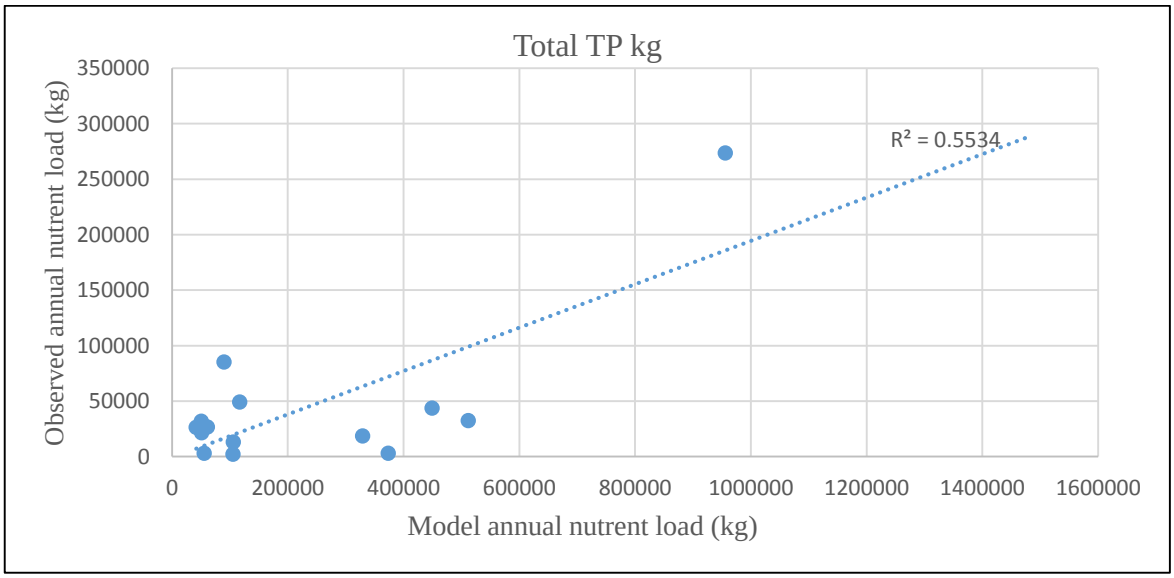


Figure 4.7. TP, $R^2$ of Model for İnanlı Stream.

Obtaining daily even monthly nutrient load data for all years is not possible for Turkey conditions. Applying constant load for short terms would be efficient for models. But calibrating or simulation is not possible with constant loads. Therefore obtaining $R^2$ over 0.5 was sufficient for our model for 3 years application.

### 4.4. Water Budget

Water budget reveals the input, process and output of amount of water by partitioning of the hydrological cycle into components such as precipitation, surface runoff, the ground water flow and lateral flow. ArcSWAT model gave results according to calibrated parameters and following hydrological cycle obtained from the model.

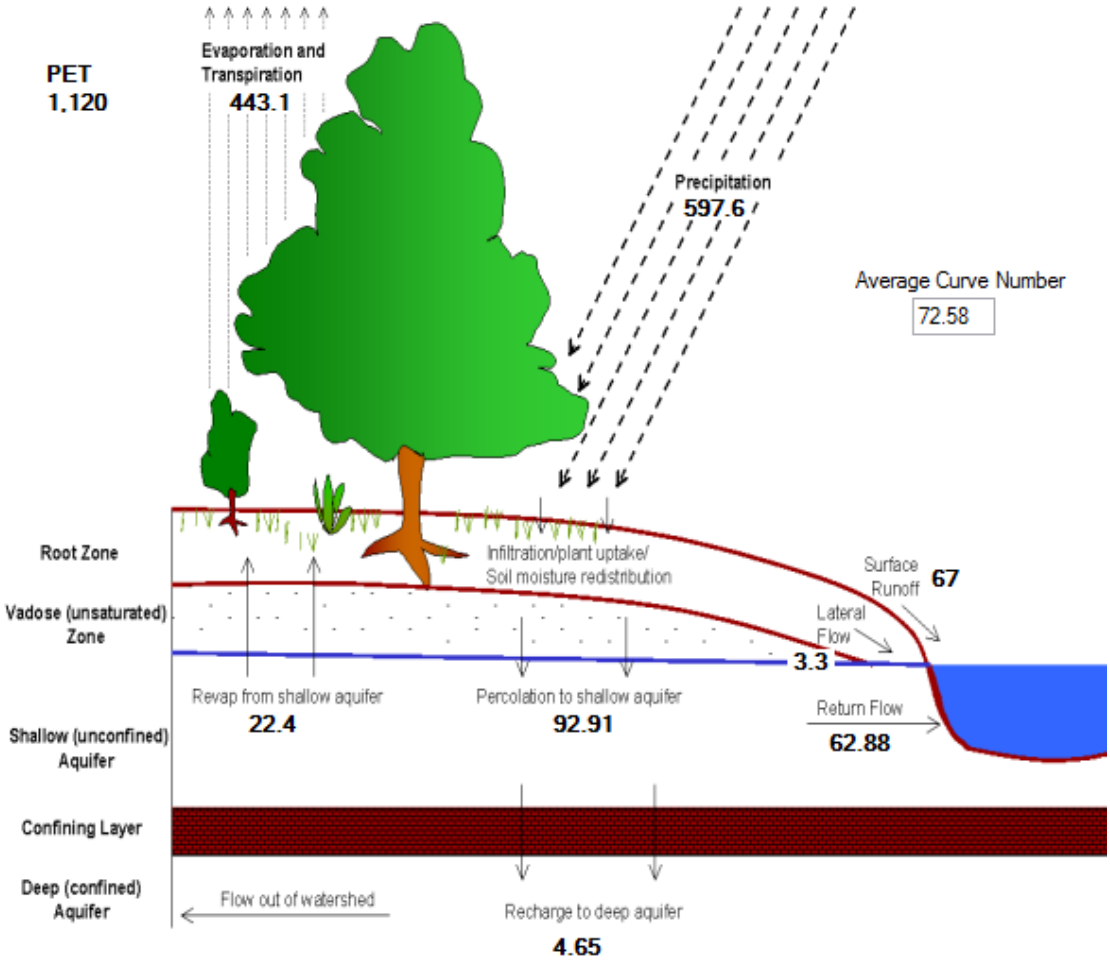


Figure 4.8. Hydrological Cycle of Model.

Hydrological cycle of Ergene Basin summarized by SWAT program as shown in Figure 4.8. Average amount of precipitation was 597.6 mm and, 443.1 mm of this source removed system by evapotranspiration. Surface run off system was 67 mm and lateral flow was around 3.3 mm. 92.91 mm water percolated to shallow aquifer. Curve number, direct run off from rainfall excess, based on the hydrological soil group and ground cover, considers the storage in ground, was 72 in this study.

Model is run through 2002-2010 years where data set was much stronger than other years. Lack of data might cause wrong estimation of stream regimes and pollution loads. But for gaining general perspective as water budget, SWAT could be applied with low data set. Therefore just by changing temperature and precipitation data set, water budget of past years was obtained. As it is known fact that before year 2000, precipitation regime was much more regular than after year 2000. Therefore SWAT model, before year 2000 and after year 2000 was compared (Table 4.4).

Precipitation of region pre 2000 year was 554 mm and post 2000 year was 581 mm. Evaporation value of pre 2000 period was nearly same with after 2000 year. Main difference was the storage of soil for this period. It was nearly 2 times of model and pre2000 years. This showed us our study period represents same behavior with pre and post weather regimes.

Table 4.4. Water Table of Ergene Basin Comparison Model, Before and After 2000 Year.

| | Model | Before2000 | After2000 |
|---|---|---|---|
| Precipitation | 597.6 | 554 | 581 |
| Evaporation | 443.1 | 419 | 415 |
| Revap from Shallow | 22.4 | 21.2 | 22.8 |
| Percolation to Shallow | 92.91 | 90.25 | 100 |
| Surface Run off | 67 | 47.52 | 57 |
| Lateral Flow | 3.3 | 3.09 | 3.44 |
| Total In | 620 | 575.2 | 603.8 |
| Total Out | 606.31 | 559.86 | 575.44 |
| Storage | 13.69 | 15.34 | 28.36 |

## 4.5. Land Use Estimation

In previous chapters, land use comparison was made with CORINE data for the years of 2006-2012 which prepared for Turkey. However, using only two land cover maps for prediction of future trends in terms of land use changes did not provide sufficient accuracy. For this reason, in this part of the study, recent land use changes and the trend of future land use changes were described for Ergene Basin. Land use maps of 1990, 2000 and 2012 were generated to quantify land cover changes from European Environmental Agency Databases (CORINE) (Figure 4.9 & 4.10).

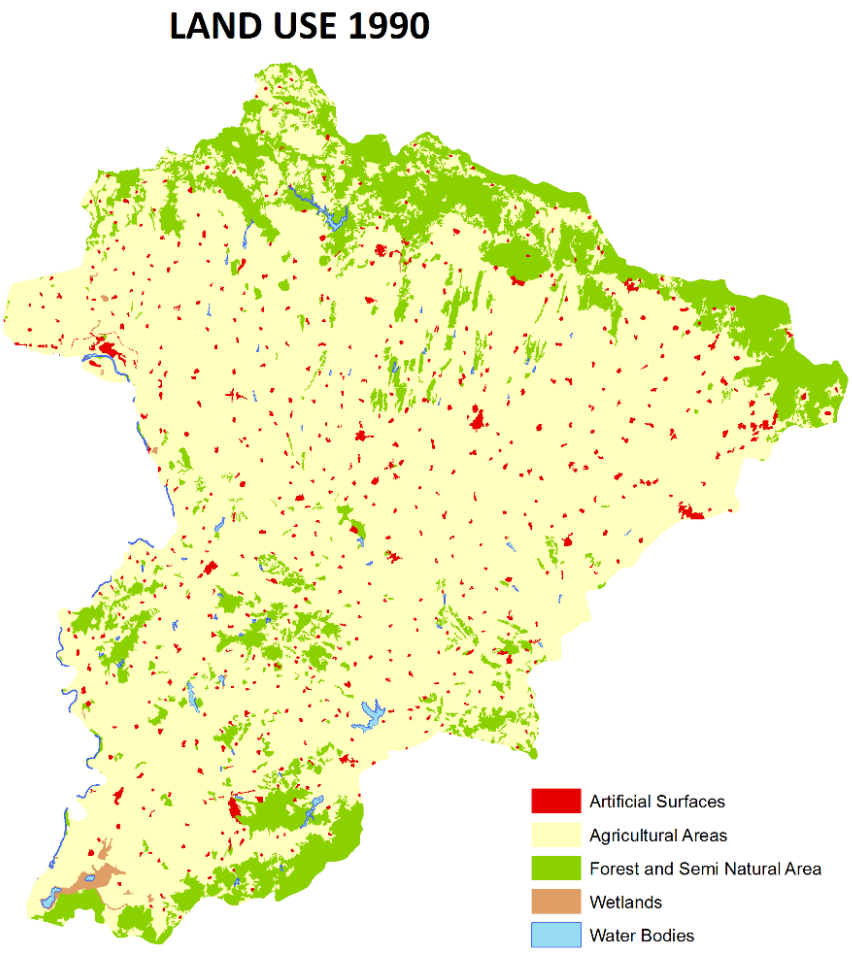


Figure 4.9. CORINE Land Cover Legend for 1990 of Ergene Basin.

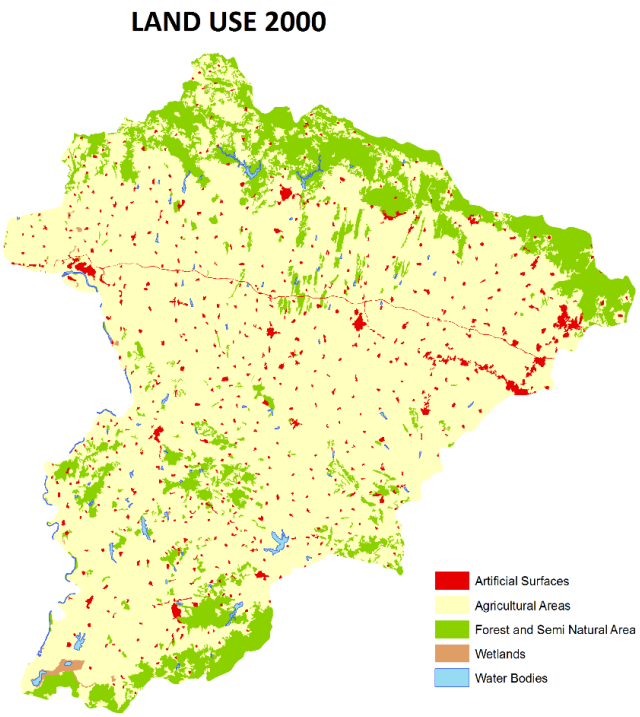


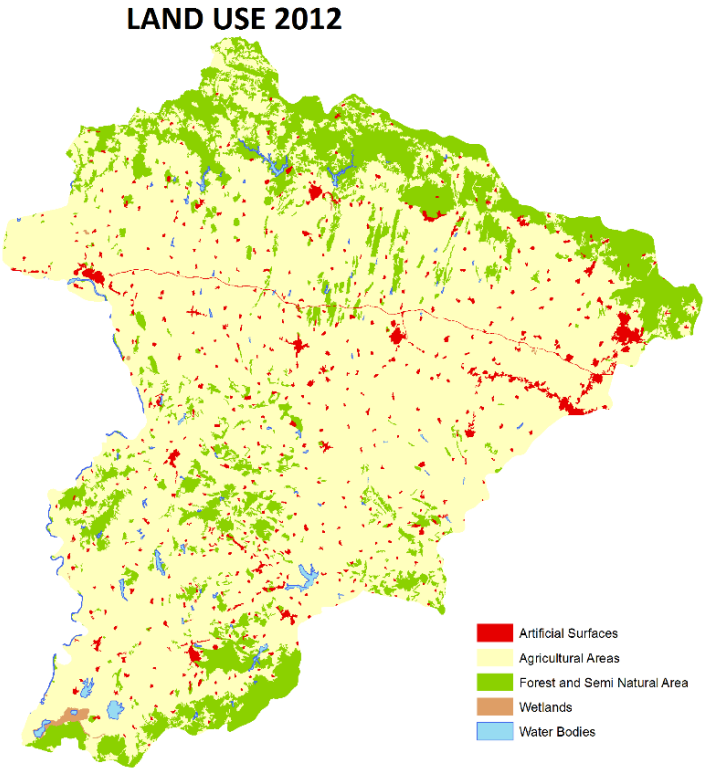


Figure 4.10. CORINE Land Cover Legend for 2000 and 2012 of Ergene Basin.

Table 4.5. Corine Land Cover Legend for Ergene Basin in Arcmap for 1990-2000-2012.

| CORINE LAND COVER LEGEND | | | | | |
|---|---|---|---|---|---|
| **Corine 1990 (ha)** | **Corine 2000 (ha)** | **Corine 2012 (ha)** | **Level 3** | **Level 2** | **Level 1** |
| 480.01 | 492.32 | 1,711.78 | 1.1.1 Continuous urban fabric | 1.1Urban fabric | 1. Artificial Surfaces |
| 28,844.30 | 32,066.28 | 29,897.07 | 1.1.2 Discontinuous urban fabric | | |
| 3,405.18 | 7,620.56 | 8,903.30 | 1.2.1 Industrial or commercial units | 1.2 Industrial, commercial and transport units | |
| 25 | 1,876.72 | 1,800.14 | 1.2.2 Road and rail networks and associated land | | |
| 147.96 | 212.51 | 83.08 | 1.2.4 Airports | | |
| 694.88 | 1,838.42 | 3,307.33 | 1.3.1 Mineral extraction sites | 1.3 Mine, dump and construction sites | |
| 60.92 | 156.05 | 302.81 | 1.3.2 Dump sites | | |
| 829.11 | 610.51 | 504.21 | 1.3.3 Construction sites | | |
| 107.65 | 147.03 | 96.57 | 1.4.2 Sport and leisure facilities | 1.4 Artificial, non-agricultural vegetated areas | |
| 686,934.59 | 682,403.47 | 684,683.15 | 2.1.1 Non-irrigated arable land | 2.1 Arable land | 2. Agricultural Areas |
| 147,921.97 | 147,984.65 | 189,034.52 | 2.1.2 Permanently irrigated land | | |
| 72,921.67 | 74,244.46 | 70,994.24 | 2.1.3 Rice fields | | |
| 820.48 | 820.48 | 204.53 | 2.2.1 Vineyards | 2.2 Permanent crops | |
| 1,089.69 | 1,089.69 | 1,488.77 | 2.2.2 Fruit trees and berry plantations | | |
| 86,834.70 | 81,763.51 | 58,566.20 | 2.3.1 Pastures | 2.3 Pastures | |
| 40,409.47 | 38,948.50 | 15,887.07 | 2.4.2 Complex cultivation patterns | 2.4 Heterogeneous agricultural areas | |
| 105,061.54 | 105,083.54 | 91,647.44 | 2.4.3 Land principally occupied by agriculture, with significant areas of natural vegetation | | |
| 71,007.84 | 75,615.04 | 81,679.39 | 3.1.1 Broad-leaved forest | 3.1Forests | 3. Forest and Semi Natural Areas |
| 13,423.31 | 18,581.28 | 23,712.84 | 3.1.2 Coniferous forest | | |
| 11,227.64 | 19,722.37 | 17,741.68 | 3.1.3 Mixed forest | | |
| 24,647.02 | 24,600.98 | 45,054.82 | 3.2.1 Natural grasslands | 3.2 Scrub and/or herbaceous vegetation associations | |
| 1,280.27 | 1,280.27 | 1,764.55 | 3.2.3 Sclerophyllous vegetation | | |
| 123,301.41 | 108,146.87 | 94,117.35 | 3.2.4 Transitional woodland-shrub | | |
| 25.09 | 25.09 | | 3.3.1 Beaches, dunes, sands | 3.3 Open spaces with little or no vegetation | |
| 3,631.96 | 3,465.63 | 4,458.10 | 3.3.3 Sparsely vegetated areas | | |
| 4,019.95 | 59.77 | 80.01 | 3.3.4 Burnt areas | | |
| 5,055.49 | 3,696.65 | 3,042.38 | 4.1.1 Inland marshes | 4.1 Inland wetlands | 4. Wetlands |
| 1,231.07 | 1,233.91 | 1,292.35 | 5.1.1 Water courses | 5.1 Inland waters | 5. Water Bodies |
| 5,538.68 | 7,192.28 | 8,923.18 | 5.1.2 Water bodies | | |

On the basis of CORINE database Ergene Basin includes 13 different land cover types. These are urban fabric, industrial, commercial and transport units, mine, dump and

construction sites, artificial, non-agricultural vegetated areas, arable land, permanent crops, pastures, heterogeneous agricultural areas, forests, scrub and/or herbaceous vegetation associations, open spaces with little or no vegetation, inland wetlands and inland waters. Land cover types are classified to five types of land uses which are artificial surfaces, agricultural areas, forest and semi natural areas, wetlands and water bodies for the purpose of analyzing the land cover changes (Table 4.5).

### 4.5.1. Driving Force Analysis of LUCC in Ergene Basin

Land use polygons were compared for change detection of land use of each time periods. And for defining of land use's intersections spatial overlay analysis was used. With using overlay method, used during evaluation phase, different cartographic layers were enabled to overlap one over the other if necessary.

Table 4.6. Land Use in the Ergene Basin for the 1990-2000-2012 Years.

| Land use types | Area by years | | | | | |
|---|---|---|---|---|---|---|
| | 1990 | | 2000 | | 2012 | |
| | in ha | in % | in ha | in % | in ha | in % |
| Artifical Surfaces | 34,595.01 | 2.400799 | 45,020.41 | 3.124294 | 46,606.28 | 3.234348 |
| Agricultural Areas | 1,141,994.10 | 79.25127 | 1,132,338.32 | 78.58119 | 1,112,505.92 | 77.20487 |
| Forest and Semi Natural Areas | 252,564.49 | 17.52729 | 251,497.30 | 17.45323 | 268,608.74 | 18.64071 |
| Wetlands | 5,055.49 | 0.350837 | 3,696.65 | 0.256537 | 3,042.38 | 0.211133 |
| Water Bodies | 6,769.75 | 0.469802 | 8,426.18 | 0.584754 | 10,215.53 | 0.70893 |

From table 4.5 and table 4.6, it was calculated that change in artificial surfaces was increased from 34,595 ha (2.40 %) to 45,020 ha (3.12%). Increasing of road, rail networks and associated land from 25.00 ha to 1,876.72 ha and discontinuous urban fabric 28,844.30 ha to 32,066.28 ha and industrial or commercial units 3,405.18 ha to 7,620.56 ha were one of the most important reasons for this change in the period 1990-2000. Also artificial areas (industrial areas and residential areas) were developed close to city center and roads. Besides roads have impact on transition "pasture to agriculture" or "forest to agriculture". On the other hand in this period wetlands area was reduced 5,055.49 ha to 3,696.65 ha.

In the period 2000-2012, there were a slow increase rate in artificial surfaces from 45,020.41 to 46,606.28 ha. The trend of reducing wetlands continued from 3,696.65 ha to 3,042.38. In addition there was a dramatic increase of forest and semi natural areas from 251,497.30 to 268,608.74 ha.

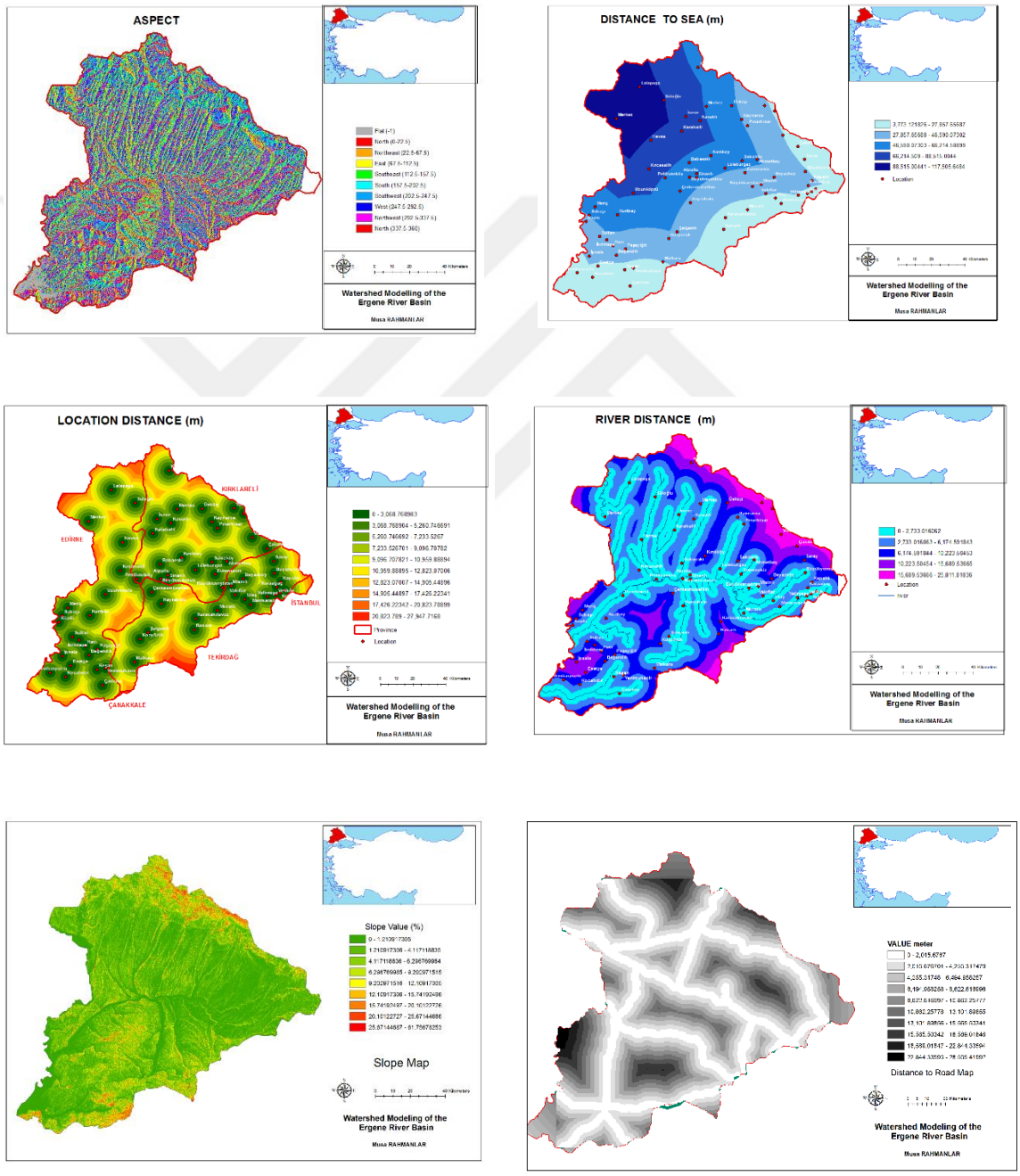


Figure 4.11. Driving Factors Map of Ergene Basin.

Obtained results showed that agricultural areas the most dominant type of land use in all of the years (79.25 %, 78.58 % and 77.20 %). In addition, artificial surfaces and forest and semi natural areas were the two important factors in characterizing land use areas of the study. In land use change projections, there are some effects which may influence the change potential of the land use. To exemplify, for forecasting increase in residential areas, distance to city centers, distance to main roads plays an important role. These factors are named as driving factors. In this study six driving factors used to predict future trends. These were aspect, proximity to sea, proximity to city center, proximity to river, slope as shown in figure 4.11. By using driving factors, definition of the future location which should changes from each pixel of land cover into another type, was obtained.

### 4.5.2. Future Land Estimation

For land comparison, CA_MARKOV model in IDRISI program was applied. By comparing land use maps for each years, CA_MARKOV model determined the transformation matrix. The Cellular Automata system established a relationship between the nearby places and the central location and predicted whether there would be a change according to the transformation matrix. Firstly, it introduced an exchange matrix by comparing two maps of certain times. As a result of this comparison, possibility of land type transformation was determined. Then, with using driving factors, prediction of future trends were obtained.

Table 4.7. Land Use Transition Matrix of 2000 to 2012.

| | | 2012 | | | | |
|---|---|---|---|---|---|---|
| | | Artificial | Agricultural | Forest and Semi Natural | Wetlands | Waterbodies |
| 1990-2000 | Artificial Surfaces | 0.9871 | 0.0073 | 0.046 | 0 | 0.001 |
| | Agricultural Areas | 0.0108 | 0.9884 | 0.0002 | 0 | 0.006 |
| | Forest and Semi Natural | 0.0025 | 0.0016 | 0.9935 | 0 | 0.0024 |
| | Wetlands | 0 | 0.1997 | 0 | 0.6731 | 0.1272 |
| | Waterbodies | 0 | 0.0007 | 0.0002 | 0.0044 | 0.9947 |

These driving factors were compared for each transformation and the correlation matrix and maps were presented. With using driving factors, transformation and correlation matrices were developed. In addition, prediction maps were produced by the transformation matrices. For instance, the relationship of “transformation of agricultural land to artificial land” with “the distance to the city center” was found to be around 80 percent.

In this study, firstly the land use data of 1990 – 2000 years were compared to obtain land use of 2012 year. And transition matrix (from 1990-2000 to 2012) was generated.

When the transition matrix was examined, the transition from artificial areas to agricultural areas and even to forest areas was observed. The main reason for this situation was thought to be due to misclassification of land or changing class of land. The land use model for the year 2012 established from the data of the year 2000 with the transition matrix (Table 4.7). A potential transitional map constructed by IDRISI program according to driving factors (Figure 4.12).

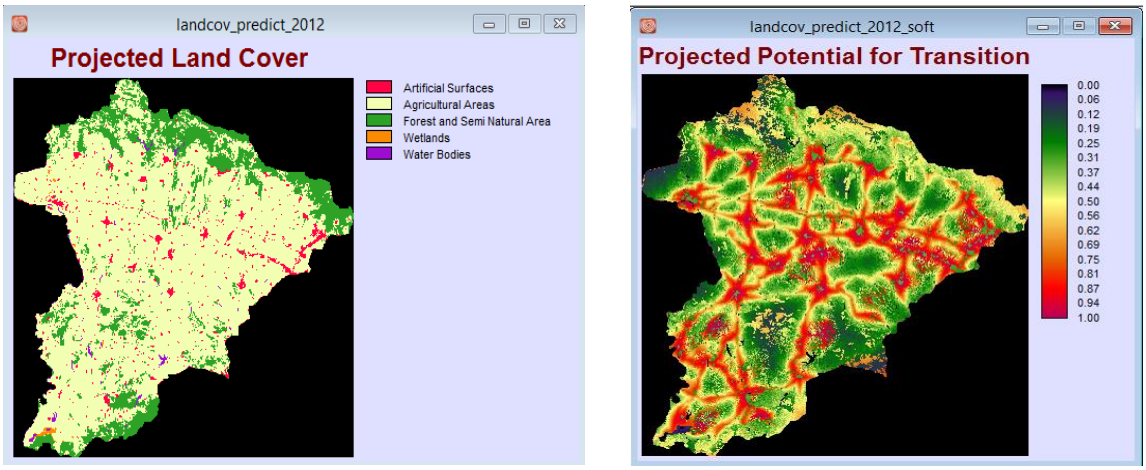


Figure 4.12. Projected 2012 Map & Projected Potential for Transition.

Generated model was compared with observed model (Figure 4.13). While in some points there was a harmony between the model and the observed data, there were changes in the point sense. There was coherence between the model and the observed data of year 2012. But there were small differences according to artificial areas in hectares. It was thought that the most important reason for this situation was the ratio of immigration and

the increase in industrial areas that established in 1990-2000. Especially in the period of 2000-2012 year, the region did not show the same trend of previous period (1990-2000 year) by reaching saturation. For this reason it can be thought that prediction from the transition matrix obtained by the 1990-2000 data was not suitable to use.

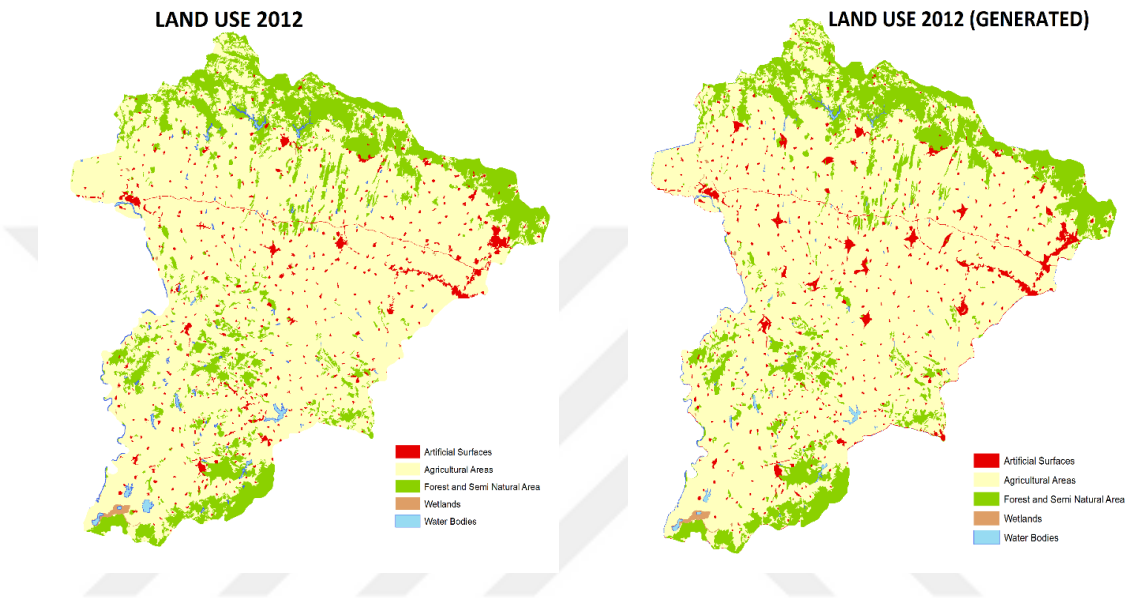


Figure 4.13. Projected 2012 Lands Use Map vs Observed 2012 Land Use Map

Area difference between CORINE 2012 and generated land use from IDRISI program as shown in Table 4.8. Due to the fact that land use change trend between 1990 to 2000 years was not same with 2000 and 2012 years. In 1990-2000 years there was a sharp increase in population, therefore expecting same result for 2000-2012 years should lead mis-projection. As can be seen from table, difference between observed and projected artificial surfaces were nearly 20% percent.

Table 4.8. CORINE 2012 & Generated 2012 Maps Area Comparison.

| | CORINE 2012 | Generated 2012 | Percent. |
|---|---|---|---|
| Artifical Surfaces (ha) | 46,606.28 | 56,806.34 | 17.96% |
| Agricultural Areas (ha) | 1,112,505.92 | 1,121,299.51 | 0.78% |
| Forest and Semi Natural Areas (ha) | 268,608.74 | 250,678.35 | -7.15% |
| Wetlands (ha) | 3,042.38 | 2,986.34 | -1.88% |
| Water Bodies (ha) | 10,215.53 | 9,027.91 | -13.15% |

In order to provide an accurate prediction for the future, the transition matrices were formed by the data of 2000-2012 which was more up-to-date. However, some of the transitions in this matrix modified by literature review (Table 4.9).

Table 4.9. Land Use Transition Matrix of 2012 to 2030.

| | | 2030 | | | | |
|---|---|---|---|---|---|---|
| | | Artificial | Agricultural | Forest and Semi Natural | Wetlands | Waterbodies |
| 2000-2012 | Artificial | 1.0000 | 0.0000 | 0.0000 | 0.0000 | 0.0000 |
| | Agricultural | 0.0094 | 0.9212 | 0.0067 | 0.0002 | 0.0000 |
| | Forest and Semi Natural | 0.0040 | 0.0642 | 0.9310 | 0.0000 | 0.0000 |
| | Wetlands | 0.0037 | 0.2625 | 0.0349 | 0.6703 | 0.0016 |
| | Waterbodies | 0.0001 | 0.0389 | 0.0095 | 0.0088 | 0.9427 |

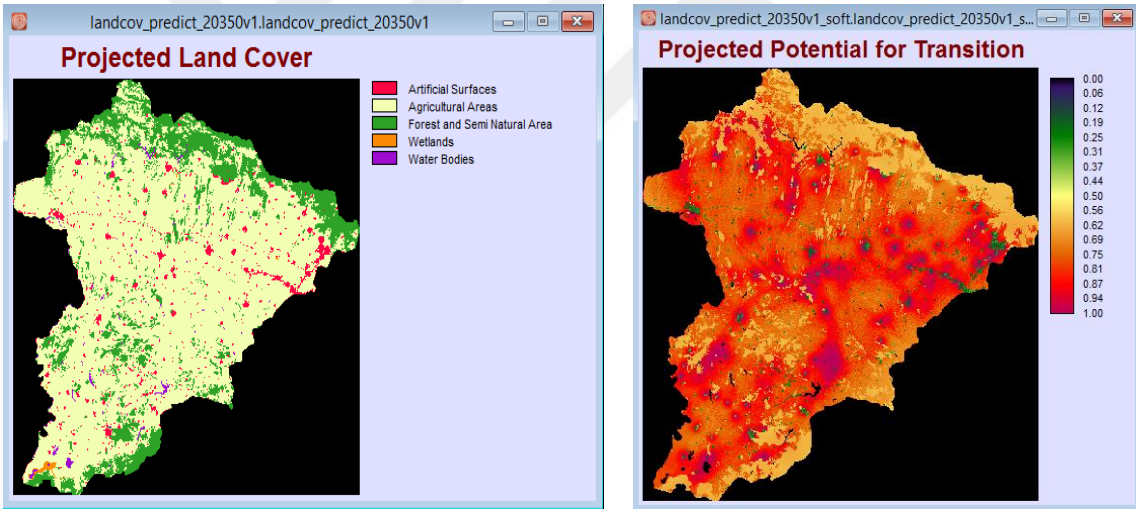


Figure 4.14. Projected Lands Use Map & Potential for Transition for 2030.

Due to the dynamic nature of the region, it was not appropriate to make a long-term forecast with the model. For this reason, land use estimation was done for 2030, and 2030 land use map was used as base map for ArcSWAT model to represent short term changes (Figure 4.14) and 2050 land use map was created for medium term changes (Figure 4.15). 2030 and 2050 transition matrices were created by taken into account regions profile (Table 4.9 and 4.10).

When the map of 2030 was examined, it was revealed that the city centers grow partially, some of the agricultural areas were abandoned and transform to forest land and some of the wetlands were turned into agricultural and artificial lands. This trend was more evident in 2050 (Figure 4.16). In addition, the model, which took into account the driving factors, stated that new settlements could occur, especially close to the main roads, the rivers and the sea.

Table 4.10. Land Use Transition Matrix of 2012 to 2050.

| | | 2050 | | | | |
|---|---|---|---|---|---|---|
| | | Artificial | Agricultural | Forest and Semi Natural | Wetlands | Waterbodies |
| 2000-2012 | Artificial | 1.0000 | 0.0000 | 0.0000 | 0.0000 | 0.0000 |
| | Agricultural | 0.0173 | 0.9048 | 0.0727 | 0.0000 | 0.0000 |
| | Forest and Semi Natural | 0.0079 | 0.1277 | 0.8628 | 0.0000 | 0.0000 |
| | Wetlands | 0.0085 | 0.4391 | 0.0690 | 0.4300 | 0.0000 |
| | Waterbodies | 0.0000 | 0.0000 | 0.0000 | 0.0000 | 1.0000 |

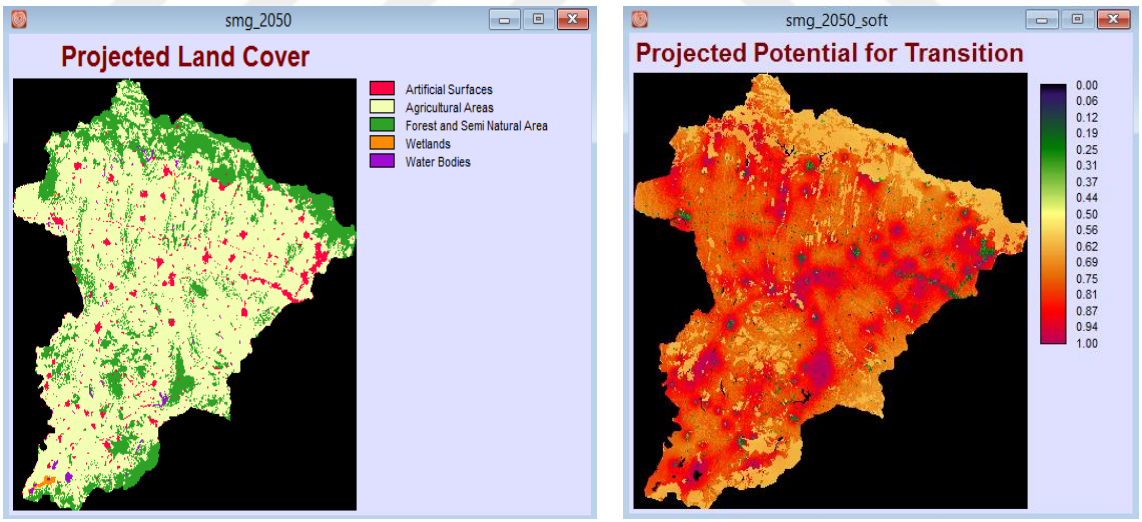


Figure 4.15. Projected Lands Use Map & Potential for Transition for 2050.

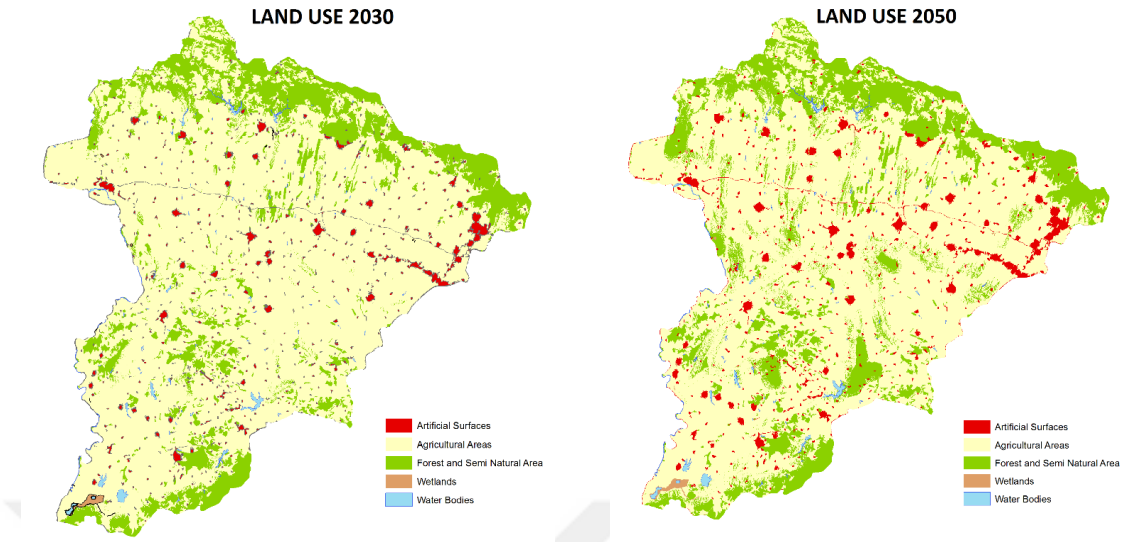


Figure 4.16. Comparison of Projected 2030 and 2050 Land Use Maps.

All of generated values and resource maps were summarized in figure 4.17. The results of the model were considered reasonable in terms of future (Table 4.11). For this reason, the model was re-classified in order to be suitable for SWAT data infrastructure so that it could be applied to SWAT program. In addition a new map of 2030 year estimation of IDRISI was constructed through 29 parameters of CORINE map. This map was used as a base map for future flow estimation model of SWAT by taking account to the effect of climate models.

Table 4.11. Comparison of Constructed Maps.

| Land Use | 2012* | 2030 | 2050 |
|---|---|---|---|
| Artificial Surfaces (ha) | 56806.34005 | 56243.5029 | 65065.13823 |
| Agricultural Surfaces (ha) | 1121299.506 | 1113508.463 | 1050335.089 |
| Forest and Semi Natural Area (ha) | 250678.3453 | 257797.9645 | 312125.9669 |
| Wetland Areas (ha) | 2986.344856 | 3036.17326 | 3039.488748 |
| Water Bodies (ha) | 9027.914654 | 10196.45502 | 10209.3956 |

*generated from 1990-2000 land use data

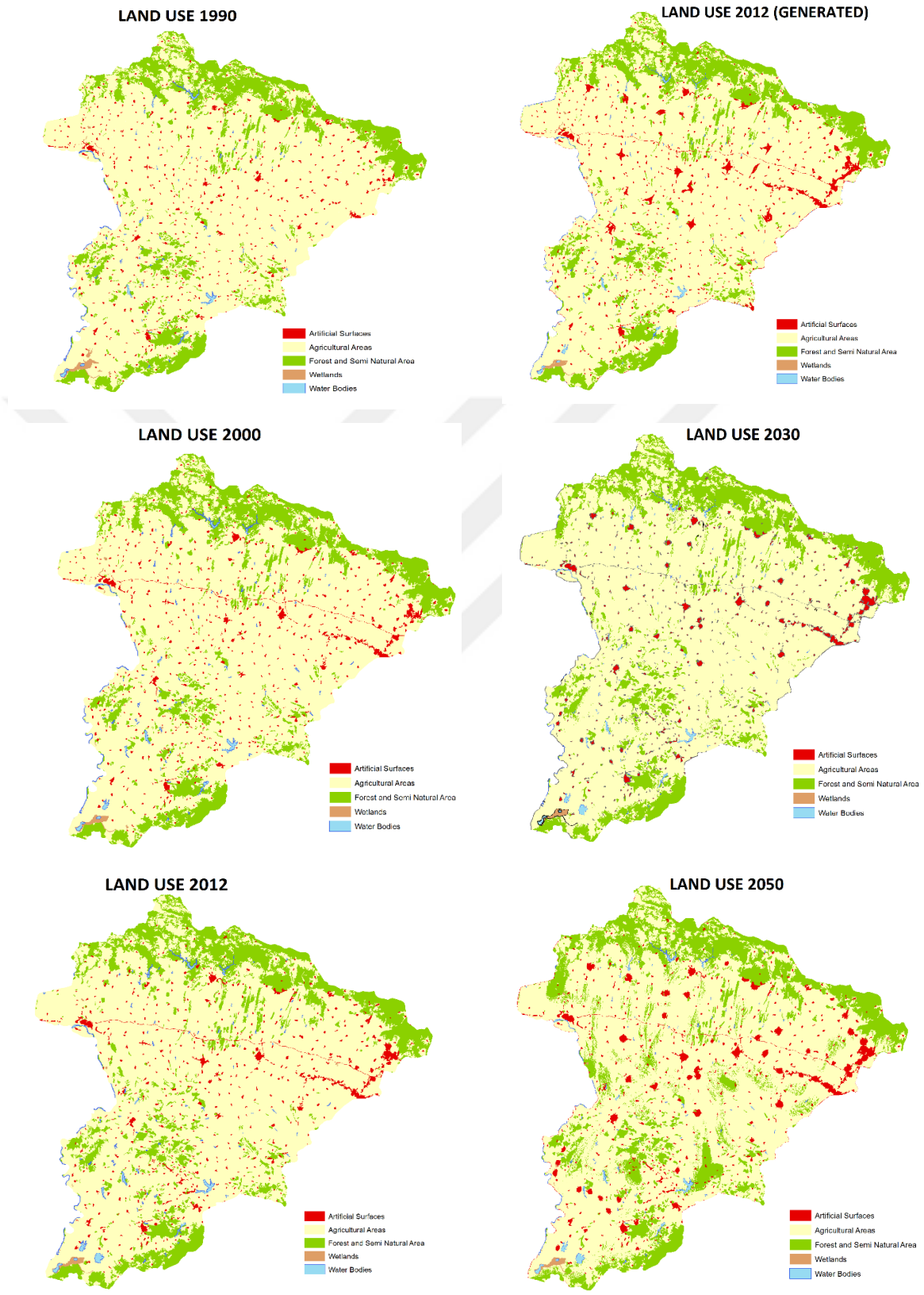


Figure 4.17. CORINE 1990,2000, 2012 Land Use Maps (right side); Constructed 2012, 2030, 2050 Land UseMaps.

### 4.6. Weather Scenarios and Effect of Climate Change

The scenario is the imagination of the future as an illusion or the depiction of alternative future situations. However, generally the scenario concept is confused with estimation concept. The scenario is not an estimate of the future, but rather a possible alternative situation (IPCC, 2000). The scenarios play an important role in understanding and evaluating the possible future development of complex systems with high uncertainty, such as climate. In this study, feature climate scenarios were used as an input for our ArcSWAT model.

For understanding region's reaction against climate change, 1960-2017 weather stations of Ergene basin was investigated (Figure 4.18 and Figure 4.19). According to precipitation vs time graph, precipitation amount decreased over last 50 years. Average trend of precipitation showed that region loses 1,56 mm precipitation per year.

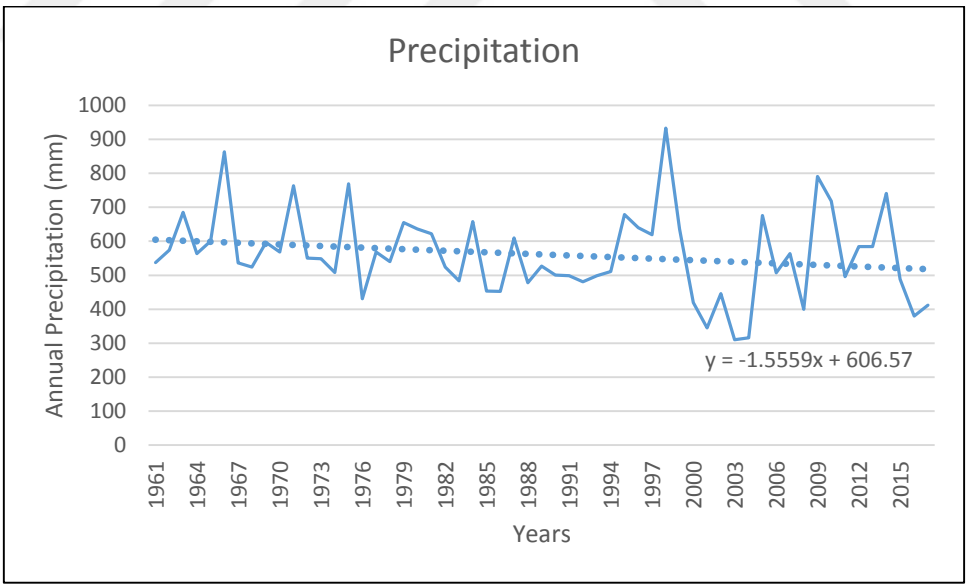


Figure 4.18. Precipitation vs Time Graph of Lüleburgaz Station.

Another important aspect is the minimum and maximum temperature changes of region. Despite both minimum temperature and maximum temperature values continued rising in years, the difference between them remained constant. Maximum temperature

value has risen 0.04 degree Celsius per year, and minimum temperature followed it with 0.03 degree Celsius per year.

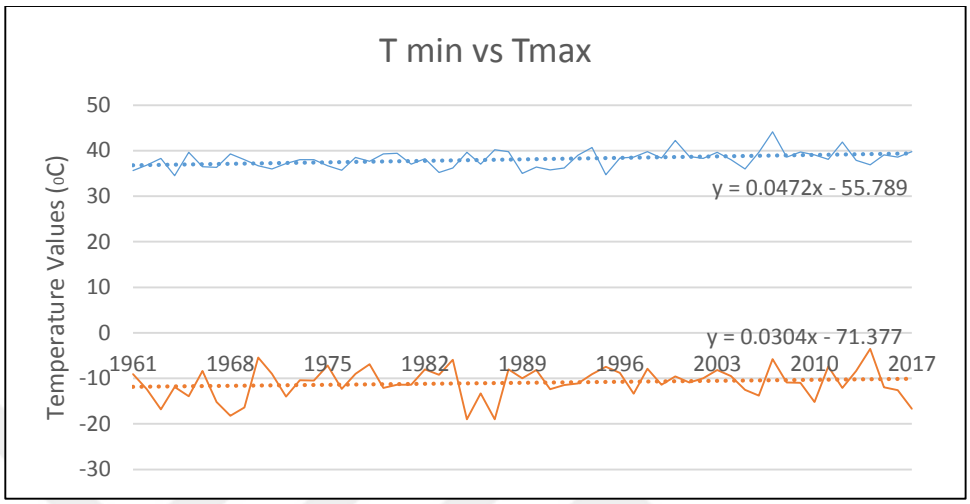


Figure 4.19. Tmin & Tmax vs Time Graph of Lüleburgaz Station.

Both results proved that climate change effect was real for this region. Thus application of a climate scenario would be useful for creating a well-designed model.

Table 4.12. RCP 4.5 and 8.5 Temperature and Precipitation Change Scenarios for Ergene Basin for 100 years.

| | Temperature | | | | Precipitation | | | |
|---|---|---|---|---|---|---|---|---|
| | Winter | Spring | Summer | Autumn | Winter | Spring | Summer | Autumn |
| RCP 4.5 | 1.5-2 | 2.0-3.0 | 2.0-3.0 | 3.0-4.0 | 5.00% | -10.00% | 10.00% | 10.00% |
| RCP 8.5 | 2.0-3.0 | 4.0-5.0 | 5.0-6.0 | 4.0-5.0 | 5.00% | -10.00% | -10.00% | -20.00% |

The General Directorate of Meteorology implemented HadGEM2-ES based models. In this study, the following results were obtained for Ergene Basin RCP 4.5 and RCP 8.5 release scenarios in order to see the effects of temperature and precipitation on the model. These scenarios were produced by using the RegCM4.3.4 regional climate model, with the dynamic scale reduction method, for Turkey and the region at 20 km temperature and rainfall projections for the years 2018-2099 obtained from the study. Table 4.12 summarizes the 100 hundred years change of temperature and precipitation according to scenarios.

The created precipitation and temperature data was new inputs for SWAT program for future scenarios. In this study, it was investigated the changes in annual mean precipitation in Ergene and its vicinity until the end of this century in periods of 2018-2040; 2041-2070 and 2071-2099 based on HadGEM2-ES/RegCM4.3.4 global/regional models' outputs both RCP4.5 and RCP 8.5 scenarios. Precipitation values of 10m x 10m grid were calculated, analyzed and maps produced in Arc GIS. All results were created by geo-referencing maps. According to findings, annual mean temperature values in the area would increase dramatically until the end of this century. Figure 4.21 summarized temperature forecast 2013-2100 years for RCP 4.5, rest estimations figure are given in Appendix A section. In this study 2015-2030 climate change scenarios were used for estimation future trends.

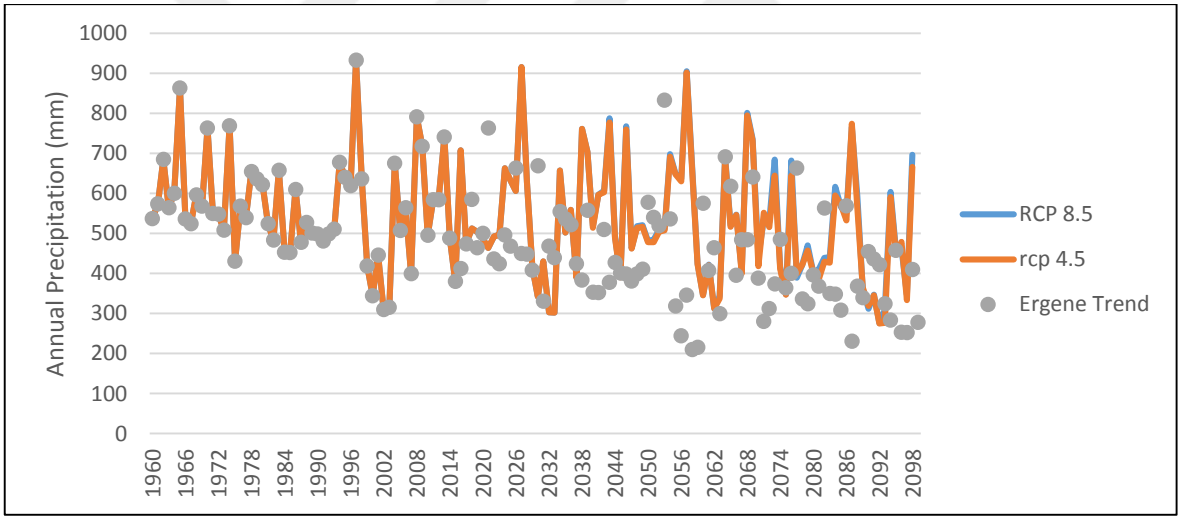


Figure 4.20. Ergene Precipitation Trend vs RCP 4.5 and 8.5 Trend

As seen from figure 4.20 Ergene Basin precipitation trend was so similar to RCP4.5 and RCP8.5 scenarios trend. Same situation exists for maximum and minimum temperature values. For comparison current weather trend and future scenarios trend, 3 datasets were constructed for SWAT model. First climate model named as base model was constructed by taking account 2000-2015 year temperature and precipitation data. RCP 4.5 model and RCP 8.5 model climate data was created according to their scenarios for years 2015-2030.

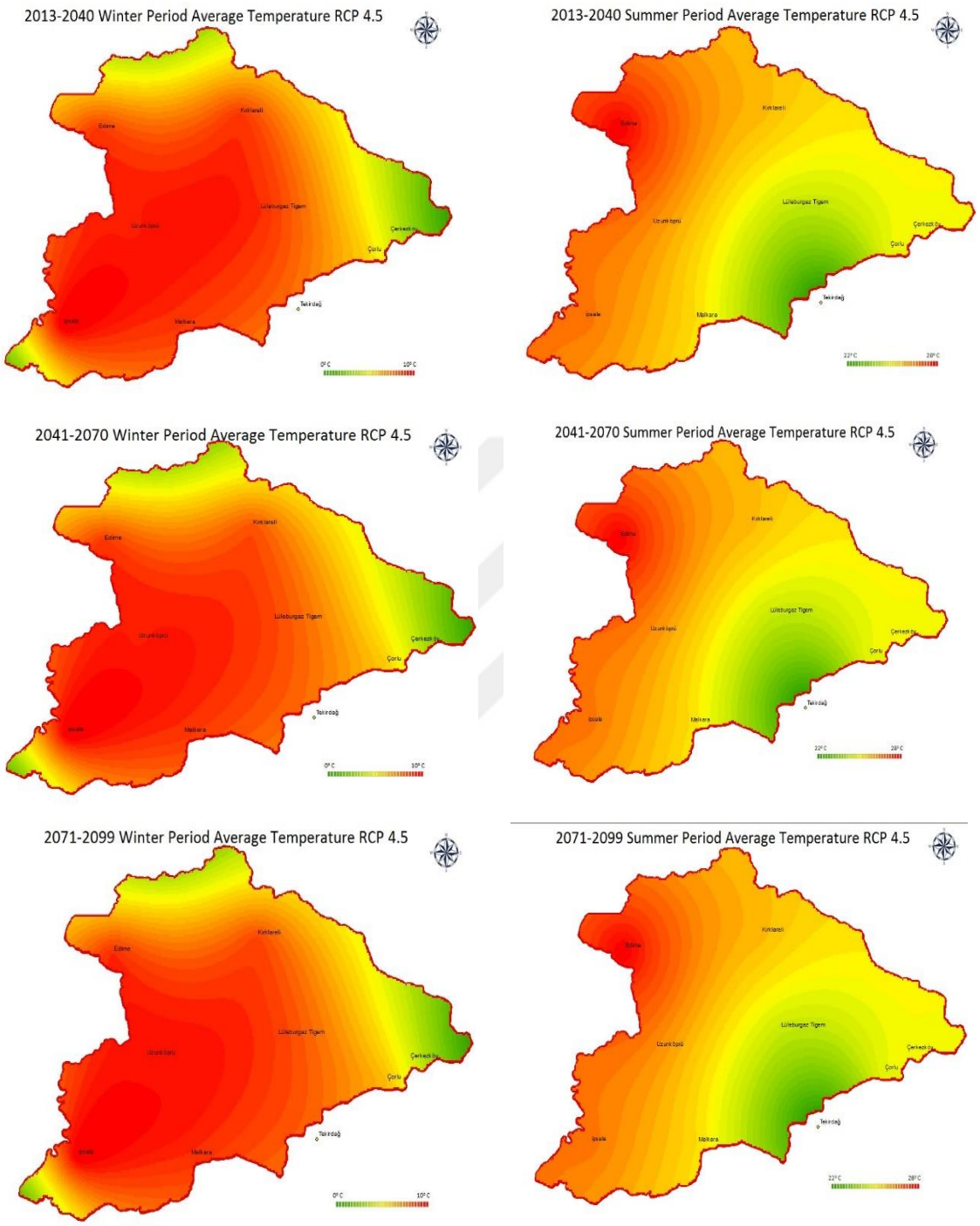


Figure 4.21. Temperature Forecast 2013-2100 RCP 4.5

## 4.7. Future Hydrology and Nutrient Estimation with SWAT

After obtaining satisfactory results from calibration and validation of the model, new data sets were constructed for future predictions. DEM, Soil and slope maps remained unchanged. 2030 generated land use map was used as base map for predictions. And predicted temperature and precipitation values were used weather input for model. İnanlı stream was used as observing point of the model. The most important task was to assess the possible changes of flow and nutrient loadings of Inanli stream according to climate and land use change scenarios.

2030 year landuse map and predicted climate scenarios were used for SWAT model comparison. SWAT model operated up to 2030 years with RCP 4.5 and 8.5 scenarios and compared with current climate scenario (2000-2015 years). Model would be used for predicting 2100 years which climate changes effect can be seen more precisely, but mis-estimation of land use changes and other factors will increase the error amount. Therefore short term estimation was done for up to year 2030.

%95 confidential plot of annual flow was obtained for İnanlı stream. Mean value of average flow changed (decreased) 7% for RCP 4.5 and 9.5% for RCP 8.5 scenario. Besides upper and lower boundaries of %95 confidence interval expanded. That means probability of facing extreme flow conditions would increase as expected (Figure 4.22).

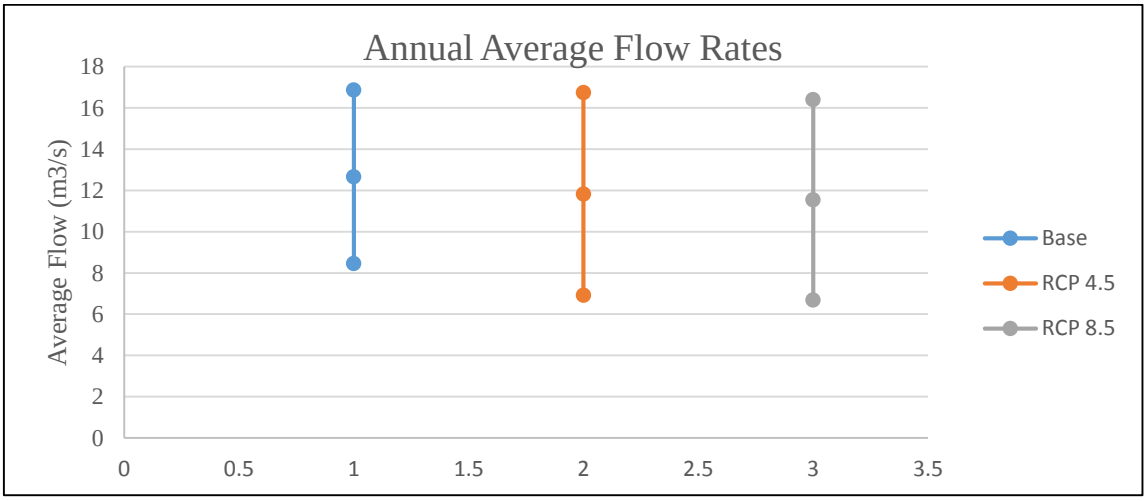


Figure 4.22. Comparison of Average Annual Flow According to Scenarios.

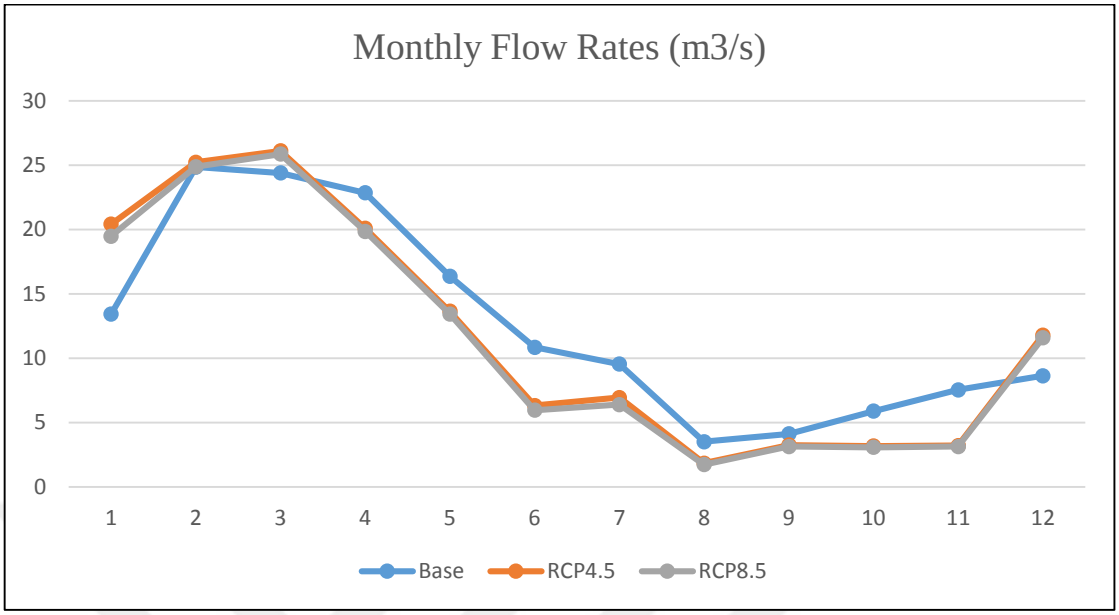


Figure 4.23. Comparison of Average Monthly Flow According to Scenarios.

According to flow regime both future scenarios reacted similarly, because the temperature and precipitation regime was not so much different up to 2030 years. But it could be seen that dry seasons flow decreases continuously also wet seasons flow capacity would increase according to Figure 4.23. Also, flood risk had a tendency to shift to earlier months due to flow regime. The difference graph easily points out that nearly all months flow regime would change. Summer and fall seasons would be much more drought. Also it was certain that flow amount would increase in winter season (Figure 4.24).

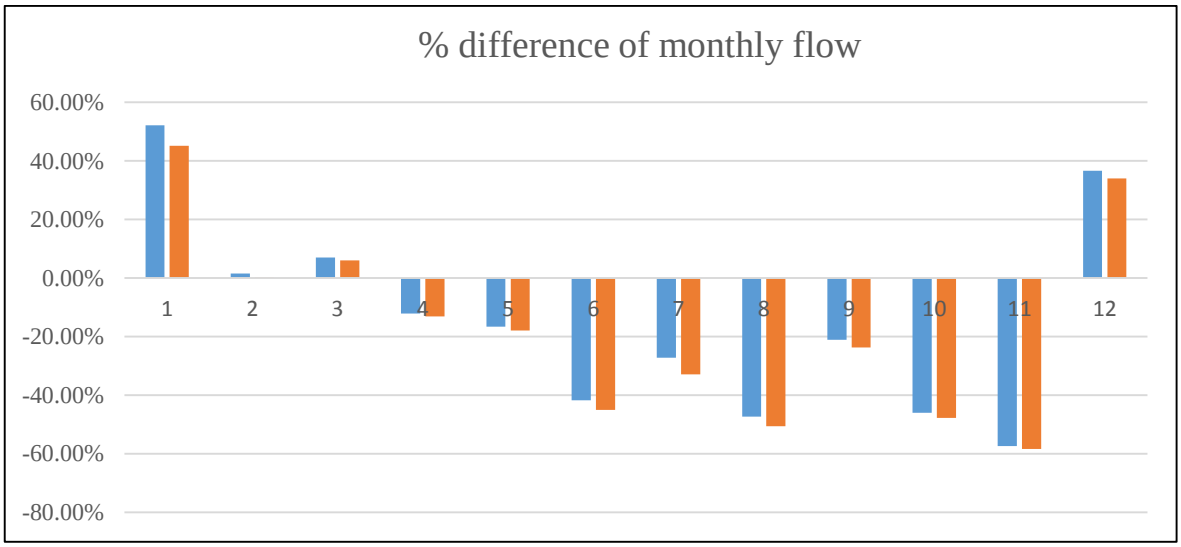


Figure 4.24. Difference Map of Current Flow with Estimated Flow Scenarios.

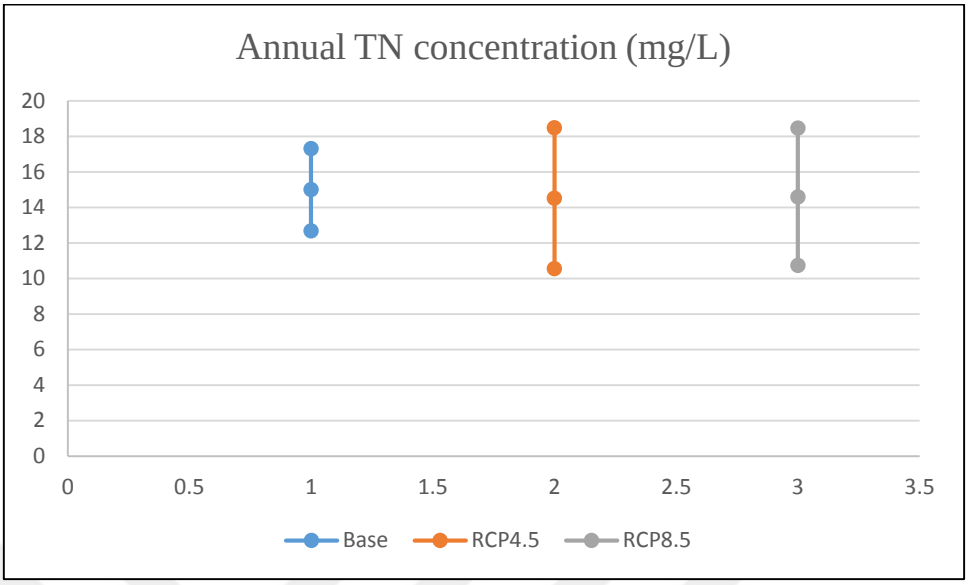


Figure 4.25. Comparison of Annual TN Concentration According to Scenarios.

Total yearly nitrogen load was expected to decrease under both RCP4.5 (by 3.2%) and RCP8.5 (by 2.7%) scenarios. The mean and median loads would be nearly same, whereas the minimum loads will decrease. The monthly load distribution was subject to decrease, especially in periods from January to March and from June to September. An increase in TN load was expected during the period from October to November. No substantial change was modeled in March and April (Figure 4.26).

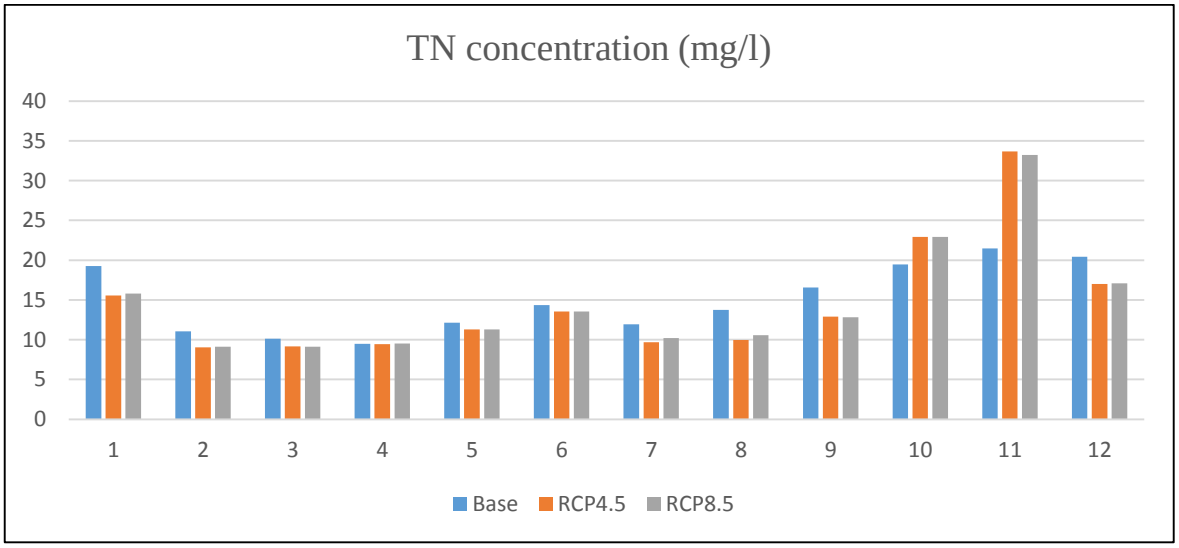


Figure 4.26. Comparison of Monthly TN Concentration According to Scenarios.

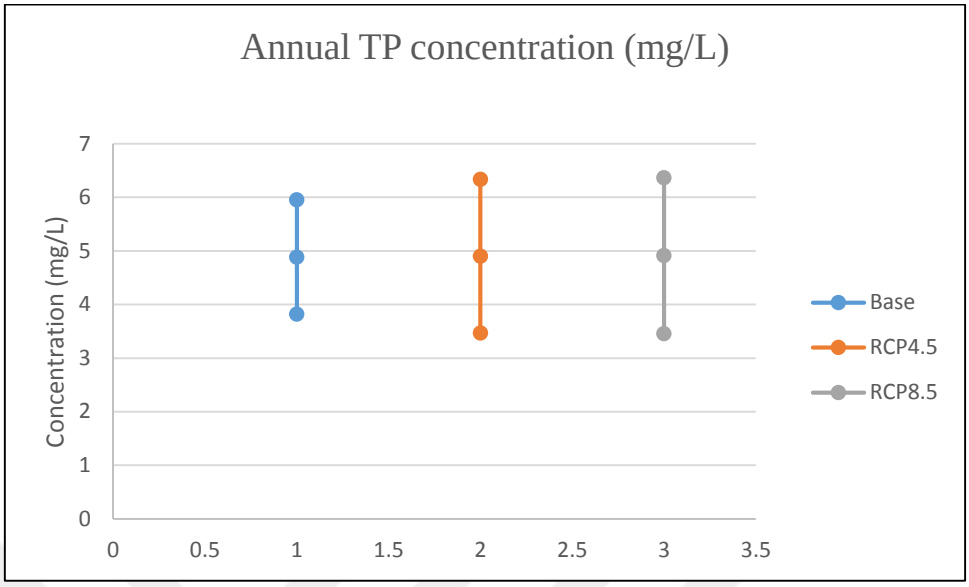


Figure 4.27. Comparison of Annual TP Concentration According to Scenarios.

As for TP loads, the model indicated nearly no change. The minimum TP load would decrease about 10% in minimal loads was modeled in the RCP 4.5 and 8.5. The maximum load would increase about 6 %. Inter-seasonal TP loads would experience substantial changes, with a large increase in the period from November to January, and a substantial decrease (by 70%) in August. A more significant increase during winter and early spring were modeled in the RCP4.5-8.5 scenario (Figure 4.27 and 4.28).

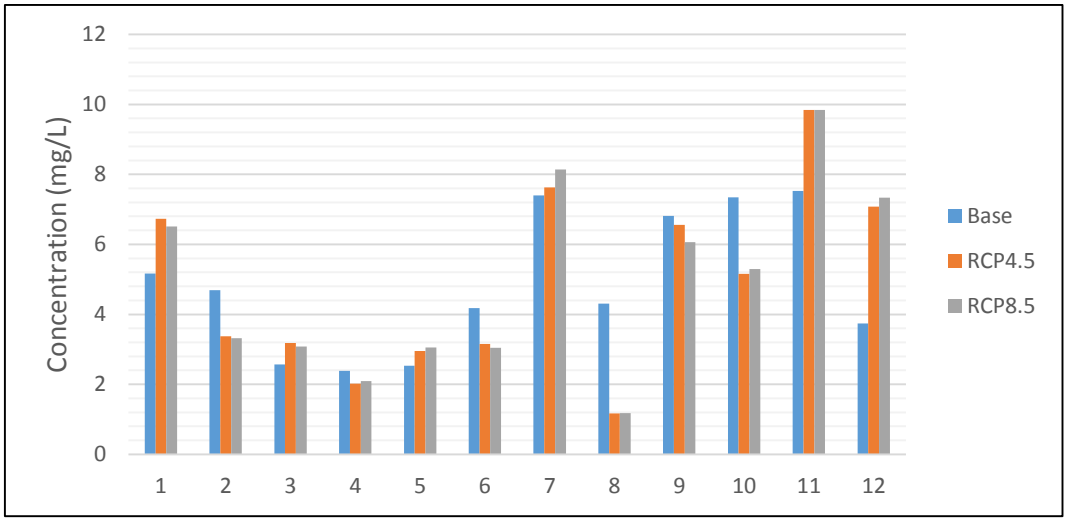


Figure 4.28. Comparison of Monthly TP Concentration  According to Scenarios.

## 4.8. Nutrient Load Estimation with Statistical Tests

As stated earlier, SWAT may show insufficient performance in order to estimate nutrient and concentration load over the basin (give some refs). To map the nutrient and concentration, non-parametric statistical tests were employed to understand the character of the recorded pollutant data in the basin. Moreover, an ARIMA model approach was offered for forecast the pollutant concentration for the certain time periods of 2010, 2020, 2030 and 2040 based on the previous trend of the available data.

### 4.8.1. Mann & Kendall Test

Mann (1945) and Kendall (1975) recommended by the non-parametric test that is independent of distribution. It is used to determine the monotonic trend in time series. The monotonic trend shows a continuously increasing or decreasing change over time. It is not affected by the actual distribution of data and is less sensitive to extreme values. The Mann Kendall trend test is more suitable for determining the trend in hydrological and meteorological time series as well as other non-parametric tests.

$$S = \sum_{i=1}^{n-1} \sum_{j=i+1}^{n} sgn(x_{j-} x_i) \tag{4.1}$$

$$sgn(\theta) = \begin{Bmatrix} +1 & (x_{j-} x_i) > 0 \\ 0 & (x_{j-} x_i) = 0 \\ -1 & (x_{j-} x_i) < 0 \end{Bmatrix} \tag{4.2}$$

Variance and Z distribution of equation is calculated from following equations.

$$Var(S) = \frac{n(n-1)(2n+5) - \sum t(t-1)(2t+5)}{18} \tag{4.3}$$

$$Zs = \begin{Bmatrix} \frac{S-1}{\sqrt{Var(S)}} \; S > 0 \\ 0 \;\; S = 0 \\ \frac{S+1}{\sqrt{Var(S)}} \; S < 0 \end{Bmatrix} \tag{4.4}$$

### 4.8.2. Spearman's Rho Test

Spearman's Rho (SR) test is another non parametric rank based test. Given a sample data set {$X_i$, I=1,2,..n} the null hypothesis Ho of the SR test against trend test is that all the $X_i$ are independent and identically distributed; the alternative hypothesis is that X increases or decreases with a trend. The test static is given by

$$D = 1 - \frac{6\sum_{i=1}^{n}[R(X_i)-i]^2}{n(n^2-1)} \tag{4.5}$$

Where R is the rank of the ith observation in the sample size n and Variance is

$$Var(D) = \frac{1}{(n-1)} \tag{4.6}$$

The p value of SR statistic is obtained from Z value

$$Zsr = \frac{D}{\sqrt{V(D)}} \tag{4.7}$$

The negative values of the Zs value show a decreasing trend, whereas the positive values show an increasing trend. The null hypothesis here is the absence of any trend in the time series, whereas when the Mann Kendall trend test is applied to a time series, when the absolute value of the Zs value is greater than the $Z_{\alpha/2}$ value found in the standard normal distribution table, the null hypothesis is rejected at the level of significance and the existence of the trend is accepted. This value is ±1,96 for the 95% confidence interval and ±2,54 for the 99% confidence interval (Köylü, 2017).

In many hydrological studies, two non-parametric rank-based statistical tests, namely the Mann–Kendall test (MK) and Spearman's Rho(SR) test are used for detecting monotonic trends in time series data. Yue *et al*. (2002) investigated the statistical power of both Spearman's Rho and Mann–Kendall at detecting monotonic trends in hydrological time-series. Statistical power of these tests are nearly identical. As sample size gets larger power of models increasing as expected. The power of tests also varies according to skewness in the data and distribution type.

In this study, MATLAB code was written for analyzing the trend of nutrient loads and other chemicals. (Figure C.1. and Figure D.1) Mann-Kendall test was used for comprehending trend of data. Due to the low quality water quality data, Spearman Rho test was conducted to elaborate existence of trend which may increase or decrease. Each average years selected for showing trend. First examine was for 5 years average moving, second one was 10 years average moving, and last one was 15 years average moving.

### 4.8.3. Time Series Models and ARIMA Model

The modeling of time series is expressed in mathematical formulas which consist of the shape of the model and a few parameters. For example, there is a need for a mathematical formula that defines the amplitude and phase to be modeled in relation to the sinusoidal wave.

Time series modeling is generally used for three purposes. These are to understand the relationship between the model and the time series, to produce future values or absent data, to obtain the trend of similar series.

<u>4.8.3.1. Autoregressive Model (AR).</u> It is the model that enables the modeling of time series in the most practical way. The values to be estimated are associated with the nearest historical value. According to the white noise, the power of correlation in the model indicates the continuity of the series. The general equation of the model was shown below.

$$(Y_t - \mu) = \sum_{l=1}^{p} \alpha_1 (Y_{t-1} - \mu) + Z_t \tag{4.8}$$

In this formula, μ is the average of the series and is shaped according to the noise (z). AR model is calculated with the number of parameters to be expressed in the model. For example, with AR model, a single parameter can be calculated as linear regression.

4.8.3.2. Moving Average Model (MA). The MA process is simply a linear filter of the previous white noise and is expressed by the overall equation of the process.

$$(Y_t) = \sum_{l=1}^{q} \beta_j \left(Y_{t-j}\right) + Z_t \tag{4.9}$$

The $\beta_j$ coefficient weights the relative contributions of the previous values. MA models are often used to model visible trends.

4.8.3.3. ARIMA Model. AR (Autoregressive) and MA (Moving Average) is the model formed by combining models. It is usually expressed in three components (p, d, q). The value p represents the sequence of the AR model, the q value is the sequence of the MA model, and the value of d represents the degree of differentiation. ARIMA model is calculated with time series and array values.

ARIMA (Autoregressive Integrated Moving Average) models are developed for prediction purposes. It is a good experimental model for modeling the observed time series. Modeling is carried out in three stages as model diagnosis, parameter estimation and diagnostic control of model conformity. These steps are repeated until the model is considered appropriate and then ready for use for model, process interpretation or prediction. ARIMA models are, in theory, the most general class of models for forecasting a time series which can be made to be “stationary” by differencing,

Control of stagnation is the first step in determining the model. If the series is not stationary, it has two indicators. Time series, different parts of the series have different general levels or auto-correlation degree is seen. Correlogram of the series (ACF, graph calculated by auto correlation function) is formed around zero.

The determination of MA and AR is the next step in model determination. MA and AR grades are determined using auto correlation and segmented auto correlation respectively. The AR (p) value to be used in the next stage refers to the interval in which the fragmented auto correlation is zero (lag ≥p + 1). In this way, the degree of AR is determined by drawing a sample fragmented auto correlation graph; in the graph of partial auto correlation values, the number of pause values exceeding the line of significance is determined.

The third step is model control and is carried out in three stages. Standardized residual values should not be in a time-varying pattern. The values of the residual values should not show significant auto correlation. Independence statistics of residual values in the time series should be determined. The model passing through these stages can be used to predict future values and missing values in the past (Köylü, 2017).

### 4.8.4. Application of Statistical Tests and ARIMA Model on Ergene Basin

With SWAT model, future flow and nutrient loads of streams were estimated. These results were helpful to obtain the trends and climate effect on study area. ArcSWAT was a good tool for observing future trends however there was a need of comparison of models results with another method due to low $R^2$ values (0.56) of nutrient loads (figure 4.6 - figure 4.7). It was estimated that, this situation stemmed from low quality input data and lack of water quality observation data. Therefore statistical methods were used for forecasting future trends according to historical values. Due to the data record of these stations was relatively high compared to other stations İnanlı, İpsala, Lüleburgaz, Uzunköprü stations water quality data was taken account for model. Orthophosphate (o-$PO_4$) and Ammonium ($NH_4$) concentrations investigated for comparison of SWAT model. And also statistical methods were applied for Alkalinity (Al) and Chlorite ($Cl^-$) where SWAT programs could not efficiently estimates future conditions.

Mann-Kendall (MK) and Spearman-Rho (SR) tests were applied for moving average of load concentrations according to 5, 10, 15 years. Both MK and SR test results measure the trend of data. Null Hypotheses Ho=0, indicates all variables are independent. Rejecting

null hypothesis H1≠0, all data has trend. If probability of SR is below “0” it means there is a decreasing trend, opposite means that there is an increasing trend. Another model named as ARIMA used for future trend of concentrations. This model is much more different from these two models. As explained above it estimates future values from historical data. Upper and Lower bounds show the % 90 confidence interval where concentration should be. In this study, test results were obtained by using MATLAB program. (Code of program are shown at Figure C.1. and Figure D.1). Where “Z” represents normal distribution Z value of tests and p represents probability value of these tests.

**o-$PO_4$ Concentration Statistical Tests**

**Mann-Kendall & Spearman Rho**
Concentration trend according to moving averages

**ARIMA**
Future Concentration Trends

a. İnanlı MA

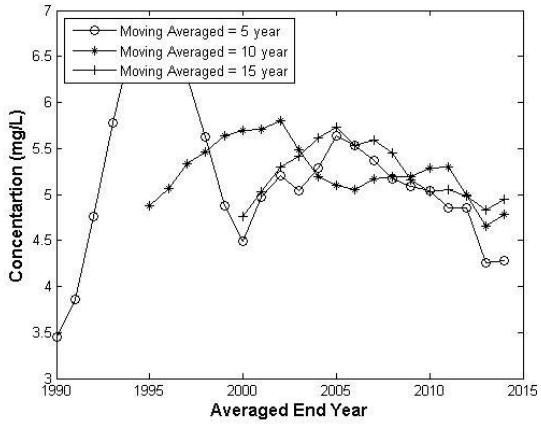


b. İnanlı ARIMA

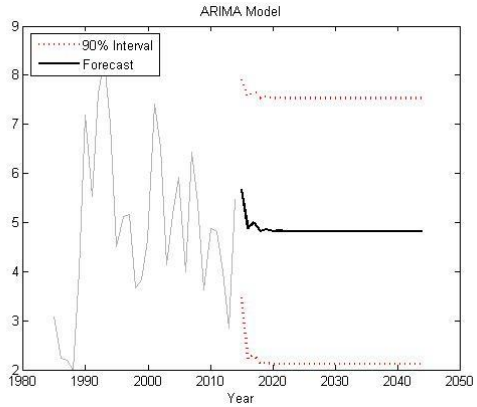


c. İpsala MA

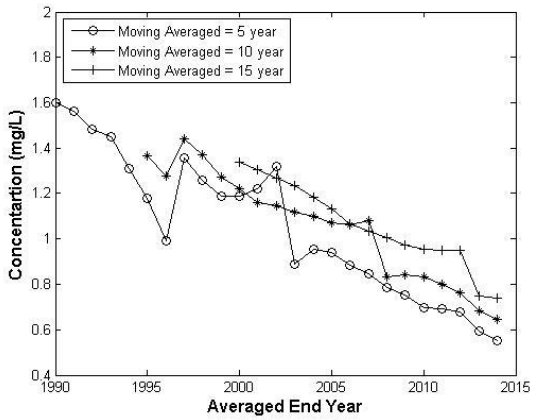


d. İpsala ARIMA

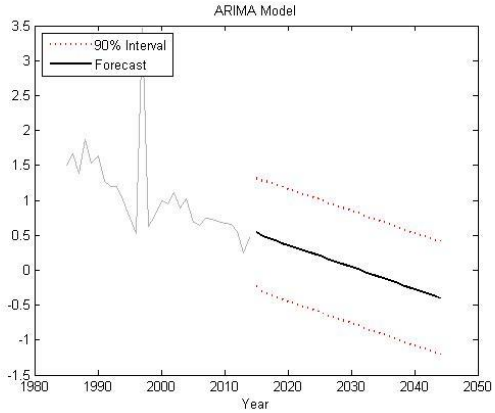


Figure 4.29. MK and SR Moving average concentration (a. and c.) and ARIMA results (b. and d.) for o-$PO_4$ İnanlı and İpsala stations

According to results İpsala rejected MK null hypotheses for o-$PO_4$ concentration that means there was a trend according to 5, 10, 15 years. And also for SR probabilities the trend would go downward. That means concentration of o-$PO_4$ would decrease among years according to statistics test. Also ARIMA model corrected these results. İpsala stream clearly showed a decreasing trend (Figure 4.29).

**o-$PO_4$ Concentration Statistical Tests**

**Mann-Kendall & Spearman Rho**
Concentration trend according to moving averages

**ARIMA**
Future Concentration Trends

a. Lüleburgaz MA

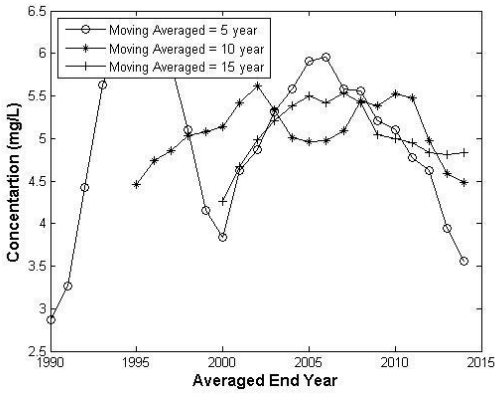


b. Lüleburgaz ARIMA

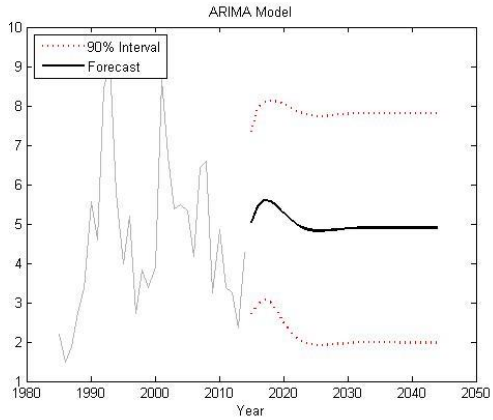


c. Uzunköprü MA

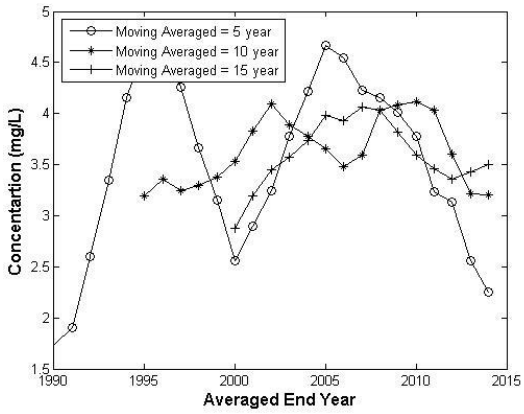


d. Uzunköprü ARIMA

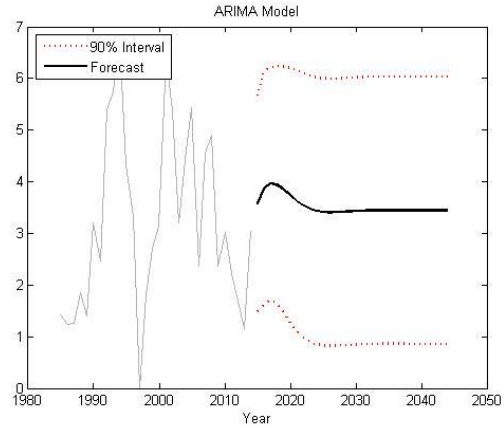


Figure 4.30. MK and SR Moving average concentration (a. and c.) and ARIMA results (b. and d.) for o-PO4 Lüleburgaz and Uzunköprü stations

On the other hand, İnanlı, Lüleburgaz and Uzunköprü did not reject MK null hypotheses. In other words, making estimation with MK and SR was not possible. But

ARIMA model can estimate future trend. As shown from figure there was a sudden increase estimated for year 2019 and after that concentration would be nearly constant after year 2025. The value of concentration would be change between 8 and 2 values (Figure 4.30).

Table 4.13. MK and SR Test Results for o-$PO_4$

| | İnanlı | İpsala | Lüleburgaz | Uzunköprü |
|---|---|---|---|---|
| MK (Z) | -1.38564 | -5.04769 | -0.3959 | 0.395897 |
| MK(p) | 0.1659 | 4.47E-07 | 0.6922 | 0.6922 |
| SR(Z) | -1.1893 | -3.7283 | -0.2272 | 0.4143 |
| SR(p) | 0.2343 | 0.000193 | 0.8203 | 0.6787 |
| Rho | -0.3179 | -0.9964 | -0.0607 | 0.1107 |

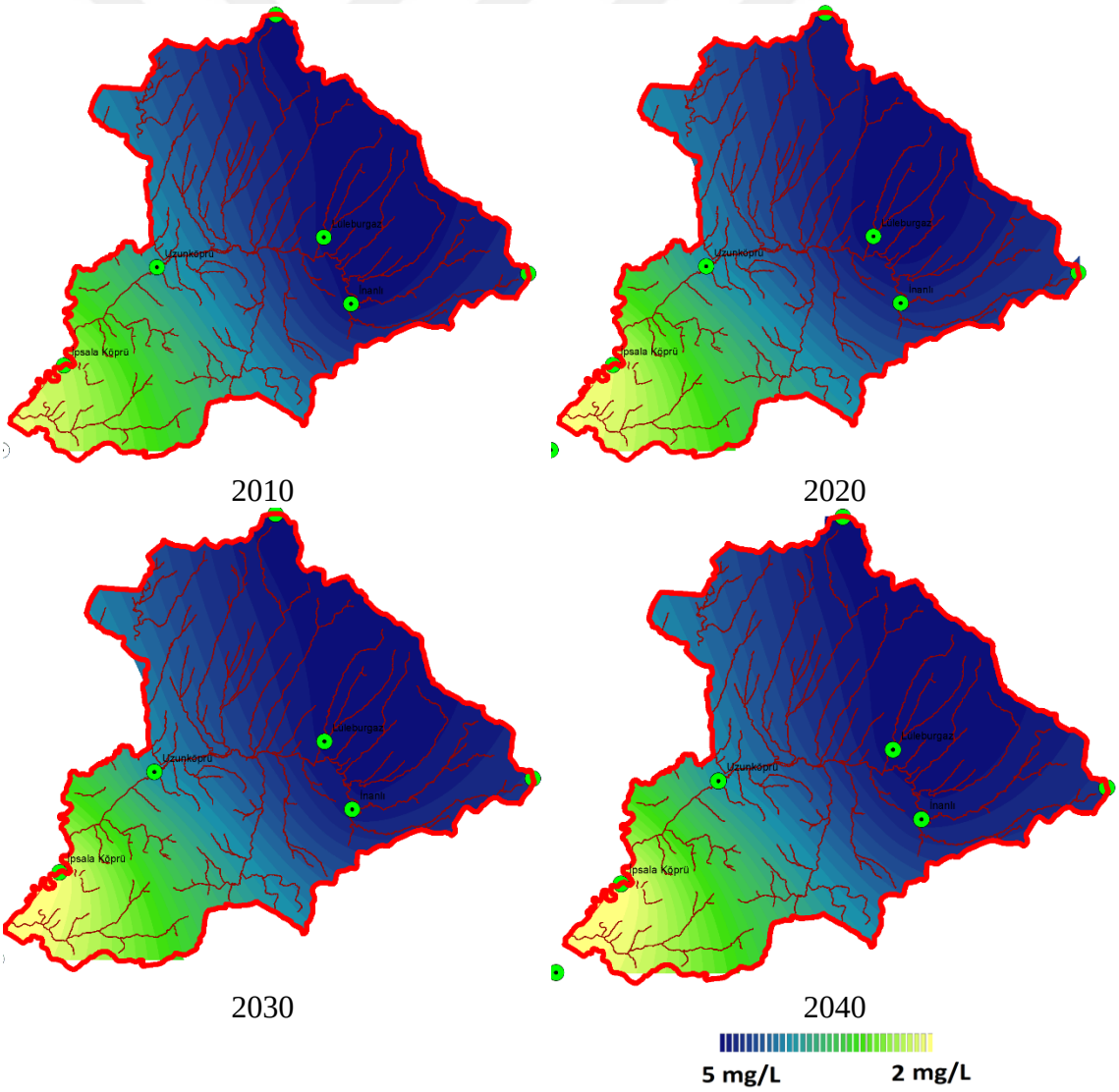


Figure 4.31. o-$PO_4$ concentration distribution of stations according to years ARIMA

As can be seen from figure 4.31, o-$PO_4$ concentration was decreasing over time. Phosphate is always a limiting nutrient for organisms. Increasing in phosphate amount will cause catastrophic environmental events like algal blooms. Therefore, phosphate concentration have to be limited for future scenarios. Also, ARIMA models phosphate concentration was close to the SWAT future estimations. Both models had similar results. This indicated that there was a potential phosphate risk threatens the region.

**$NH_4$ Concentration Statistical Tests**

**Mann-Kendall & Spearman Rho**
Concentration trend according to moving averages

**ARIMA**
Future Concentration Trends

a. İnanlı MA

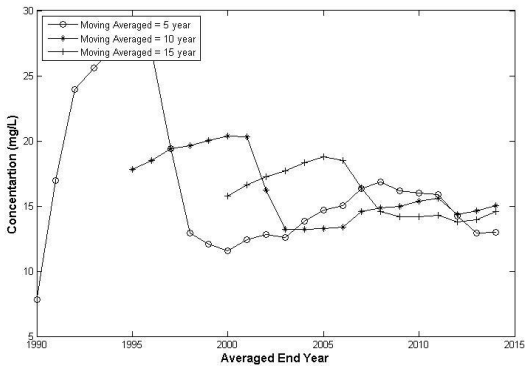


b. İnanlı ARIMA

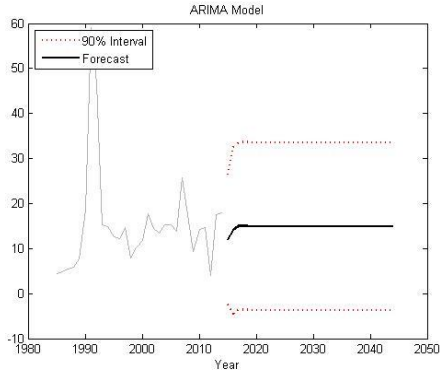


c. İpsala MA

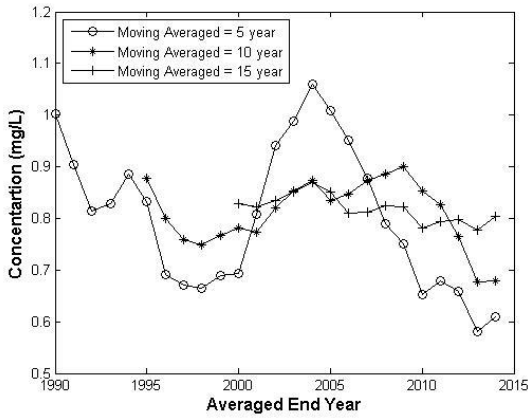


d. İpsala ARIMA

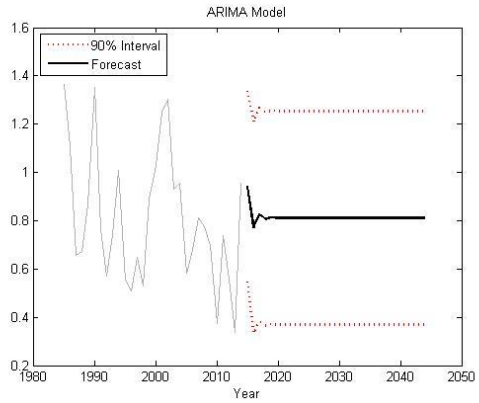


Figure 4.32. MK and SR Moving average concentration (a. and c.) and ARIMA results (b. and d.) for $NH_4$ İnanlı and İpsala stations

According to results İnanlı, İpsala, Lüleburgaz, Uzunköprü rejected MK null hypotheses for $NH_4$ concentration that means there was a trend according to 5, 10, 15 years.

For stations İnanlı, İpsala SR probabilities the trend would go upward. There was an opposite condition for Lüleburgaz and Uzunköprü stations. According to ARIMA model İnanlı and Uzunköprü had small amount increasing trend, while İpsala and Lüleburgaz had decreasing trend (Figure 4.32 and 4.33).

**$NH_4$ Concentration Statistical Tests**

**Mann-Kendall & Spearman Rho**
Concentration trend according to moving averages

**ARIMA**
Future Concentration Trends

a. Lüleburgaz MA

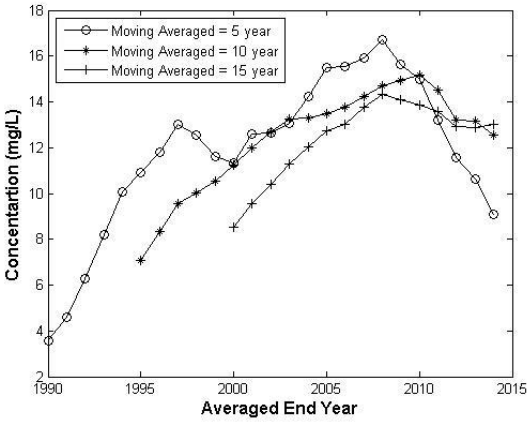


b. Lüleburgaz ARIMA

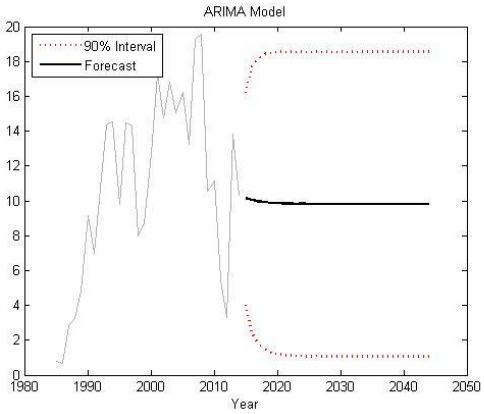


c. Uzunköprü MA

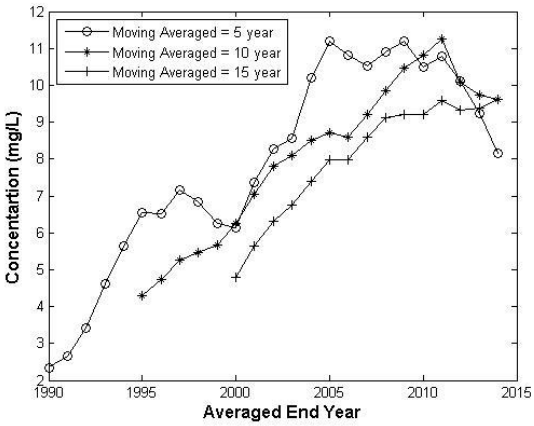


d. Uzunköprü ARIMA

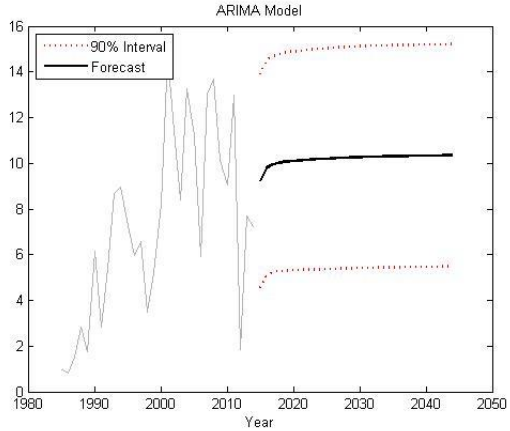


Figure 4.33. MK and SR Moving average concentration (a. and c.) and ARIMA results (b. and d.) for NH4 Lüleburgaz and Uzunköprü stations

Table 4.14. MK and SR Test Results for $NH_4$

| | İnanlı | İpsala | Lüleburgaz | Uzunköprü |
|---|---|---|---|---|
| MK (Z) | -2.17744 | -2.57333 | 2.672307 | 4.849742 |
| MK(p) | 0.0294 | 0.0101 | 0.0075 | 1.24E-06 |
| SR(Z) | -2.5791 | -2.8196 | 2.5657 | 3.6882 |
| SR(p) | 0.0099 | 0.0048 | 0.0103 | 0.000226 |
| Rho | -0.6893 | -0.7536 | 0.6857 | 0.9857 |

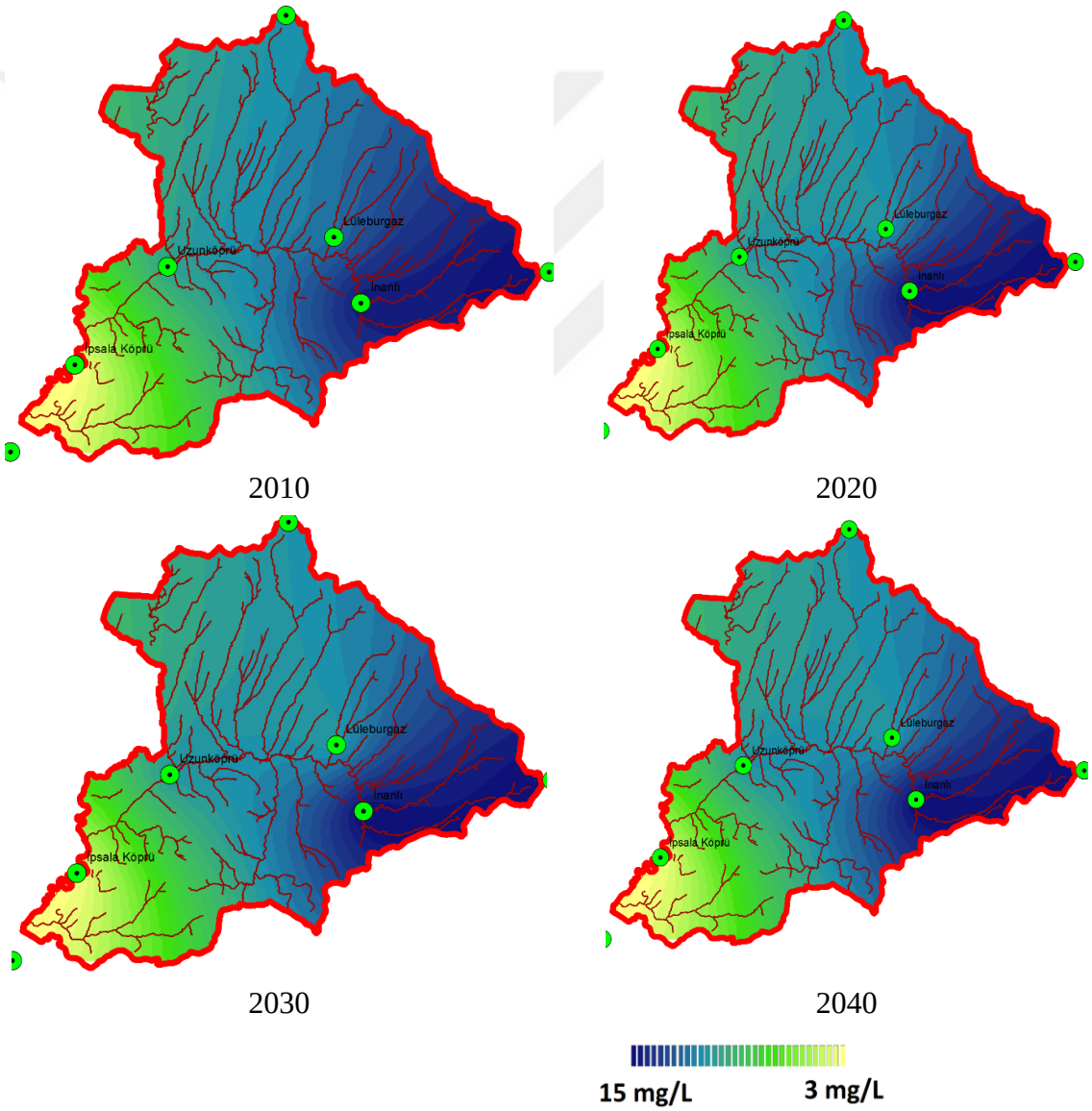


Figure 4.34. $NH_4$ concentration distribution of stations according to years for ARIMA

Ammonia is used in fertilizer and animal feed production and in the manufacture of fibres, plastics, explosives, paper, and rubber. It is used as a coolant, in metal processing, and as a starting product for many nitrogen-containing compounds. Ammonia and ammonium salts are used in cleansing agents and as food additives and ammonium chloride is used as a diuretic. As can be seen from figure 4.34, $NH_4$ concentration decreased over time. Despite decreasing concentration was beneficial for environment, the concentration amount was still high for up to year 2040. Therefore precautions have to be taken against $NH_4$ usage.

**Al Concentration Statistical Tests**

**Mann-Kendall & Spearman Rho**

Concentration trend according to moving averages

**ARIMA**

Future Concentration Trends

a. İnanlı MA

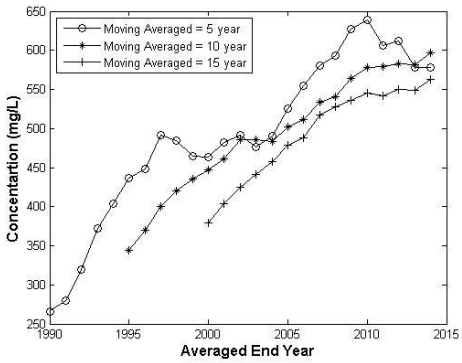


b. İnanlı ARIMA

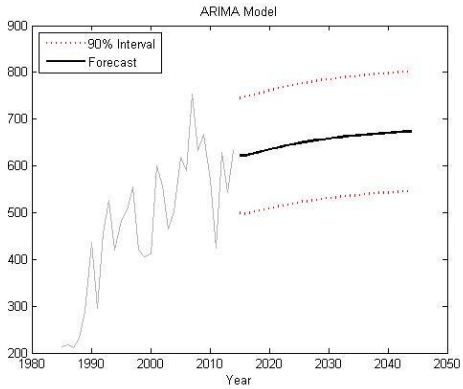


c. İpsala MA

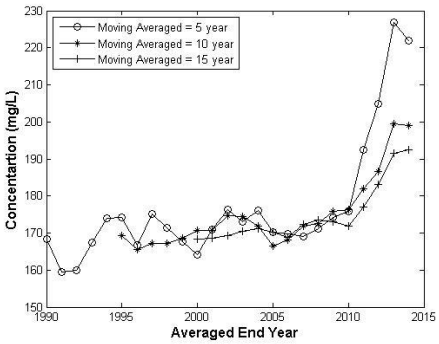


d. İpsala ARIMA

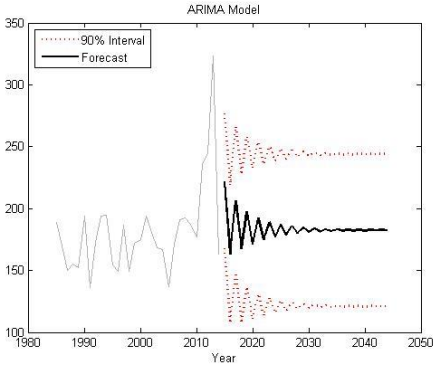


Figure 4.35. MK and SR Moving average concentration (a. and c.) and ARIMA results (b. and d.) Al İnanlı and İpsala stations

**Al Concentration Statistical Tests**

**Mann-Kendall & Spearman Rho** **ARIMA**

Concentration trend according to moving averages

Future Concentration Trends

a. Lüleburgaz MA

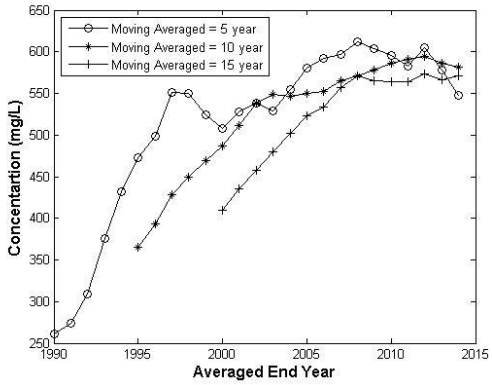


b. Lüleburgaz ARIMA

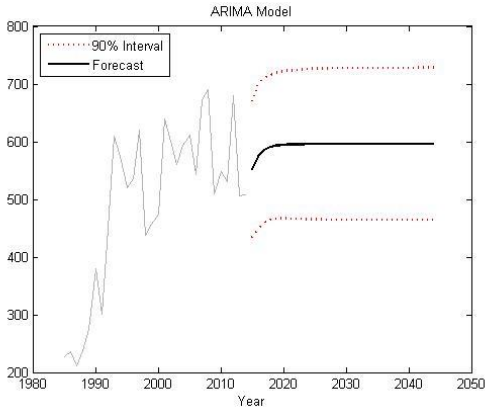


c. Uzunköprü MA

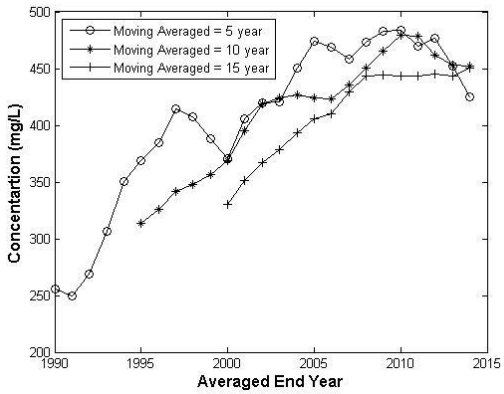


d. Uzunköprü ARIMA

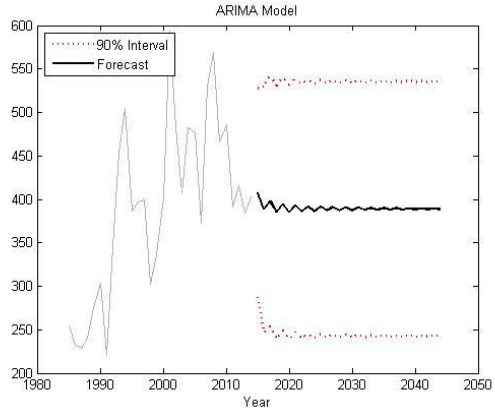


Figure 4.36. MK and SR Moving average concentration (a. and c.) and ARIMA results (b. and d.) for Al Lüleburgaz and Uzunköprü stations

MK and SR test rejected the null hypotheses for Alkalinity (Al) concentration. And also all Z values showed there was an expected increase in concentration of Al values. ARIMA clearly showed increasing trend for İnanlı and Lüleburgaz stream, and some fluctuations were expected for İpsala and Uzunköprü streams. As can be seen figure 4.37, the Al concentration shifting towards to south west of the region.

Table 4.15. MK and SR Test Results for Al

| | İnanlı | İpsala | Lüleburgaz | Uzunköprü |
|---|---|---|---|---|
| MK (Z) | 4.948717 | 4.156922 | 4.255896 | 4.552819 |
| MK(p) | 7.47E-07 | 3.23E-05 | 2.08E-05 | 5.29E-06 |
| SR(Z) | 3.7149 | 3.4744 | 3.4343 | 3.5679 |
| SR(p) | 0.000203 | 0.000512 | 0.000594 | 0.00036 |
| Rho | 0.9929 | 0.9286 | 0.9179 | 0.9536 |

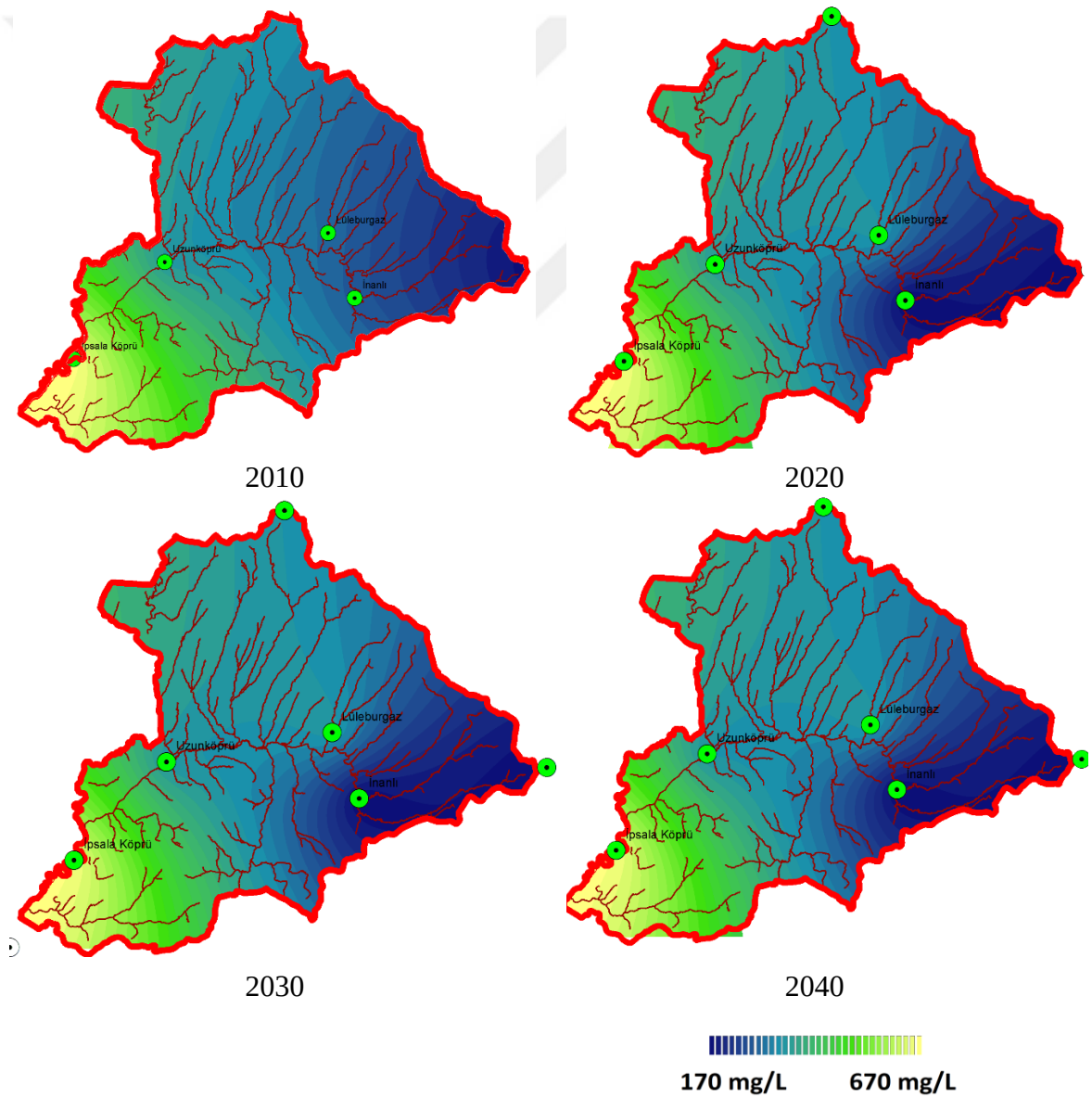


Figure 4.37. Al concentration distribution of stations according to ARIMA

For Cl concentration MK and SR test rejected the null hypotheses. And also all Z values showed there was an expected increase in concentration of Cl values. All ARIMA results expected an increase the trends of Cl concentrations.

**Cl Concentration Statistical Tests**

**Mann-Kendall & Spearman Rho**
Concentration trend according to moving averages

**ARIMA**
Future Concentration Trends

a. İnanlı MA

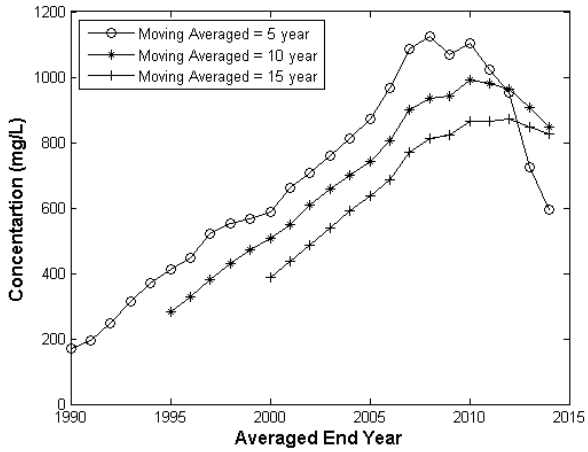


b. İnanlı ARIMA

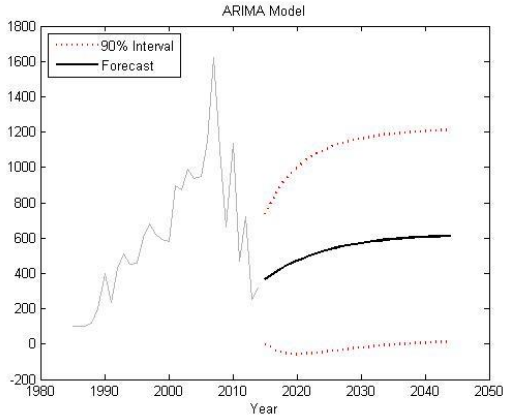


c. İpsala MA

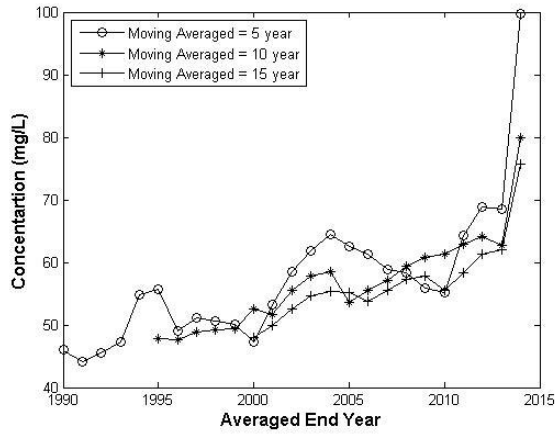


d. İpsala ARIMA

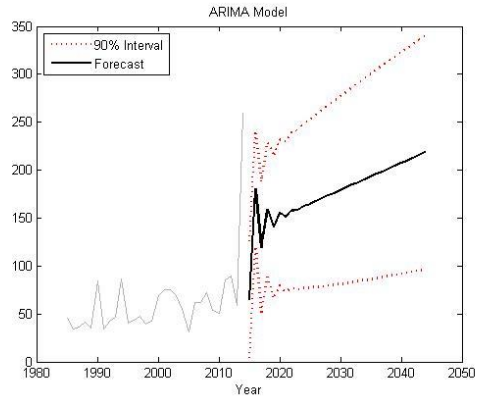


Figure 4.38. MK and SR Moving average concentration (a. and c.) and ARIMA results (b. and d.) for Cl İnanlı and İpsala stations

Table 4.16. MK and SR Test Results for Cl.

| | İnanlı | İpsala | Lüleburgaz | Uzunköprü |
|---|---|---|---|---|
| MK (Z) | 4.453845 | 4.552819 | 4.453845 | 4.849742 |
| MK(p) | 8.43E-06 | 5.29E-06 | 8.43E-06 | 1.24E-06 |
| SR(Z) | 3.5278 | 3.608 | 3.5278 | 3.6882 |
| SR(p) | 0.000419 | 0.000309 | 0.000419 | 0.000226 |
| Rho | 0.9429 | 0.9643 | 0.9429 | 0.9857 |

**Cl Concentration Statistical Tests**

**Mann-Kendall & Spearman Rho**

Concentration trend according to moving averages

**ARIMA**

Future Concentration Trends

a. Lüleburgaz MA

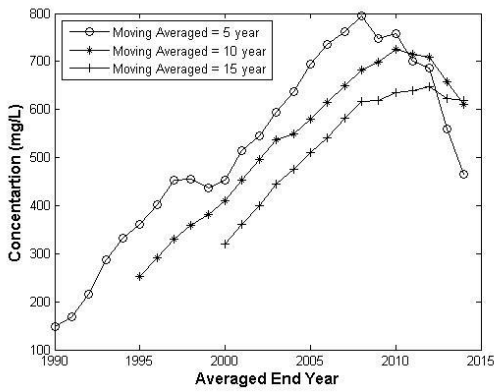


b. Lüleburgaz ARIMA

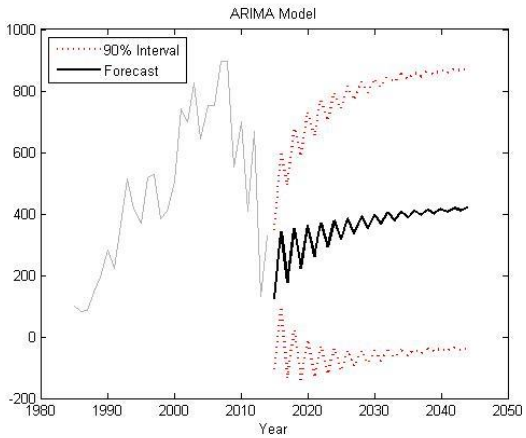


c. Uzunköprü MA

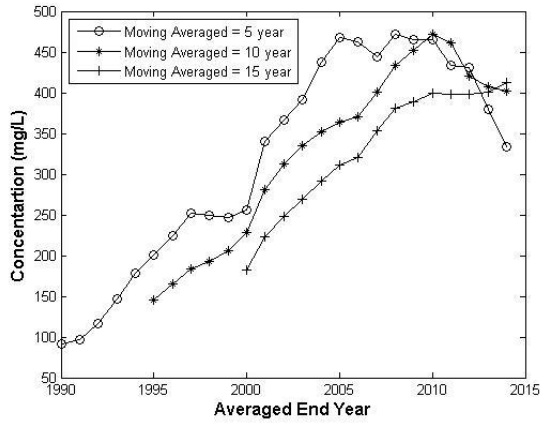


d. Uzunköprü ARIMA

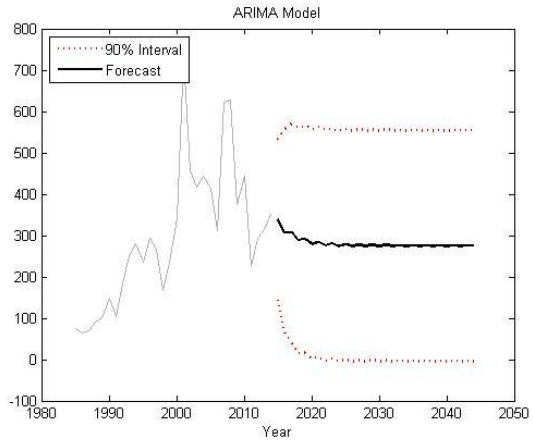


Figure 4.39. MK and SR Moving average concentration (a. and c.) and ARIMA results (b. and d.) for Cl Lüleburgaz and Uzunköprü stations

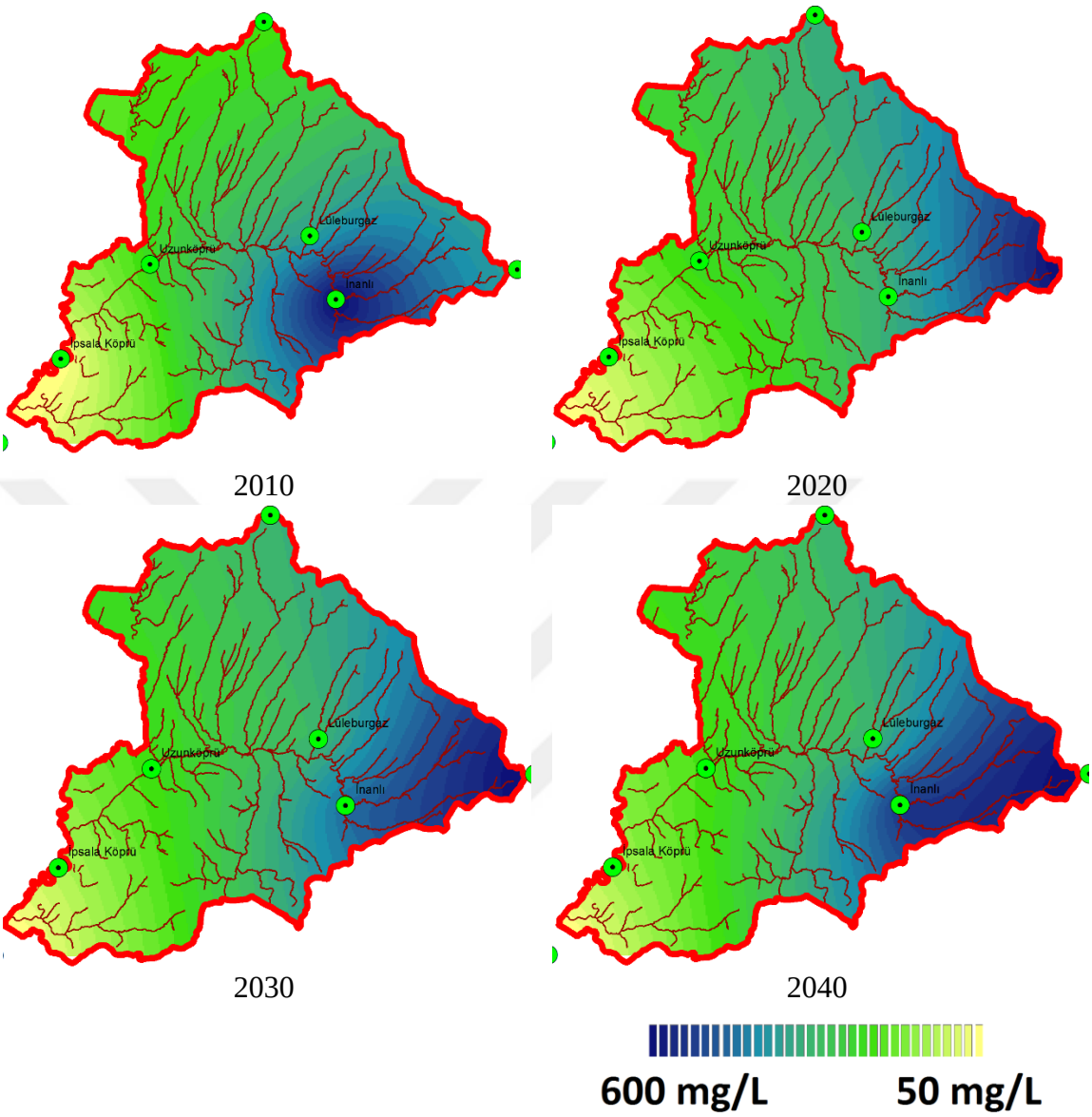


Figure 4.40. Cl concentration distribution of stations according to ARIMA

Chlorides are widely distributed in nature as salts of sodium (NaCl) and potassium (KCl). Sodium chloride is widely used in the production of industrial chemicals such as caustic soda, chlorine, sodium chlorite, and sodium hypochlorite. Sodium chloride, calcium chloride, and magnesium chloride are extensively used in snow and ice control. Potassium chloride is used in the production of fertilizers. It could be seen from figure 4.40. Main source of chloride seemed as İnanlı point which represents the source of industry. Therefore it seemed sodium chlorite was much more dominant than potassium chloride.

The outlined forecasting processes indicated the following key points:

- For a basin, the recorded data for certain pollutants include hydrological data such as flow rate, precipitation, evaporation, temperature etc implicitly. In other words, ARIMA model tries to extrapolate information from “what happened the past under some circumstances” to “what will happen under the same circumstances.” Thus, the entire process inherently includes bias and errors in the estimation.
- For a real interpretation of the proposed ARIMA model, the result of statistical tests for the specific stations were compared with the trend of the ARIMA model, and the results are consistent.
- Unless the necessary precautions are taken into account, Cl concentration will increase in İnanli, Lüleburgaz and İpsala stations where close to agricultural and industrial facilities are. The kriging analysis was applied to map the overall Cl concentration for the certain times. The propagation of Cl to Uzunköprü station is slow as shown in the figure 4.40. This result also verifies that of ARIMA model since the Cl concentration seems more or less constant over the years.
- Similar to above comment, the results can be extended to the findings of Al concentration analysis.
- Although the consistent results obtained from ARIMA, the data have uncertainty, so model capability should be considered as limited.

As a conclusion, these analyses show us Ergene basin is under attack by a considerable amount of pollutants which creates some risks for the environment as well as the human’s life.

# 5. RESULTS AND DISCUSSIONS

The concept of modeling is generally defined as a tool to assist people for solving the problems they face in the real world by simplifying them. This concept has been used in various fields for humanity, especially with the development of mathematical concepts and calculation techniques.

Hydrological models are used to formulate the issues such as flow potential, pollution, flood risk, especially the hydrological structure of water. In particular, physical-based models can provide consistent results in hydrological systems. With the development of satellite and computer technology, the use of physical-based models has increased and integrated modeling concept has become more prominent and basin model applications have become widespread.

In Turkey, lots of hydrological models were designed for river or lake systems. But, number of comprehensive watershed model for Turkey is limited. The main aim of this study is to be pioneer and instructive for other integrated watershed studies. Ergene Basin, which has been exposed to population growth, migration, industrial development and agricultural pollution since the 1980s, was the focus of this study. In addition, public institutions make researches about Ergene Basin, due to the policy makers decisions. This situation helped to get data about the region.

Ergene basin, is located in the northeast of Turkey, is at risk because it is neighbor to the Turkey's largest growth potential city, Istanbul. The organized industrial zones in the region creates point load risk, and also the agricultural potential of the region threatens the Ergene River, which is the biggest river in the region, and its networks. In addition, the Ergene Basin has been under pressure of immigration to the region's major cities, Tekirdag and Edirne.

The basin was modeled by ArcGIS-based SWAT model named as “ArcSWAT”. SWAT model has been preferred because it is widely used in the world. Such models need

high amount of data which increases the error probability. Therefore, it is important to prefer a common model, which is also used by other researchers, in order to solve the problems that may arise during modeling phase. As a matter of fact that, many problems were encountered from data acquisition to validation of the model. These problems were solved by the help of the information gathered from national and international sources.

Land use, land slope, soil classification, weather data are basic data needs of SWAT model. CORINE 2012 data and soil classification data was obtained from Ministry of Agriculture and Forestry, slope of basin was created by ArcGIS program. Climate data was obtained from the General Directorate of Meteorology (1960-2017). Pollution loads were calculated from the report outputs prepared by the Ministry of Agriculture and Forestry in 2017. The most important data of the model is daily meteorological data. The flow and pollution data required for the calibration and validation of the model were obtained from state hydraulic works (SHW). SHW constructed flow data for meet daily demand and pollution data for only few months of years due the missing data.

After the SWAT model was constructed according to the input data, a 2-year warm-up period was applied to model for years 2003-2004, model was calibrated with the years 2005-2007 data. 2008-2010 years were used for validation. The main reason for the 2-year warm up was to produce reasonable values for groundwater outputs. Hayrabolu and İnanlı observation points from the basin were used for the calibration phase. The model operated with monthly data. Due to the low accuracy of the outputs given by the daily data, monthly data were preferred.

SWAT-CUP program was preferred for calibration of the model. In the calibration process, it was determined that which parameters were more sensitive by the help of SUFI-2 module. 11 parameters were evaluated considering literature reviews. In the study, İnanlı and Hayrabolu flow data used for calibration parameters among these parameters, CN2 (moisture parameter) and CANMX (density of plant cover) values were found to be more sensitive than other parameters. The parameters were calculated as follows. CN2 0,073, ALPHA_BF 0.15, GW_DELAY 387, GWQMN 1.9, CANMX 18.33, EPCO 0.98, ESCO 0.75, SOL_AWC 0.92, GW_REVAP 0.179, OV_N 0.58, RAINHMX 89.5. Model

calibration $R^2$ value for Hayrabolu was 0.72 and 0.55 for İnanlı. Nash Sucliffe model efficiency coefficient was found 0.68 and 0.49 respectively. Values over 0.5 for NSE for stream flow calibration suggested acceptable. Calibration was completed for 2005-2008 years. After calibration period, new parameters applied and following $R^2$ values obtained for Hayrabolu (0.77) and İnanlı (0.72) stream. And also NSE values for Hayrabolu was 0.64 and İnanlı 0.48. The existence of water quality data was not valid for whole stations therefore İnanlı stream was chosen for nutrient load testing. Ministry of Agriculture and Forestry 2017 load data were used as constant load. Due to the fact that absence of data lead to decrease in $R^2$ values. The coefficient of determination ($R^2$) was 0.56 for TN and 0.55 for TP respectively. The water budget of Ergene Basin was created by SWAT model. Briefly according to model, precipitation amount was 597.6 mm and 443.1 mm evapotranspiration. Surface runoff system was 67 mm, lateral flow was 3.3 mm. 92.91mm water percolated to shallow aquifer.

The CA_Markov model was used to demonstrate future land use map of the region. The model can predict the change of region in the future by means of the given factor maps. It is an integration of Cellular Automata and Markov Chain systems. IDRISI model was chosen as the interface for application of the model. However, despite Turkey has high resolution 2006 and 2012 CORINE land use maps, the number of these maps were not sufficient for this study. Thus, 1990, 2000 and 2012 CORINE land use data has been downloaded from European Environmental Agency database. Although these maps have a low image resolution, they were preferred because of number of (3) different dated maps which are build up for 10 year intervals. These maps are reorganized with ArcGIS program to obtain same coordinate system. For testing model efficiency 2012 year map was created from 1990-2000 year data by the help of IDRISI program. There was a difference around %17 for artificial areas between projected and observed 2012 maps. This stems from the development trend of the region in the period 1990-2000 was not consistent with the period of 2000-2012. Therefore using most recent trends will decrease potential of error of land use estimation of upcoming years. For this reason, the 2000-2012 trend of change was used for future forecasting. According to the research, it was expected to that agricultural areas will be 77.28 % and artificial land area will be 3.90 % of total area in 2030 year. In 2050, this ratio was expected to be 72.90 % for agriculture and 4.52 % for artificial areas.

1960-2017 years meteorological data showed that the region will be effected by climate changes. In recent 50 years average trend of precipitation showed that region loses 1,56 mm precipitation per year. Maximum temperature has risen 0.04 degree Celsius per year, and minimum temperature follows it with 0.03 degree Celsius per year. Under these circumstances forecasting climate effects was a need for watershed model. RCP 4.5 and RCP 8.5 estimation scenario models which were prepared by the general directorate of meteorological services for climate change were used in this study. SWAT future climate data were generated according to these scenarios by downscaling temperature and precipitation data.

The model which can predict future scenarios is much more vulnerable than models present current situations for decision makers. For this reason, modeling future trends will contribute to the studies and academic researches in this area. Therefore, the input data were recreated in order to point out the effects of climate and land use change. The future SWAT model was established on 2030 land use map and RCP4.5 and RCP8.5 climate scenarios data. These results were compared with current land use and climate data. The model was run in terms of hydrology, TP and TN, and the results were compared for three scenarios. According to the results, mean value of average flow decreased 7% for RCP 4.5 and 9.5% for RCP 8.5. Also it was expected that during summer and spring periods flow rates will be decreased up to 57 percent. And flow amount would increase in winter period. Annual TN average will be expected to decrease 3.2% for RCP 4.5 and 2.7% for RCP 8.5. Despite average annual TP concentrations of all scenarios were nearly same, monthly distribution differed from month to month. TP loads would experience substantial changes, with a large increase in the period from November to January, and a substantial decrease (by 70%) in August.

Since the future climate of region trend wass consistent with RCP 4.5 and 8.5 scenarios, the concentration regimes were tested for their tendencies with Mann-Kendall and Spearman-Rho tests. These statistical models showed that the concentration values of certain dates were independent or dependent. It means, if concentration parameters were dependent, the concentrations had a tendency (increasing or decreasing). Statistical model could give information about future values. Beside these models, ARIMA model was

constructed for estimation values of concentrations. ARIMA could estimate concentrations with 95% confidence interval for future dates. ARIMA model could provide consistent results. These three tests were operated for İnanlı, Lüleburgaz and İpsala, Uzunköprü stations. o-$PO_4$, $NH_4$, $Cl^-$, Al quality values were used for testing model. According to Mann-Kendal and Spearman-Rho tests showed that only Lüleburgaz and Uzunköprü stations o-$PO_4$ values were independent, all rest 4 stations values had a tendency for all concentrations.

Model also consistent with SWAT output results, both models estimated TN concentration as close to 15 and TP concentration as 5mg/l. Besides ARIMA model could estimate future concentrations of ions like Cl which SWAT could not. Therefore using ARIMA would be a simple but consistent way for decision makers. Results of ARIMA model were visualized by krigging method with ArcGIS program. The resultant map showed the distribution of concentrations around Ergene Basin. It was seen from figures that industrial locations were the source of pollution for region. If this scenario continued up to 2040, nearly whole basin would be effected. These analyses showed us Ergene basin was under attack by a considerable amount of pollutants which creates some risks for the environment as well as the human's life.

To sum up, when the land use change models are taken into consideration, it is understood that the density of the city center will increase and some agricultural lands will decrease or become inefficient. In addition this scenario is not far away due to the basin's proximity to İstanbul province. Despite the land use transition potential of Ergene basin is not so high in recent years, there is a probability that ongoing investments in basin may trigger again land use changes. As a result, the increase of area defined as artificial area will continue to pose a risk on water sources and nature. According to climate models, the maximum and minimum temperatures of the region are expected to increase and the precipitation regime is expected to decrease. Although there is not much change in annual average in the short term, it is seen that the region is risky in monthly distribution. It may be likely that the region will be exposed to flood risk in the following years. The water quality models and statistical tests carried out within the scope of the thesis show that the region is at risk for pollution. If no regulations or investments are made in order to prevent

pollution in the region, the western part of the basin, which is now less polluted than in the east, will be affected by this pollution. In addition to the elements that trigger environmental pollution such as nitrogen and phosphorus, also chlorine and alkalinity values are a threat for the region. The presence of sectors such as leather and textiles in the region shows that heavy metals and toxic chemicals are present in water resources. Therefore, it is important to identify and monitor the risky substances and to model them according to these values.

This study in which land use and climate adaptation of the region was handled in the regional sense will contribute to the academic researches and the strategic plans of the Thrace region and we hope that it will lead to a larger scale of regional and national studies. It is expected that study will provide a decision support mechanism to national and regional decision makers in the development, planning and implementation stages of strategies in land and water resources management.

# REFERENCES


Abbaspour, C. K. (2008). SWAT Calibrating and Uncertainty Programs. *A User Manual. Eawag Zurich, Switzerland*.

Abdelwahab, O. M. M., Ricci, G. F., De Girolamo, A. M., & Gentile, F. (2018). Modelling Soil Erosion in a Mediterranean Watershed: Comparison between SWAT and AnnAGNPS Models. *Environmental Research*, *166*, 363-376.

Akın, M., & Akın, G. (2007). Suyun Önemi, Türkiye'de Su Potansiyeli, Su Havzaları ve Su Kirliliği. *Ankara Üniversitesi Dil ve Tarih-Coğrafya Fakültesi Dergisi*, *47*(2), 105-118.

Akıner, M. E., & Akkoyunlu, A. (2012). Modeling and Forecasting River Flow Rate from the Melen Watershed, Turkey. *Journal of Hydrology*, *456*, 121-129.

Altın, B. N. (2000). Trakya'da Yerşekillerinin Neotektonik Dönem Jeomorfolojik Gelişimleri. 28. *Coğrafya Meslek Haftası (Edirne) Bildiriler, Geçmişte, Günümüzde ve Gelecekte Trakya, Editör: Prof. Dr. Suna Doğaner, Türk Coğrafya Kurumu Coğrafya Meslek Haftaları Serisi*, *2*, 10-12.

Altürk, B. (2017). Arazi Kullanım/Arazi Örtüsü Değişikliğinin ve Su Kaynaklarına Etkisinin Belirlenmesi: Ergene Havzası Örneği. *Ph. D Thesis. Namık Kemal Üniversitesi. Tekirdağ*.

Anand, J., Gosain, A. K., & Khosa, R. (2018). Prediction of Land Use Changes Based on Land Change Modeler And Attribution of Changes İn The Water Balance of Ganga Basin To Land Use Change Using the SWAT model. *Science of the Total Environment*, *644*, 503-519.

Arnell, N. W. (1999). Climate Change and Global Water Resources. *Global Environmental Change*, *9*, 31-49.

Arnold, J. G., Srinivasan, R., Muttiah, R. S., & Griggs, R. H. (1995). Watershed Modeling and GIS with SWAT and GRASS. SWAT User's Manual. *Blackland Research Center. Texas Agricultural Experimental Station: Temple, TX*.

Bicknell, B. R., Imhoff, J. C., Kittle Jr, J. L., Donigian Jr, A. S., & Johanson, R. C. (1996). Hydrological Simulation Program-FORTRAN. *User's Manual for Release 11. US EPA.*

Biswas, A. K. (1970). *History of Hydrology*. Elsevier Science Limited.

Čerkasova, N., Umgiesser, G., & Ertürk, A. (2018). Development of A Hydrology and Water Quality Model for a Large Transboundary River Watershed to İnvestigate The İmpacts of Climate Change–a Swat Application. *Ecological Engineering*, *124*, 99-115.

Cox, P. M., Betts, R. A., Jones, C. D., Spall, S. A., & Totterdell, I. J. (2000). Acceleration of Global Warming due to Carbon-cycle Feedbacks in a Coupled Climate Model. *Nature*, *408*(6809), 184.

Danielopol, D. L., Griebler, C., Gunatilaka, A., & Notenboom, J. (2003). Present State and Future Prospects for Groundwater Ecosystems. *Environmental Conservation*, *30*(2), 104-130.

Devi, K. G., Ganasri, B. P., & Dwarakish, G. S. (2015). A Review on Hydrological Models, Aquatic Procedia, 4, 1001–1007.

Donigian, A. S., & Imhoff, J. (2006). History and Evolution of Watershed Modeling Derived from the Stanford Watershed Model. *Watershed Models*, 21-45.

Eagleson, P. S. (1970). *Dynamic Hydrology* (No. GB661 E23).

EEA (2006). *European Environment Agency CORINE Land Cover 2006 Legend*, https://www.eea.europa.eu/data-and-maps/figures/corine-land-cover-2006-by-country-1/legend/fancybox.html, accessed at December 2018.

Erdoğan, N., Nurlu, E., Guvensen, A., & Erdem, U. (2015). Land Use/Land Cover Change Detection for Environmental Monitoring in Turkey. A Case Study in Karaburun Peninsula. *Journal of Environmental Protection and Ecology*, *16*(1), 252-263.

Ertürk, A., Gurel, M., Ekdal, A., Tavsan, C., Ugurluoglu, A., Seker, D. Z., ... & Ozturk, I. (2010). Water Quality Assessment and Meta Model Development in Melen Watershed–Turkey. *Journal of Environmental Management*, *91*(7), 1526-1545.

Ertürk, A., Ekdal, A., Gürel, M., Karakaya, N., Guzel, C., & Gönenç, E. (2014). Evaluating the İmpact of Climate Change on Groundwater Resources in a Small Mediterranean Watershed. *Science of the Total Environment*, *499*, 437-447.

Ficklin, D. L., Luo, Y., Luedeling, E., & Zhang, M. (2009). Climate Change Sensitivity Assessment of a Highly Agricultural Watershed Using SWAT. *Journal of Hydrology*, *374*(1-2), 16-29.

Flato, G., Marotzke, J., Abiodun, B., Braconnot, P., Chou, S. C., Collins, W., ... & Forest, C. (2013). Evaluation of Climate Models. *Cambridge University Press*. 741-882.

Friedlingstein, P., Cox, P., Betts, R., Bopp, L., von Bloh, W., Brovkin, V., ... & Bala, G. (2006). Climate–carbon Cycle Feedback Analysis: Results from the C4MIP Model Intercomparison. *Journal of Climate*, *19*(14), 3337-3353.

GDM (2015).Yeni Senaryolar ile Türkiye İklim Projeksiyonları ve İklim Değişikliği. *Meteoroloji Genel Müdürlüğü. Ankara*. 62-68.

Gök, C. (2015). Havza Sürdürülebilirlik İndeksinin Türkiye'de Uygulanması: Ergene Havzası Örneği. *Master Thesis. Hacettepe University. Ankara*.

Gölpınar, M. S. (2017). Determination of Surface Flow with SWAT Model: A Case Study in the Akarsu Irrigation District. *Master Thesis. Çukurova University. Adana.*

Güneş, E. H. (2009). Havzalar için Zehirlilik Parametresi ile Deşarj Etki İndeksi Geliştirilmesi. *Ph.D Thesis. Istanbul Technical University. Istanbul.*

Güngör (2018). SWAT Modeli Kullanılarak Filyos Çayı Havzası'nın Hidrolojik Analizi. *Ph.D Thesis. Bulent Ecevit University. Zonguldak.*

Güzel, Ç. (2010). SWAT Modelinin Türkiye'deki Bir Havzada Uygulanması. *Ph.D Thesis. Istanbul Technical University. Istanbul.*

Haines, C., & Crouch, R. (2007). Mathematical modelling and applications: Ability and competence frameworks. In *Modelling and applications in mathematics education* (pp. 417-424). Springer, Boston, MA.

Haktanır, K., Cangir, C., & Boyraz, D. (2005). Toprak Kaynakları Kullanımı. *TMMOB Ziraat Mühendisleri Odası, Türkiye Ziraat Mühendisliği VI. Teknik Kongresi*, 3-7.

Hallı, M., Sari, E., & Kurt, M. A. (2014). Assessment of Arsenic and Heavy Metal Pollution in Surface Sediments of the Ergene River, Turkey. *Polish Journal of Environmental Studies*, *23*(5).

Han, H., Yang, C., & Song, J. (2015). Scenario simulation and the prediction of land use and land cover change in Beijing, China. *Sustainability*, *7*(4), 4260-4279.

Hazar, K. (1997). Ergene Nehri Kirlilik Raporu. *DSİ. Genel Müdürlüğü, XI. Bölge Müdürlüğü, Edirne*.

IPCC (2001). Climate change 2001: impacts, adaptation, and vulnerability: contribution of Working Group II to the third assessment report of the Intergovernmental Panel on Climate Change (Vol. 2). *Cambridge University Press*.

IPCC (2007). Climate Change 2007: The Scientific Basic. Contribution of Working Group I to the Fourth Assessment Report of the Intergovernmental Panel on Climate Change. Summary for Policy Makers.

IPCC (2007a). Climate Change 2007: Impacts, Adaptation and Vulnerability. *Cambridge, United Kingdom and New York, NY, USA. Cambridge University Press.*

IPCC (2013). Summary for Policymakers Climate Change 2013. The Physical Science Basis Contribution of Working Group I to the Fifth Assessment Report of the Intergovernmental Panel on Climate Change. *Ed: Thomas F. Stocker, Dahe Qin, Gian- Kasper Plattner, Tignor Simon K. Allen, Judith Boschung, Alexander Nauels, Yu Xia, Vicent Bex, Pauline Midgley. Cambridge University Press. Cambridge.*

IPCC (2018). Summary for Policymakers. In: Global warming of 1.5°C. An IPCC Special Report on the impacts of global warming of 1.5°C above pre-industrial levels and related global greenhouse gas emission pathways, in the context of strengthening the global response to the threat of climate change, sustainable development, and efforts to eradicate poverty. *World Meteorological Organization. Geneva. Switzerland.* 32.

Jajarmizadeh, M., Harun, S., & Salarpour, M. (2012). A review on theoretical consideration and types of models in hydrology. *Journal of Environmental Science and Technology*, *5*(5), 249-261.

Kocaman, H., Akin, Y. K., & Oğuzhan, A. (2011). The Effects of Ergene River's Pollution on Agricultural Production in Thrace: A Case Study of Edirne. *The Black Sea Journal of Science*, *2*(3), 89-104.

Köycegiz, C., & Büyükyıldız, M. (2019). Calibration of SWAT and Two Data-Driven Models for a Data-Scarce Mountainous Headwater in Semi-Arid Konya Closed Basin. *Water*, *11*(1), 147.

Lambin, E. F., Rounsevell, M. D. A., & Geist, H. J. (2000). Are Agricultural Land-Use Models Able to Predict Changes in Land-use Intensity?. *Agriculture, Ecosystems & Environment*, *82*(1-3), 321-331.

Lee, K. S., & Chung, E. S. (2007). Hydrological Effects of Climate Change, Groundwater Withdrawal, and Land Use in a Small Korean Watershed. *Hydrological Processes: An International Journal*, *21*(22), 3046-3056.

Lin, B., Chen, X., Yao, H., Chen, Y., Liu, M., Gao, L., & James, A. (2015). Analyses of Landuse Change Impacts on Catchment Runoff Using Different time Indicators Based on SWAT Model. *Ecological Indicators*, *58*, 55-63.

Milly, P. C. D., Betancourt, J., Falkenmark, M., Hirsch, R. M., Kundzewicz, Z. W., Lettenmaier, D. P., & Stouffer, R. J. (2008). Stationarity is Dead: Whither Water Management? *Science*, *319*(5863), 573-574.

Ministry of Development. (2012). 2012 Yılı Yatırım Programı. *Kalkınma Bakanlığı. Ankara*.

MoFWA (2013). Basin Protection Action Plans: Ergene Basin Report. *Ministry of Forestry and Water Affairs. Ankara*.

MoAF (2017). Ergene Pollution Report. *Ministry of Agriculture and Forestry. Ankara*.

Moriasi, D. N., Arnold, J. G., Van Liew, M. W., Bingner, R. L., Harmel, R. D., & Veith, T. L. (2007). Model Evaluation Guidelines for Systematic Quantification of Accuracy in Watershed Simulations. *Transactions of the ASABE*, *50*(3), 885-900.

Nash, J. E., & Sutcliffe, J. V. (1970). River Flow Forecasting Through Conceptual Models Part I—A Discussion of Principles. *Journal of Hydrology*, *10*(3), 282-290.

Neitsch, S. L., Arnold, J. G., Kiniry, J. R., & Williams, J. R. (2011). Soil and Water Assessment Tool Theoretical Documentation Version 2009. *Texas Water Resources Institute.*

Ordu, Ş., & Demir, A. (2007). Determination of water quality of Ergene River by planning environmental information system. *Sigma Journal of Engineering and Natural Sciences*, *25*(1), 101.

Özcan, Z. (2016). Evaluation of the Best Management Practices to Control Agricultural Diffuse Pollution in Lake Mogan Watershed with SWAT Model. *Ph.D Thesis. Middle East Technical University. Ankara.*

Özdemir, A., & Leloglu, U. M. (2014, September). Climate Change Impact Assessment on River Basin: Sarisu-Eylikler River, Turkey. *In 2nd International sustainable watershed management conference, SuWaMa*. 103-112.

Özkan, E., Kubaş, A. & Toprak, A. (2008). Ergene Havzasındaki Kirliliğin Sosyo Ekonomik Etkileri. *Havza Kirliliği Konferansı*, 15.

Paçal, M. (2017). Hydrological and Water Quality Modeling Of Ergene River Basin. *Master Thesis. Yıldız Technical University. Istanbul.*

Piao, S., Ciais, P., Huang, Y., Shen, Z., Peng, S., Li, J., ... & Friedlingstein, P. (2010). The Impacts of Climate Change on Water Resources and Agriculture in China. *Nature*, *467*(7311), 43.

Price, B., Kienast, F., Seidl, I., Ginzler, C., Verburg, P. H., & Bolliger, J. (2015). Future Landscapes of Switzerland: Risk Areas for Urbanisation and land Abandonment. *Applied Geography*, *57*, 32-41.

Stocker, T. F., Qin, D., Plattner, G.-K., Alexander, L. V., Allen, S. K., Bindoff, N. L., et al. (2013). Technical Summary. In T. F. Stocker, D. Qin, G.-K. Plattner, M. Tignor, S. K. Allen, J. Boschung, et al. (Eds.), *Climate Change 2013: The Physical Science Basis. Contribution of Working Group I to the fifth Assessment Report of the Intergovernmental Panel on Climate Change* . Cambridge, UK, New York: Cambridge University Press. 33–115.

Sullivan, A., Ternan, J. L., & Williams, A. G. (2004). Land use change and hydrological response in the Camel catchment, Cornwall. *Applied Geography*, *24*(2), 119-137.

Thavhana, M. P., Savage, M. J., & Moeletsi, M. E. (2018). SWAT modEl Uncertainty Analysis, Calibration and Validation for Runoff Simulation in the Luvuvhu River Catchment, South Africa. *Physics and Chemistry of the Earth, Parts A/B/C*.

TURKSTAT (2017). National Population and Demographic Statistics. *Ankara.*

Usul, N. (2005). Engineering Hydrology. METU Press. *Ankara.*

Veldkamp, A., & Lambin, E. F. (2001). Predicting Land-use Change. Elsevier Science Limited.

Verburg, P. H., & Overmars, K. P. (2009). Combining Top-down and Bottom-up Dynamics in Land Use Modeling: Exploring the Future of Abandoned Farmlands in Europe with the Dyna-CLUE Model. *Landscape Ecology*, *24*(9), 1167.

Verschaffel, L., Greer, B., & De Corte, E. (2002). Everyday Knowledge and Mathematical Modeling of School Word Problems. In *Symbolizing, Modeling and Tool use in Mathematics Education*(pp. 257-276). Springer, Dordrecht.

Xu, Z. X., Pang, J. P., Liu, C. M., & Li, J. Y. (2009). Assessment of runoff and sediment yield in the Miyun Reservoir catchment by using SWAT model. *Hydrological Processes: An International Journal*, *23*(25), 3619-3630.

# APPENDIX A: CLIMATE SCENARIOS

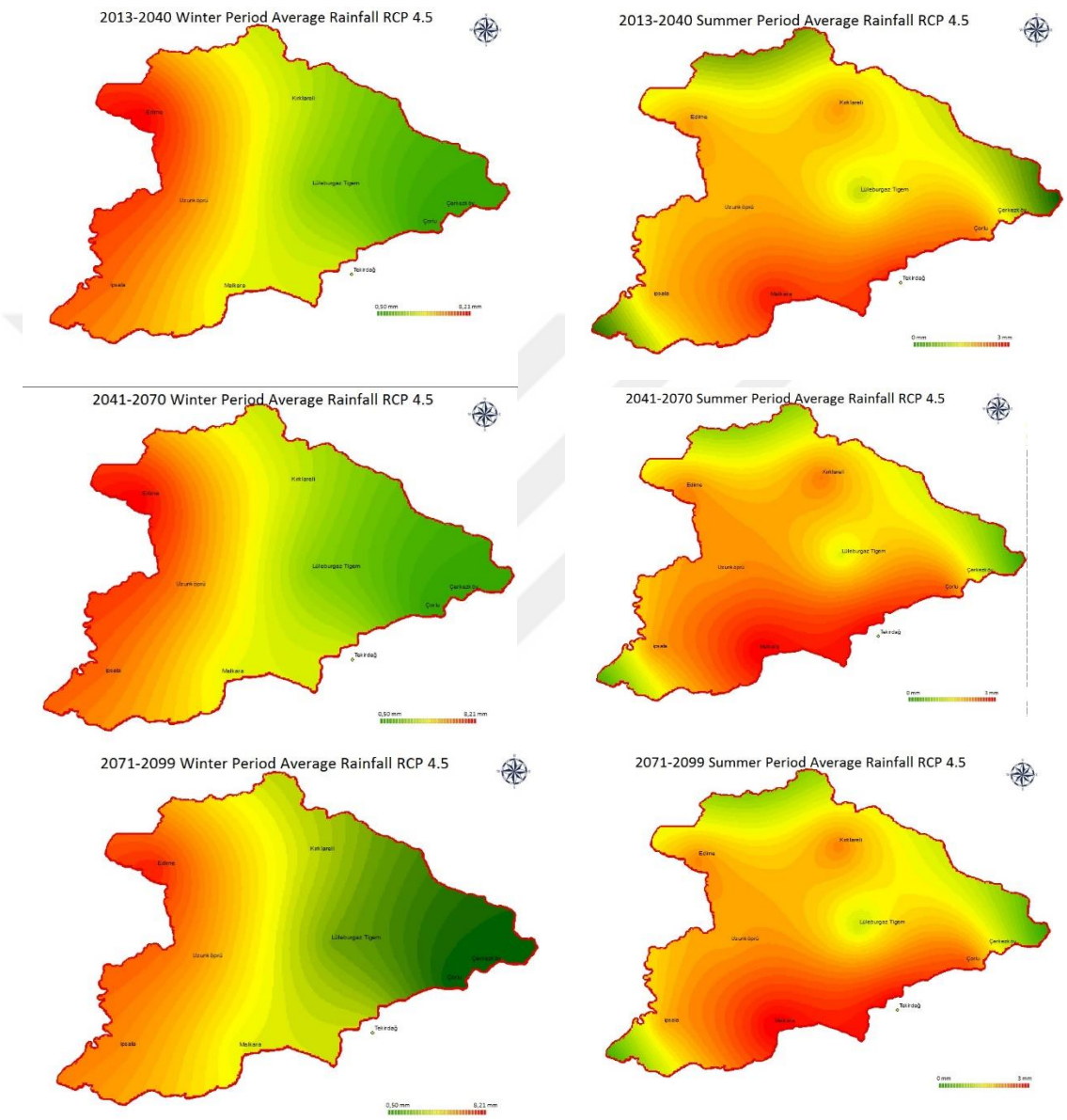


Figure A.1 Precipitation Forecast 2018-2100 RCP 4.5.

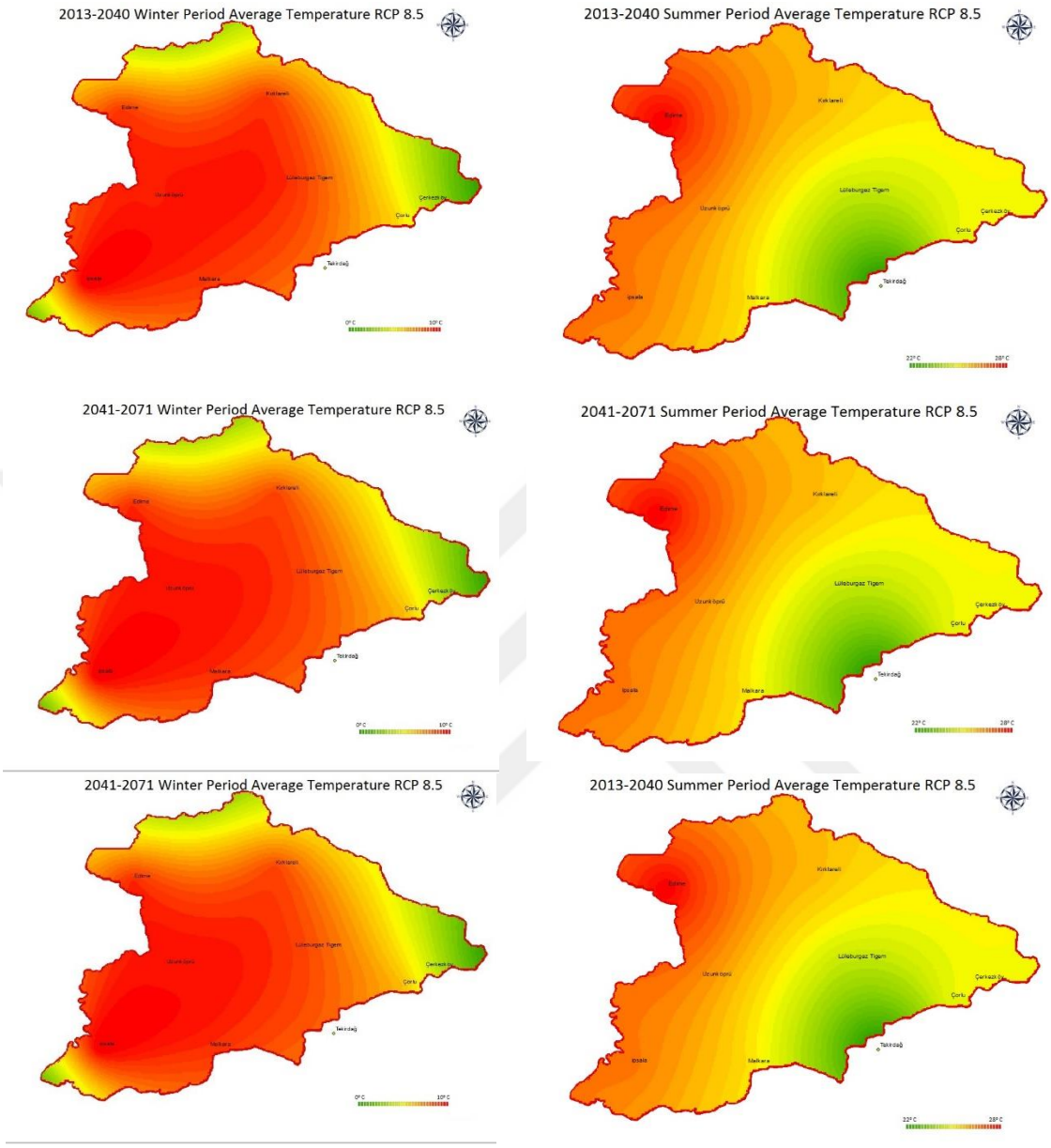


Figure A.2. Temperature Forecast 2013-2100 RCP 8.5.

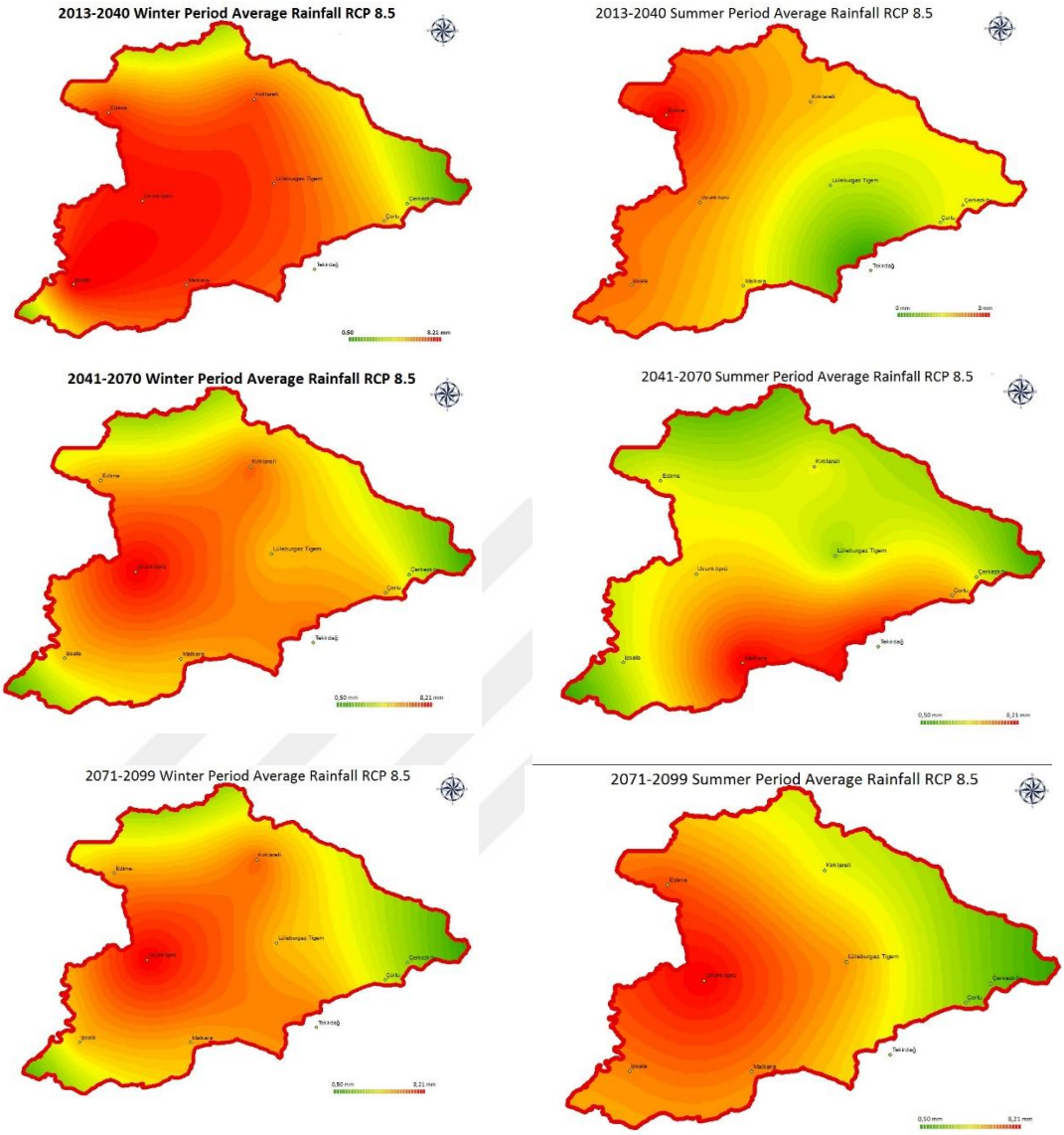


Figure A.3 Precipitation Forecast 2013-2100 RCP 8.5.

# APPENDIX B: 2006 AND 2012 CORINE MAPS

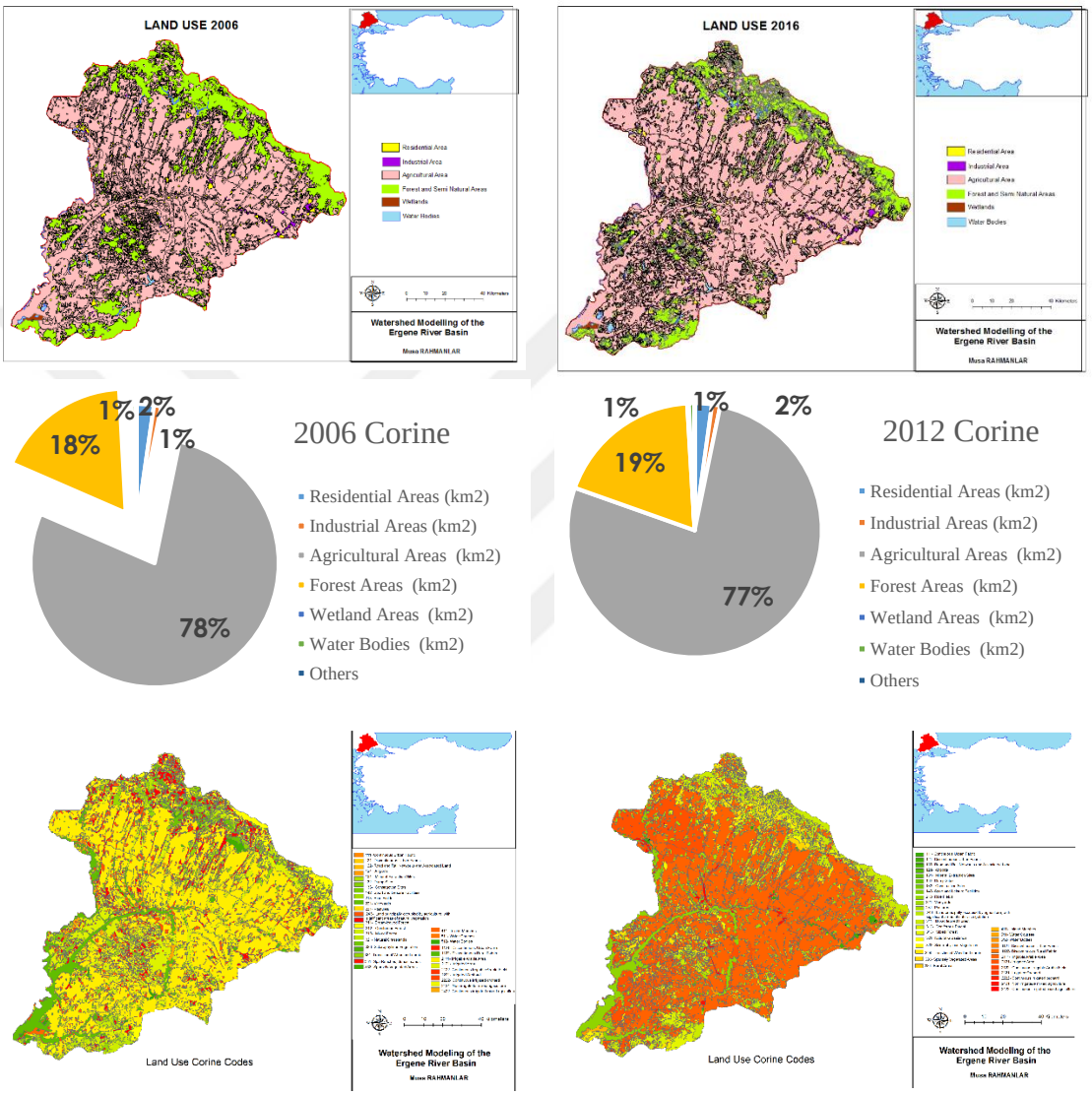


CORINE 2006 CORINE 2012

Figure B.1. CORINE 2006 and 2012 Map Comparison.

# APPENDIX C: MATLAB CODE OF MOVING AVERAGE TEST

```
clear all
close all
clc
 K=dlmread('musa.txt');
z=size(K);
t=K(:,1);
C=K(:,2:z(2));

n=length(t);

p=[ 5 10 15 ];
mark={'ko-','k*-','k+-','k^-'};
for j=1:length(p)


    off{j}=['Moving Averaged =' blanks(1) num2str(p(j)) blanks(1)
'year'];

    for i=1:n-p(j)

        os(j,i) =mean(C(i:p(j)+i,1));


    end

        [H2,p_value2,rho,Z2]=Spearmanrho(os(j,1:i),0.05);
   Result2(j,:)=[H2,p_value2,rho,Z2];


    [H,p_value,S,VarS]=Mann_Kendall(os(j,1:i),0.05);


        Result(j,:)=[H,p_value,S,VarS];

    figure(1)
    plot(p(j)+t(1:n-p(j)),os(j,1:n-p(j)),char(mark{1,j}))
    hold on
    xlabel('Averaged End Year','FontSize',12,'FontWeight','bold')
    ylabel('Concentartion (mg/L)','FontSize',12,'FontWeight','bold')


end

figure(1)
legend(off,2)
```

Figure C.1. MATLAB Code of Moving Average Test.

# APPENDIX D: MATLAB CODE OF ARIMA TEST

```
clear all
close all
clc

K=dlmread('musa.txt');
z=size(K);
t=K(:,1);
C=K(:,5);

%model = arima('ARLags',1,'Variance',garch(1,1))

%arima model fit

musaModel = arima(2,0,1);
modelFit = estimate(musaModel,C);

%forecast for future trend i.e after 500 days
[Y,YMSE] = forecast(modelFit,30,'Y0',C);


lower = Y - 1.64*sqrt(YMSE);
upper = Y + 1.64*sqrt(YMSE);



figure
plot(t,C,'Color',[.7,.7,.7]);
 hold on
h1 =
plot(t(length(t))+1:t(length(t))+30,lower,'r:','LineWidth',2
);

plot(t(length(t))+1:t(length(t))+30,upper,'r:','LineWidth',2
)
 h2 =
plot(t(length(t))+1:t(length(t))+30,Y,'k','LineWidth',2);
legend([h1 h2],'90% Interval','Forecast',...
         'Location','NorthWest')
title('ARIMA Model')
xlabel('Year')
hold off
```

Figure D.1. MATLAB Code of ARIMA Test

```
function[H,p_value,rho,Z]=Spearmanrho(Y,alpha)


Ynew=sort(Y);

n=length(Y);
indy=zeros(1,n);
for i=1:n

    os=find(Y(i)==Ynew);

    m=length(os);
    if m>1
        dum=os;
        indy(i)=-1;

    else
        indy(i)=os;
    end

end

a=find(indy==-1);

if isempty(a)~=1
    indy(a)=dum;
end



indx=1:n;
d2=sum((indx-indy).^2);
rho=1-6*d2/n/(n^2-1);
Z=rho*sqrt(n-1);
p_value=2*(1-normcdf(abs(Z),0,1)); %% Two-tailed test
pz=norminv(1-alpha,0,1);
H=abs(Z)>pz; %%
```

Figure D.1. MATLAB Code of ARIMA Test (cont.)